Philipp Marco Neu, BSc.

Identification of di- and oligomeric oxidation products in biodiesel

Master Thesis

to obtain the academic degree

Diplom-Ingenieur (Dipl.-Ing.)

Masterstudium Technische Chemie

submitted at the

Graz University of Technology (NAWI-Graz)

supervised by:

Ao. Univ.-Prof. Dr.phil. Martin Mittelbach

Dr.rer.nat. Sigurd Schober

Stephanie Flitsch, MSc.

Renewable Resources Group

Institute of Chemistry, University of Graz

Graz, Mai 2014

EIDESSTATTLICHE ERKLÄRUNG
AFFIDAVIT

Ich erkläre an Eides statt, dass ich die vorliegende Arbeit selbstständig verfasst, andere als die angegebenen Quellen/Hilfsmittel nicht benutzt, und die den benutzten Quellen wörtlich und inhaltlich entnommenen Stellen als solche kenntlich gemacht habe. Das in TUGRAZonline hochgeladene Textdokument ist mit der vorliegenden Masterarbeit identisch.

I declare that I have authored this thesis independently, that I have not used other than the declared sources/resources, and that I have explicitly indicated all material which has been quoted either literally or by content from the sources used. The text document uploaded to TUGRAZonline is identical to the present master's thesis.

_____   _____
Datum / Date   Unterschrift / Signature

Danksagung

Ich möchte mich hier bei all jenen Personen bedanken, die mich während des Studiums und bei der Erstellung dieser Masterarbeit maßgeblich unterstützt haben.

In erster Line danke ich Prof. Dr. Martin Mittelbach für die Bereitstellung des Themas und der fachlichen Betreuung,

Dr. Sigurd Schober und Stephanie Flitsch, MSc sowie Herrn Dr. Jörg Ullmann für die Unterstützung, Ideen und Kommentare.

Ich danke Prof. Dr. Robert Saf für die Anfertigung und Bereitstellung der hochauflösenden Massenspektren sowie der weiteren hilfreichen Beratung.

Außerdem bedanke ich mich bei allen aktuellen und ehemaligen Mitgliedern der AG NAWARO die, während meiner Zeit hier, mir immer hilfsbereit zur Seite standen.

Ich bin meinen Eltern herzlichst dankbar für die Ermöglichung meines Studiums und die ständige Unterstützung sowohl finanziell als auch moralisch.

Abschließend danke ich meiner Familie und meinen Freunden.

Content

Abstract

Biodiesel as renewable resource is a well-established substitute or blending component for petrodiesel. It is produced by transesterification of a plant oil, waste oil or animal fat with methanol to obtain fatty acid methyl esters (FAME).

Biodiesel tends to degrade when stored or stressed for a long time, due to its chemical composition. From lipid aging, it has been known that many reaction steps are involved in this degeneration, like fragmentation, oxidation or di- and oligomerization. The oxidative attack occurs on the double bonds of the fatty acids. When blended with petrodiesel and after a long aging time, precipitation of polar dimers and oligomers in the nonpolar petrodiesel can occur. The identification of these compounds is difficult and characterization of di- and oligomeric aging products is not reported in literature. But there are different reaction types known in the lipid oxidation to form dimers and oligomers like the linkage with oxygen, reaction of esters or epoxides and Diels-Alder reaction.

The aim of the research was the time-resolved analysis of the change of the biodiesel's (B100) and biodiesel blends' (B50 and B7) composition during accelerated aging. The aging was performed in a Rancimat or PetroOxy device with increased temperature and air/oxygen supply. The investigation of formed molecules with a higher molecular mass could be achieved with a chromatographic separation of the polar and nonpolar content of the samples, followed by size-exclusion chromatography (SEC) of the fractions. With a longer aging time, the amount of polar compounds increases because of the reaction with oxygen and also the formation of molecules with a higher mass is increasing with longer aging time.

Furthermore, an identification of aging products of oleic acid methyl ester (OAME) via high resolution mass spectrometry (GC-TOF-MS and MALDI-TOF-MS) was performed. In the spectra of aged OAME a wide range of molecular masses appear besides the obvious binding of two molecules of OAME from the oxidizing step, so there are far more reactions occurring during the aging process than expected. It can be demonstrated that with a longer aging time the regions of molecular masses shift to higher molecular masses. A further saponification and transesterification step shows the presence of ester-linked di-and oligomers.

Kurzfassung

Biodiesel als erneuerbarer Rohstoff ist ein bewährter Ersatz oder eine bewährte Mischungskomponente für fossilen Diesel. Er wird durch die Umesterung von Pflanzenölen, Altspeiseölen oder Tierfetten mit Methanol zu Fettsäuremethylester (FAME) hergestellt.

Aufgrund seiner chemischen Zusammensetzung ist Biodiesel oxidationsempfindlich, wenn er für einen längeren Zeitraum gelagert oder thermisch beansprucht wird. Von der Lipidalterung ist bekannt, dass dieser Abbau durch viele Reaktionsschritte wie Fragmentierung, Oxidation, oder Di- bzw. Oligomerisierung, stattfindet. Der oxidative Angriff erfolgt an den Doppelbindungen der im Biodiesel vorhandenen Fettsäuren. Falls er mit fossilem Diesel vermischt wird, entsteht bei langer Alterungsdauer eine Abscheidung der zunächst gelösten polaren Di- und Oligomeren im unpolaren Mineralöldiesel. Die Identifikation dieser höhermolekularen Stoffe gestaltet sich als schwierig und die Charakterisierung von Di- und Oligomeren ist in der Literatur kaum beschrieben. Verschiedene Reaktionstypen werden bei der Lipidoxidation vorgeschlagen, die zu einer Bildung von Di- bzw. Oligomeren führt, wie die Verknüpfung über Sauerstoff, eine Reaktion von Estern oder Epoxiden oder über die Diels-Alder Reaktion.

Die Zielsetzung dieser Untersuchung war die zeitaufgelöste Analyse der veränderten Zusammensetzung während der beschleunigten Alterung von Biodiesel (B100) und Biodieselmischungen (B50, B7). Die Alterung wurde in Rancimat und PetroOxy-Analysensystemen, bei erhöhter Temperatur und Luft- bzw. Sauerstoffzufuhr, durchgeführt. Die Untersuchung der gebildeten höhermolekularen Alterungsprodukte konnte mittels chromatographischer Trennung der unpolaren und polaren Bestandteile und anschließender Größenausschlusschromatographie (SEC) der Fraktionen erreicht werden. Mit der Alterungsdauer erhöht sich auch, wegen der Aufnahme von Sauerstoff, die Menge an polaren Molekülen, außerdem wird die Bildung von höhermolekularen Stoffen durch die längere Alterungsdauer begünstigt.

Weiters wurden Alterungsprodukte von Ölsäuremethylester (OAME) über hochauflösende Massenspektroskopie (GC-TOF-MS und MALDI-TOF-MS) identifiziert. Im Massenspektrum des gealterten OAME tauchen eine Vielzahl an Molekülmassen, abseits von dem offensichtlichen Verknüpfen zweier OAME-Monomer-Molekülen durch den Oxidationsschritt, auf. Also entstehen durch die Alterung von FAME viel mehr Verbindungen als bisher angenommen. Es kann gezeigt werden, dass diese gefunden Komponenten bei längerer Alterung eine höhere Molekülmasse erreichen. Ein erneuter Veresterungsschritt zeigt die Verknüpfung von Di- und Oligomeren über Esterbrücken.

1   Introduction

Biodiesel tends, due to its chemical composition, to degradation. During these degradation processes precipitates can be formed when the biofuel is blended with petrodiesel. With the development of higher efficient engines the fuel gets more and more stressed due to higher temperatures and pressures in the injection systems.

Manufacturers of fuel carrying parts and injector systems are interested to investigate the degeneration of biodiesel, because cases of damage are reported due to these precipitations. An identification of the aging products and their properties are helpful for those manufacturers to develop more robust parts and systems.

The aim of this work is the investigation and identification of these aging products with a special attention to the high molecular mass range.

The time-resolved analysis of the formed di- and oligomers was performed by accelerated aging of biodiesel (B100) and biodiesel blends (B50, B7) and separation of the polar aging products by column chromatography and size-exclusion chromatography (SEC).

For a more accurate identification of the biodiesel aging products, an analysis of aged oleic acid methyl ester (OAME) was performed. This analysis includes high resolution time-of-flight mass spectrometry with MALDI and gas chromatography-electron ionization. The investigation of the aging of OAME was selected because of its high content in rape seed oil and the presence of double bonds as well as the lower tendency to isomerization than linoleic or linolenic acid methyl ester. Furthermore, a renewed mass analysis after a transesterification reaction should show the presence of monomers linked with an ester group to form di- and oligomers.

2   Background and Theoretical Part

2.1   B100 Biodiesel

Biodiesel is a mono alkyl ester produced via transesterification reaction of triacylglycerol with short chain monovalent alcohols like methanol or ethanol. The most commercially used one is esterified with methanol (fatty acid methyl ester (FAME)).

The fatty acids are mono carboxylic acids with a saturated or unsaturated carbon chain. The source of the fatty acids can be plant, waste and used frying oils or animal fats. The fatty acids are available in this oils and fats as triglycerides (Figure 1).

Triglyceride   + 3 Alcohol $\xrightarrow{\text{Cat.}}$ 3 Alkyl ester   + Gylcerol
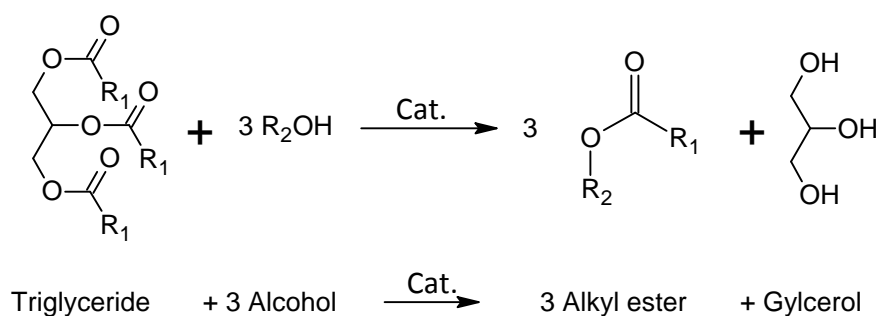
Figure 1: Scheme of the transesterification reaction. R_1 is the carbon chain of various fatty acids; R_2 is the alcohol (methanol for the production of FAME) modified from [1]

Typically, strong acids or bases are used as catalyst for the industrial production of biodiesel. Studies have shown that the base-catalyzed reaction is much faster than the reaction with an acid as catalyst [2], [3]. For that reason, the alkali-catalyzed process is commercially used for the biodiesel production. The acid-catalyzed reaction is used by the transesterification of feedstocks with a high content of free fatty acids, so the catalyst does not produce soaps [4]. Furthermore, catalytic reactions with enzymes [5], [6] and with non-ionic bases [7] as well as non-catalytic supercritical trans-esterification [8], [9] reactions have been reported.

Glycerol is obtained as by-product during the transesterification of fats and oils to biodiesel. The amount of the received glycerol is about $10\%_{wt}$ of the yield of the fatty acid methyl esters [10]. This glycerol has various applications [1] and can be used as chemical intermediate [2], [10]. Some applications are in the cosmetic and pharmaceutical industry, as component to form alkyd resin, as moistener in tobacco products or as antifreeze or in cleaner or polishers [11].

Depending on the used feedstock, the fatty acid composition is different for the produced biodiesel. Table 1 summarizes the average content in rape seed oil with a low erucic acid concentration.

Table 1: Common fatty acids and their content in rape seed oils (low erucic acid)

Fatty acids		Trivial name	IUPAC name	Content in rape seed oil [%] [12]
Saturated	C14:0	Myristic acid	Tetradecanoic acid	ND-0.2
	C16:0	Palmitic acid	Hexadecanoic acid	2.5-7.0
	C18:0	Stearic acid	Octadecanoic acid	0.8-3.0
	C20:0	Arachidic acid	Eicosanoic acid	0.2-1.2
Unsaturated	C16:1	Palmitoleic acid	(9Z)-Hexadec-9-enoic acid	ND-0.6
	C18:1	Oleic acid	(9Z)-Octadec-9-enoic acid	51.0-70.0
	C18:2	Linoleic acid	(9Z,12Z)-Octadec-9,12-dienoic acid	15.0-30.0*
	C18:3	α-Linolenic acid	(9Z,12Z,15Z)-Octadec-9,12,15-trienoic acid	5.0-14.0*
	C20:1	Gondoic acid	(11Z)-Eicos-11-enoic acid	0.1-4.3*
	C22:1	Erucic acid	(13Z)-Docos-13-enoic acid	ND-2.0
				(>2.0-60 high erucic acid rape seed oil)

ND: not detectable (<0.05%) *double bond position isomers are possible

2.1.1 Ecological Aspects

The combustion of fossil fuels releases the long-term stored carbon from the earth´s lithosphere to the atmosphere. Without considering the indirect land use change, life-cycle analyses show, that the use of 1 L rape seed oil biodiesel, in comparison to fossil petrodiesel, saves 2.2 kg CO_2-equivalents of greenhouse gases [13]. A 57% reduction of greenhouse gas emissions can be achieved by replacing petrodiesel with biodiesel [14]. Furthermore, the sustainability of biodiesel, because of the use of renewable resources for the production, is an ecological advantage in contrast to the use of fossil fuel for transportation. But renewable biofuels are also not totally neutral in the global carbon cycle [15], [16]. The biodiesel emissions of green house gases are caused by fertilizing (N_2O), the use of methanol or the processing steps [17].

Within the European Directive 2009/28/EC all member states have to meet the following target, until 2020: 10% share of biofuels in all forms of transportation [18]. For Germany, the share of biofuels in transportation, was 5.7% in 2012 [19]. This amount has almost to be doubled to reach the EU goal. Until 2020 the objective target of 10% of renewable fuels will be mainly covered by the so-called 1st Generation of biofuels like biodiesel blends with fatty acid methyl esters or bioethanol as petrol substitute from the fermentation of sugars or other carbohydrates.

In the year 2011 8,607,000 tons of biodiesel were produced in the EU-27 [20] and 10,816,616 tons of biofuels [21] were consumed for transportation. With 2,800,000 tons (33% of the EU-27) Germany produced the highest amount of biodiesel [20]. Rape seed oil is commonly used for the German biodiesel production (87%) and also waste oils get transesterified (5%). Further feedstocks were soybean oil (2%), palm oil (0.5%) and animal fats (2%) [22].

Because of the properties of biodiesel, it can be used as 100% substitute or blending component for petrodiesel. The EN 590 [23] specification allows an addition of 7%$_{vol}$ biodiesel to petrodiesel and manufactures give warranty for the use of this blending ratio in all diesel engines. The use of FAME as fuel is covered in the European Standard EN 14214 [24]. Important properties are specified in this standard with the corresponding analytical methods and values which the FAME has to meet.

2.1.2   Technical Aspects

The relatively low stability of biodiesel in contrast to petrodiesel against oxidation leads to aging of the fuel. Oxidation of the fuel can occur when it is in contact with oxygen over a longer time or at elevated temperatures, e.g. at long term storage or in the tank and injection parts like common rail.

A result of the aging of the fuel is the formation of deposits. These deposits are a problem for all fuel carrying parts in the engine and become a bigger issue by the invention and development of the common-rail fuel injection system. The fuel gets compressed up to 1,800 bar [25] and also thermally stressed before it gets injected. Furthermore, unused fuel drains back as recycle flow to the tank, gets mixed with fresh fuel and the combustion cycle is started again (Figure 2). Deposits are also produced when free fatty acids form soaps with metals.

A deposit in the injector system leads to a bad nebulizing of the fuel or a complete plug of the fuel filter or injector, which can cause a damage of the engine. New injector-systems get tested in long term experiments, with biodiesel blends and under real engine conditions [26].

Furthermore, oxidation of biofuel also produces short chain acids like formic or acetic acid. The corrosivity is increasing with the concentration of these acids and further oxidation is also promoted because of the catalytic factor. Events of damage are reported, caused by corrosion of fuel carrying parts [27], [28].
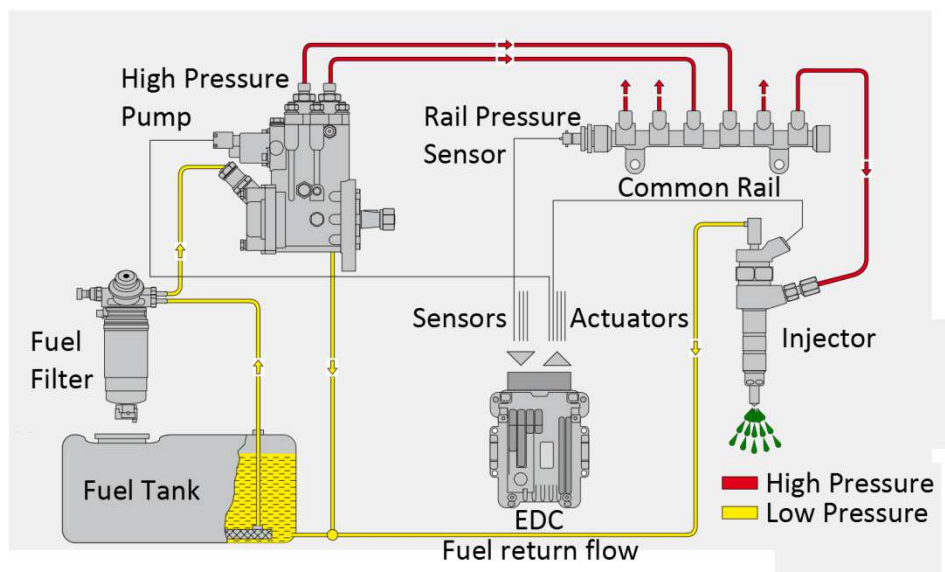

Figure 2: Scheme of a common rail injection system from [29]

2.2 Aging of Biodiesel

The degeneration of fats and lipids is well known [30], [31], [32]. The aging of biodiesel is similar because of the similar chemical functional groups like double bonds or the ester group.

The stability of biodiesel is primarily depending on the amount of double bonds in the fatty acids (Table 1). Polyunsaturated fatty acids tend more to autoxidation than a monounsaturated fatty acid, because of the much more reactive bis-allylic methylene group (Figure 3). The reported relative oxidation rates from C18:1 to C18:2 to C18:3 fluctuate from 1:10:25 [33] and 1:41:98 [34] or C18:0 to C18:1 to C18:2 to C18:3 is 1:100:1200:2500, [35] depending on the method of measurement. The oxidation starts with a free radical initiation step, then the reaction on the allylic carbon and at last the termination step to form stable oxidation products, primarily hydroperoxides (Figure 4).

The first initiation step is the abstraction of an allylic hydrogen, with a delocalized allyic radical as result (Figure 3). A double bond migration can happen because of this delocalization and form all kinds of conformational- and cis/trans-isomers [30]. An addition of molecular oxygen on the radical takes place. The formation of peroxyl radicals out of oleic acid and termination with a hydrogen radical to form hydroperoxides is shown in Figure 4. With a higher grade of unsaturation a variety of isomers are possible [36].
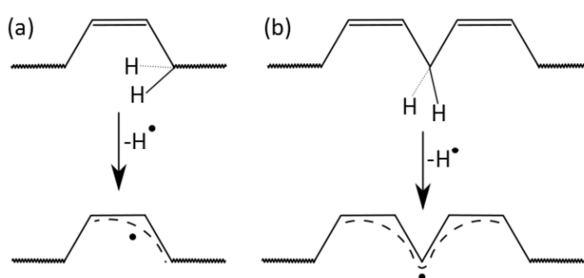
Figure 3: Initiation step and formation of a delocalized allylic radical from (a) a monounsaturated fatty acid like oleic acid and a bis- allylic radical (b) from a polyunsaturated fatty acid like linoleic acid based on [32]
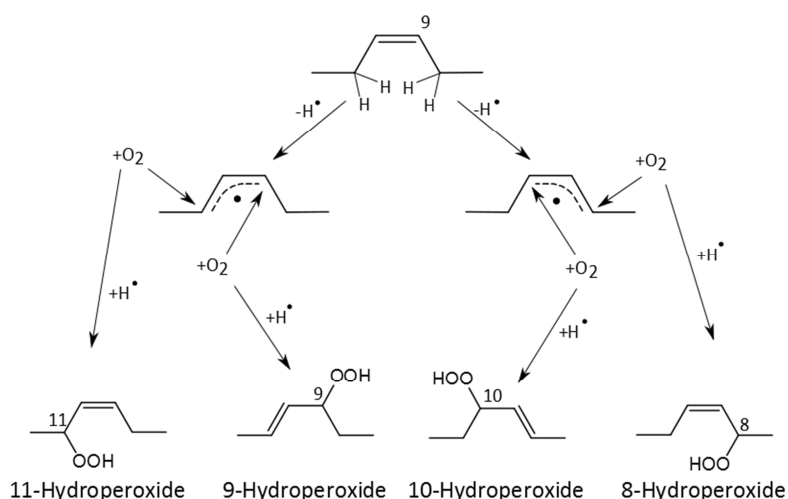
Figure 4: Formation of hydroperoxide isomers from oleic acid (methyl ester) based on [30]

Further decomposition reactions of the hydroperoxides lead to secondary oxidation products. These oxidation reactions can be classified by the molecular weight of the formed products, where the mass can decrease by fragmentation, stays almost constant by addition of oxygen or is increasing with the formation of dimers and oligomers.

- Polar Monomers

The formation of epoxides out of hydroperoxides is one of the dominant reactions during biodiesel oxidation [30], but also reactions of hydroperoxides to form ketones or alcohols have been reported [37] (Figure 5). These reactions form oxidation products with a slight increase of the molecular mass, because of the addition of oxygen to the fatty acid methyl ester.
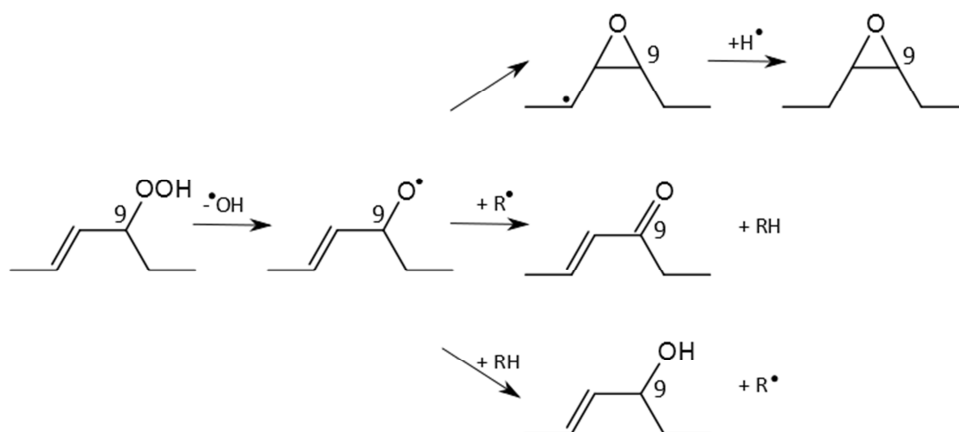

Figure 5: Formation of epoxystearate out of the hydroperoxide based on [30] **and the formation of ketones or alcohols as aging poducts** based on [37]

- Fragmentation

Smaller molecules are formed by the thermal hydroperoxide decomposition of the hydroperoxides. These fragmentation reactions form aldehydes, alkyl and olefinic radicals by β-scission. Further reactions of the radicals produce stable secondary oxidation products [30] (Figure 6). The high isomer variety of the formed hydroperoxides leads to a high variety of this secondary oxidation products. The formed aldehydes can undergo further oxidation to form carboxylic acids.
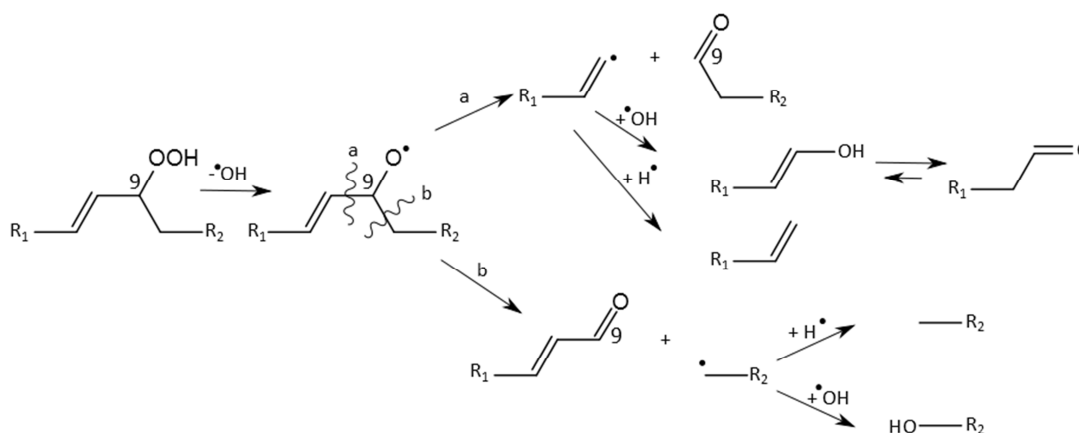

Figure 6: β-Fragmentation of the oleic acid- 9-hydroperoxide based on [30]

- Di-and Oligomerization

Oxidation products with a higher molecular mass are formed mainly in the termination step of the free radical reaction, where the recombination of two radicals takes place (Figure 7, a). Furthermore, reactions of radicals with a double bond lead to an unstable radical, which can undergo further reactions [38] (Figure 7, b).
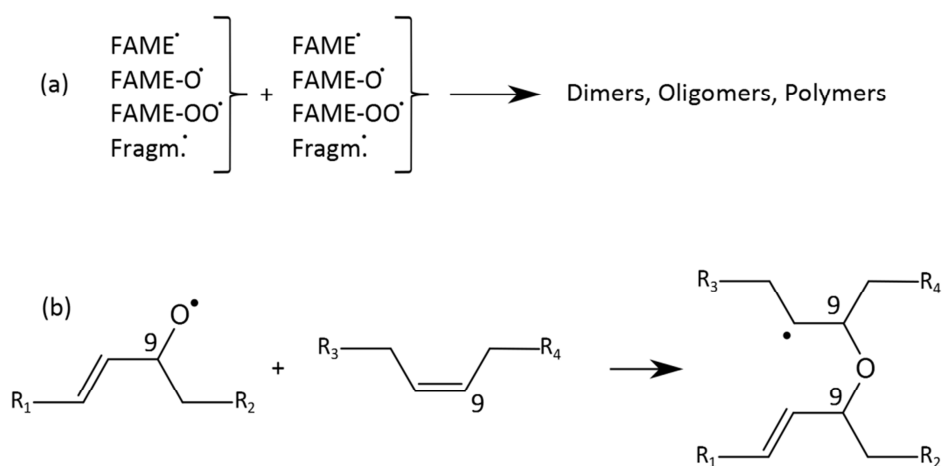

Figure 7: Formation of aging products with a higher molecular mass [38]

A further possible pathway to form dimers is the cyclization via a Diels-Alder reaction. Decades ago, this reaction became from a theoretically possible to an accepted reaction, which occurs under certain conditions [30], [39], [40]. A previous isomerisation step of a poly unsaturated fatty acid is needed to form a conjugated diene. But Arca et al. (2012) [41] and also Hwang et al. (2013) [42] could not identify any of these Diels-Alder products as aging product via the characteristic methine-carbon NMR-signals of the ring system (Figure 8).
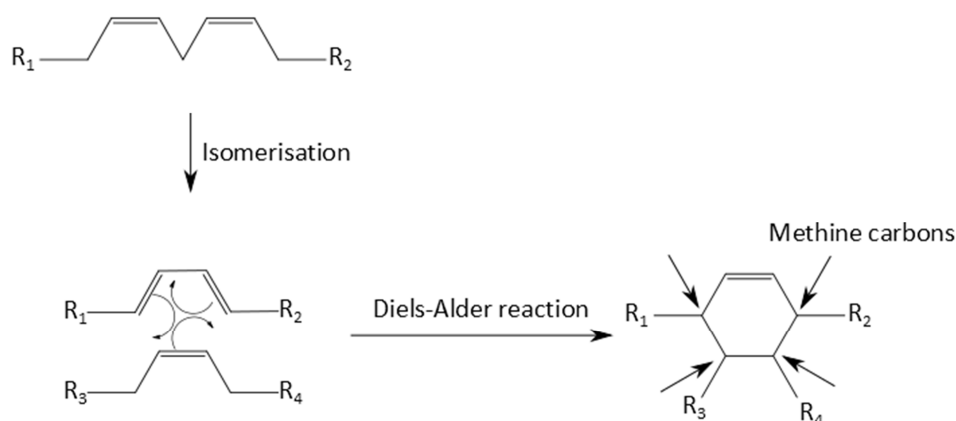

Figure 8: Dimerization reaction via the Diels-Alder cyclization based on [42]

The amount of oligomers in used frying oils can be more than 21% of the sample and also a dimer-content of 14% of the used frying oil sample was found from Ruiz-Méndez et al. (2008) [43]. Pereira et al. published 2013 their results of the determination of di- and oligomers in oxidized soybean-oil-biodiesel (methyl ester). They found a content of 0.8% oligomers and a dimeric content of 1.4% in the FAME-sample, after an oxidation time of 6 hours (Rancimat conditions (see chapter 2.2.1.1)) [44]. The quantification of these di-and oligomers were performed by size-exclusion-chromatography (SEC (see chapter 2.3.1.3)).

Figure 9 summarizes the oxidation reactions discussed here for lipid aging and further suggested pathways [45].
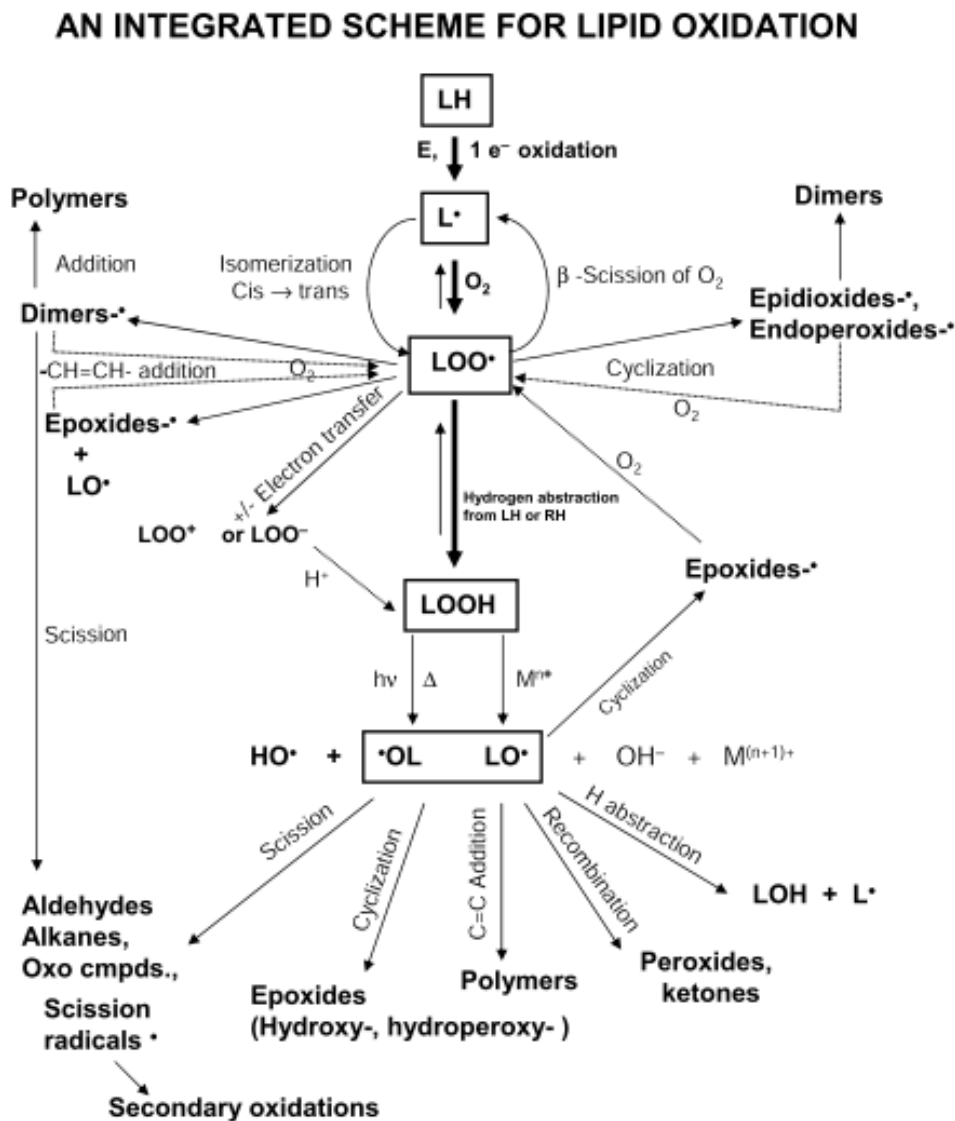

Figure 9: Scheme of lipid oxidation from [38]

2.2.1 Oxidation stability

Different strategies are performed to increase the oxidation stability of biodiesel. The inactivating, reduction or eliminating of catalytically working metals [46], [47], [48], the addition of antioxidants [47], [49], [50], the reduction of polyunsaturated compounds by hydrogenation [30] or blending [48] are reported.

The induction period (IP) is the time that is needed to reduce the biodiesel´s oxidation reserve and the start of the formation of oxidation products. The IP can be determined with different devices.

2.2.1.1 Rancimat

The standard method EN 15751 [51] describes the determination of the oxidation stability value with the Rancimat device of FAME and their blends with a minimum amount of 2%$_{vol}$ FAME content.
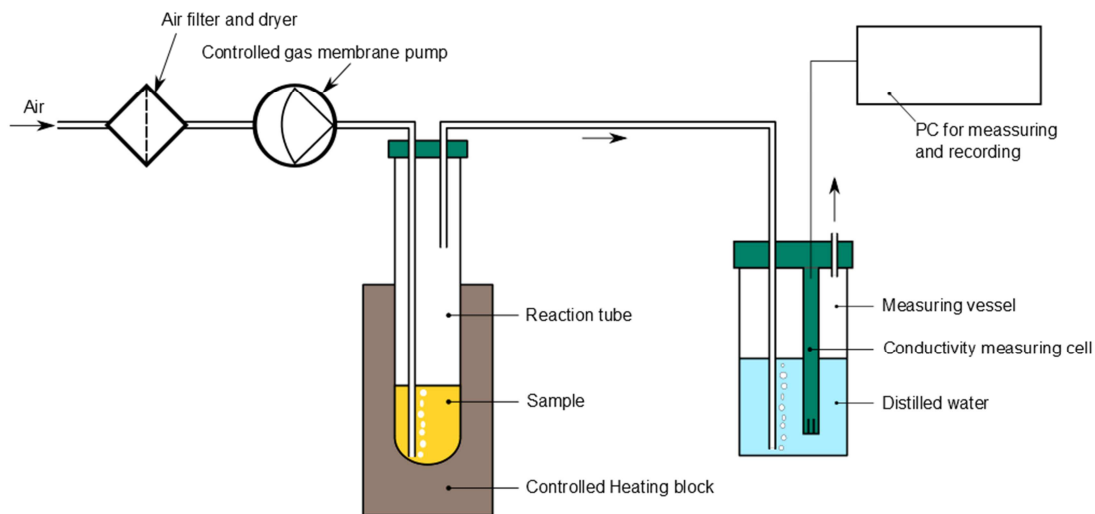
Figure 10: Scheme of a Rancimat device used for the determination of the IP of a biodiesel sample (modified scheme from Stephanie Flitsch [52])

For the IP determination the biodiesel samples are heated up to 110°C in the commercially available Rancimat device. A permanent dry air flow with 10 L/h is blown through the sample and volatile components are carried out of the system. They are transferred into a beaker with distilled water and get dissolved in it. Volatile aging products like formic or acetic acid increase the conductivity of the water. A measuring cell analyses this increase of conductivity continuously and transmits the data to the evaluation unit. The software calculates the IP with the maxima of the second derivative of the conductivity graph. A manual method of the determination is to create a tangent at the inflection point and the base line. The intersection point of the two lines also gives the IP (see Figure 11). Both methods are approved in the standard EN 15751 [51]. Figure 11 shows a typical conductivity trend for the IP determination of a biodiesel out of rape seed oil with the manual determination of the IP.
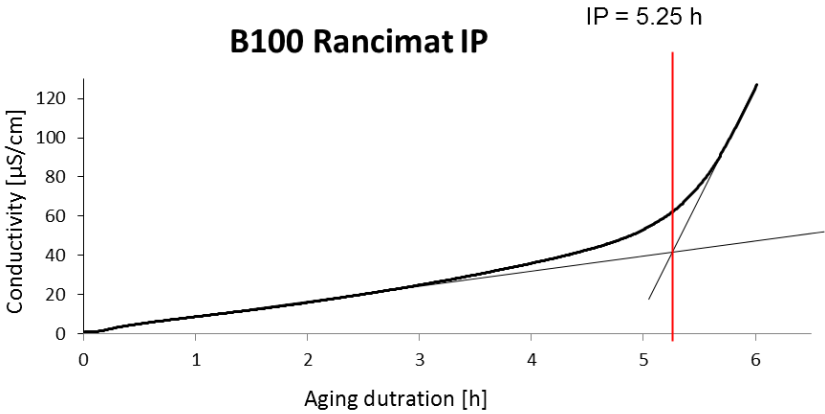
Figure 11: Conductivity trend of the determination of the oxidation stability value of a rape seed oil biodiesel.

In the beginning the oxidation reserve of the biodiesel is consumed. Natural and synthetic antioxidants extend the induction period. After the full use of the oxidation reserve a strong increase in conductivity occurs. The biodiesel gets degenerated and aging products are formed.

2.2.1.2   PetroOXY

The oxidation stability can also be determined with the use of the European standard EN 16091 [53]. For this standard method the biofuel or petrodiesel sample is heated up to 140°C in a sealed reactor under a pure oxygen atmosphere with a pressure of 7 bar. Because of the oxidation process of the sample, the oxygen gets consumed and a pressure drop occurs. The IP is defined as the time it takes for a 10% pressure drop of the maximum pressure. In Figure 12 a typical PetroOxy IP determination test of a B100 biodiesel out of rape seed oil is shown.
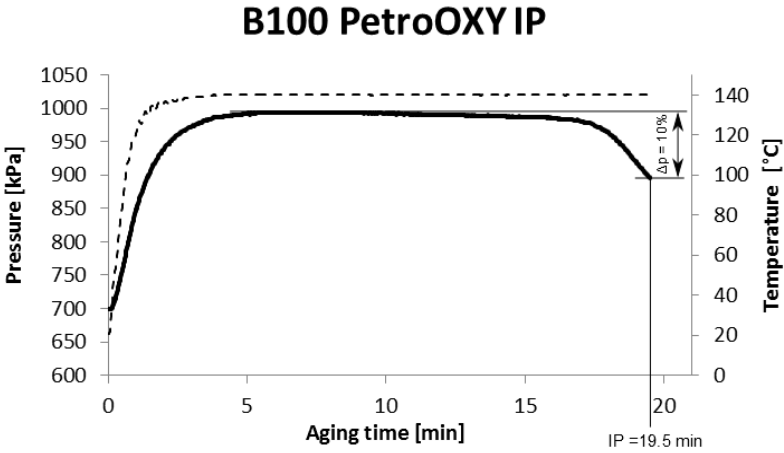

Figure 12: Determination of the induction period of rape seed oil biodiesel

The reactor is closed and charged with a pressure of 7 bar of oxygen. The pressure is also increasing during the heating up stage of the reactor from room temperature to 140°C. In this time some of the aging reserve gets already consumed. The maximum pressure is reached after approximately 5 minutes. After this time the pressure slowly begins to decrease. When the oxidation reserve is consumed, the pressure drops immediately. The IP is determined after a pressure drop of 10%.

2.3   Analytical Methods

2.3.1   Chromatography

The IUPAC defines chromatography as a physical separation method for components which are distributed differently between two immiscible phases. One phase is stationary and the other one moves as mobile phase in a defined direction [54]. The different distribution occurs because of different interaction, due to various properties of the analytes, with the stationary or mobile phase. The interactions lead to a slower velocity of the molecules and to a defined retention time for each component.

Chromatography can be classified depending on the various separation properties of the analytes. The commonly used techniques are adsorption, partition, exclusion, ion-exchange, or affinity chromatography. The methods used for this work should be viewed on detail.

For instrumental analytics, any kind of continuous detector can be used at the end of the stationary phase to detect the compounds. Different detector devices are UV-VIS, refraction index, evaporate light scattering for liquid and flame ionization, thermal conductivity detectors for gaseous mobile phases. Depending on the ionization method, also a mass selective detector can be used for liquid or gaseous mobile phases.

2.3.1.1   Adsorption Chromatography

The separation in the adsorption chromatography of the compounds in a sample happens because of repeated adsorption and desorption processes of the analytes on the surface of an active solid phase like silica gel. Polar compounds in the sample have a longer retention time because they are held back longer on the polar hydroxyl groups of the silica gel. Hydrogen bonds and Van-der-Waals interactions slow down the more polar compounds on their way through the column. A higher retention time is the result [54].

This principle is used in the liquid column chromatography to separate nonpolar and polar analytes in a sample. The sample amount in the column chromatography can be a few milligram (solid phase extraction, SPE) or, depending on the column size, several tens of gram. Because of the defined retention times of the analytes, this technique is used for analytical applications to characterize samples qualitatively. The columns for HPLC- applications for adsorption chromatography either have a polar package like silica gel (normal phase) or a nonpolar one with long chain hydrocarbons (C8 or C18) (reverse phase) [55].

2.3.1.2   Partition Chromatography

In the partition chromatography the analytes are distributed between the stationary and mobile phase because of their different solubility in one of the two phases [54].

Gas chromatography represents a special case for the partition chromatography. Here the separation is based on the boiling points of the analytes and then the vaporized molecules are separated by partition processes with the stationary phase in the column.

2.3.1.3   Size-Exclusion Chromatography

In the size-exclusion chromatography (SEC) the separation is effected by the size and shape of the anlytes in solution, precisely their hydrodynamic volume. As stationary phase porous solids are packed in a column. The analytes get distributed in the pores, whereby three cases can occur. First, when the analyte is too big in size, it does not fit in the pore and gets excluded (V_0). Second, analytes with a too small hydrodynamic volume totally permeate the whole volume of the pores and elute with the column volume (V_t). In the third case, the analyte has a retention volume between V_0 and V_t, where the solid phase gets selective permeated. In this range the separation of the analytes occurs [56]. The slope and position of the selective separation graph (Figure 13, left) depends on the column package, the absolute pore size, and the pore size distribution [57]. Figure 13 (right) shows the selective separation of two analytes. The smaller molecule A has a longer distance in each of the pores and is therefore slower than the molecule B, which has a bigger size. This delay leads to a higher retention time of the smaller analyt A. A calibration of SEC-columns is performed with standards with known molecular masses and a comparison of the retention times. With a higher retention time the analyzed molecules get smaller and therefore their molecular mass decreases [58].
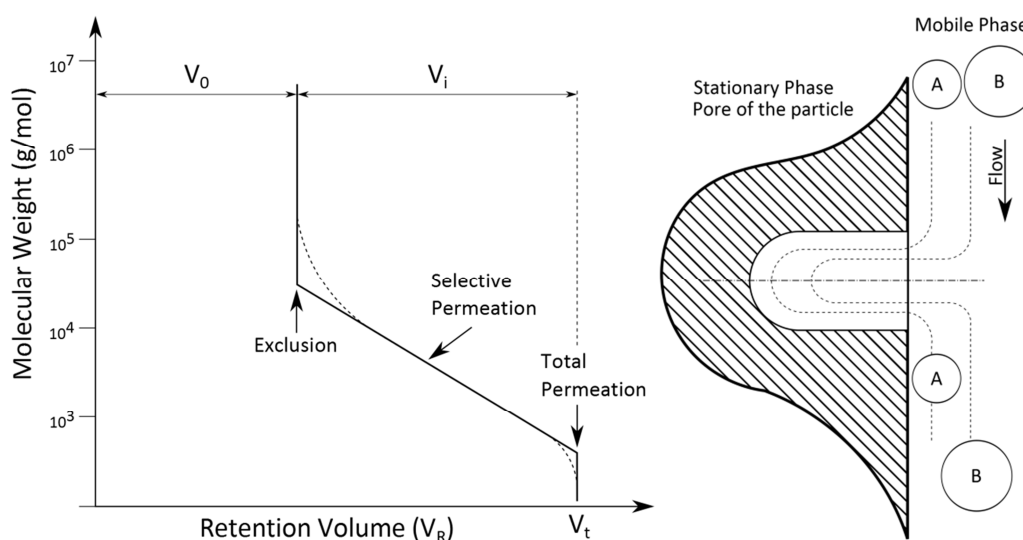

Figure 13: Size exclusion chromatography calibration and separation range modified scheme from [57] **and scheme of the selective separation in the size exclusion chromatography** modified scheme from [58]

2.3.2   Mass Spectrometry

Mass spectrometry allows the measurement of the atom or molecule masses of samples. Because of the separation and detection technique the mass to charge ratio (m/z) is analyzed.

2.3.2.1   Ionization

Ionization is required for the analytes to measure their mass to charge ratio. Different types of ionization methods are established in the mass spectrometry like electron impact (EI), atmospheric pressure chemical ionization (APCI), electrospray ionization (ESI), inductive coupled plasma (ICP) or matrix assisted laser desorption/ionization (MALDI). The preferred ionization method generally depends on the physical state of the samples or sample preparation (Figure 14). Depending on the energy input of the used ionization method a hard (EI) or soft (APCI) ionization occurs and the measurement of fragments (hard) or molecule peaks (soft) is preferred.Furthermore, if the analytes are not gaseous, a vaporization of the analytes is required for the mass analysator and is processed simultaneously with (MALDI) or after (ESI) the ionization. Figure 14 shows the broad variety of applications for ionization.
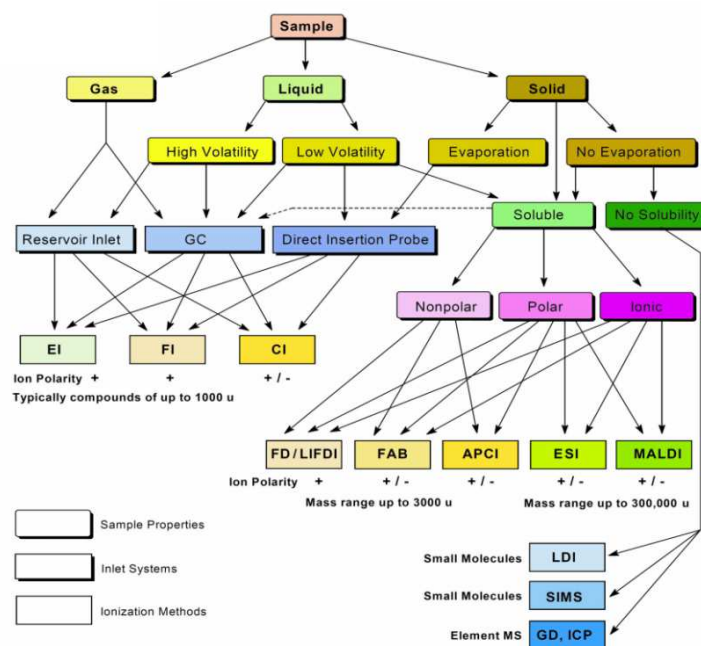
Figure 14: Ionization methods for mass spectrometry from [59]

- Electron Ionization (EI)

Electron ionization is widely used in gas chromatography coupled with a mass spectrometry as detector unit. A filament generates electrons, through thermoionic emission. These electrons are accelerated to a collision zone with the analyte. The acceleration energy is usually set at 70 eV, which corresponds to a de Broglie wavelength of 1.4 Å. The energy of the electrons is transferred to the molecules, if this wavelength is disturbed by the bond length of the analyte [60]. As result a radical ion is generated. A fragmentation of this radical ion occurs because of a further reaction to reach the thermodynamically most stable molecule [61]. Each molecule has its own specific fragmentation pattern and can therefore be characterized, when found in databases [62], [63], [64], [65] or by their typical fragmentation like α-cleavage, formation of carbeniumions, loss of neutral particles or rearrangement reactions like McLafferty or retro Diels-Alder [66].
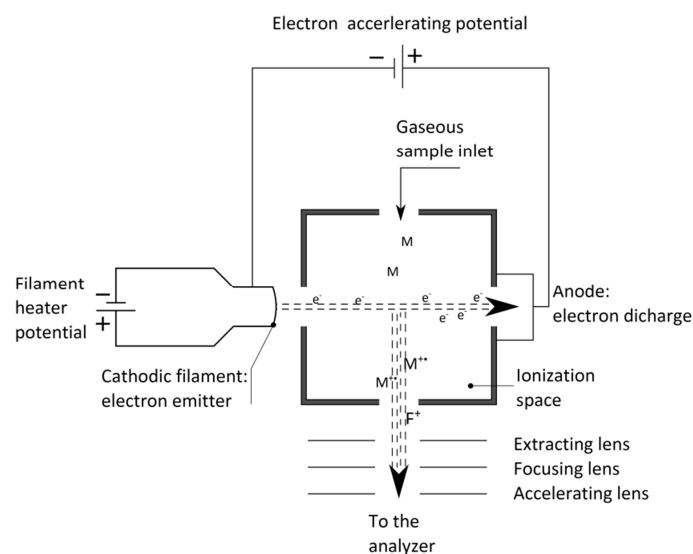

Figure 15: Scheme of the Electron Ionization technique modified from [60]

- Matrix Assisted Laser Desorption/Ionization (MALDI)

The analysis of synthetic polymers or biopolymers by mass spectrometers with MALDI as ion source has become an established characterizing method. In the sample preparation the analytes are mixed with a matrix of organic molecules, which can absorb the laser energy like substituted cinnamic acids and acetophenones or dithranol and other additives. The ablation of the matrix-analyte mixture occurs by a short intense laser pulse on the solid sample. The energy of the laser causes sublimation of the matrix molecules and the analyte is also ejected with this matrix [67]. A charge transfer occurs in the gas phase to ionize the analytes to form mainly single charged pseudo molecule ions [60]. This technique of ionization is unsuitable for coupling with a continuous chromatographic method, but discontinuous off-line techniques have been designed [68].
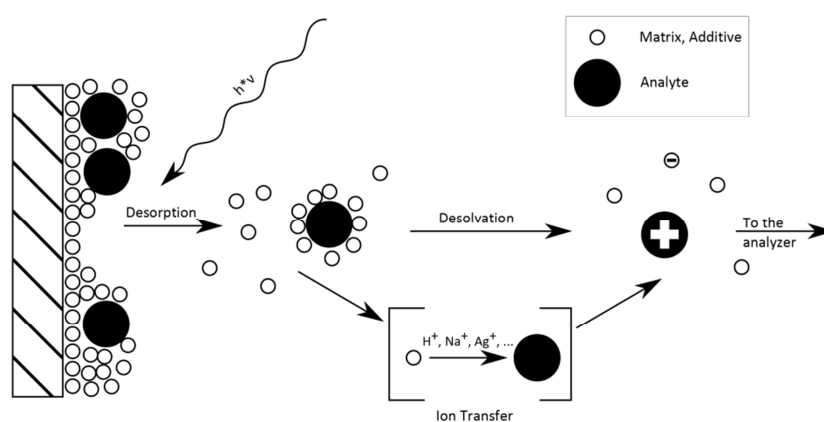

Figure 16: Scheme of the MALD Ionization technique modified from [60]

2.3.2.2 Mass Analyzers

The gaseous ionized analytes are separated according to their mass to charge ratio in the mass selective analyzer. Different methods can be used for mass separation, such as quadrupole mass filter, magnetic sector instruments, time of flight analyzator or ion traps.

- Quadrupole Mass Analyzer

A quadrupole mass analyzer consists of four parallel electrode rods, ordered in a square. The generated ions from the ion source are accelerated before entering the quadrupole mass analyzer and fly along these rods. On these rods a direct current and an oscillating radio frequency voltage are applied and generate an electromagnetic field. A selection occurs because this field allows just a certain m/z a complete passing on a stable path. Other m/z are filtered out and collide with the wall of a rod. By sequentially changing the radio frequency or the voltages on the rods, the field is set so that other smaller or larger ions can reach the ion detector and give a signal [69].
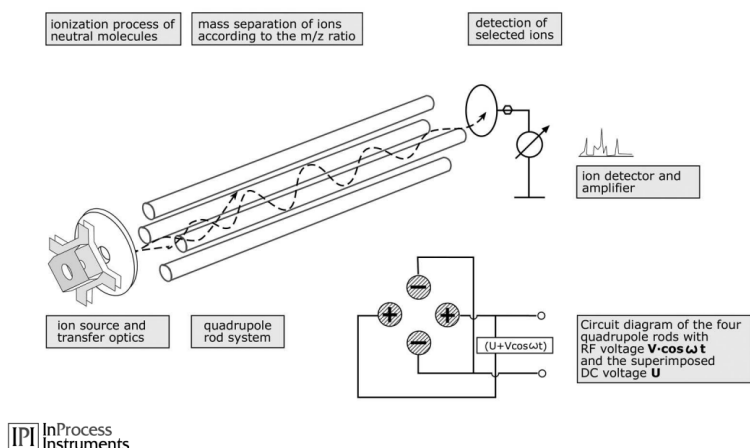
Figure 17: Scheme of a quadrupole mass analyzer [from [70]]

- Time of Flight Mass Analyzer

Heavier ions need a longer time for a certain distance, when accelerated with the same kinetic energy. This effect is used in the analytsis of charged molecules or fragments with a time of flight separator. With the correlation of mass and flight time over $m/z = 2e * E * s \left(\frac{t}{d}\right)^2$ the m/z are analyzed by a measured time the analytes need to pass the flight tube and reach the detector. Where "e" is the elementary charge, "E" the extraction pulse potential, "s" is the length of the acceleration field and "d" is the length of the field free drift zone [61]. The flight tube can be constructed linear or with a reflector design. The reflector corrects possible kinetic energy dispersions and gives a higher mass resolution [60].

The big advantage of using a TOF mass analyzer is the much higher resolution that can be achieved than with a quadrupol mass analyzer (**Fehler! Verweisquelle konnte nicht gefunden werden.** left). A higher mass resolution allows the determination of the elemental formula, because of the identification of the exact masses. A separation of the ions with the same nominal masses (isobaric molecules) is possible. Also the identification of the molecular formula of the fragmental pattern (with EI) is possible, which supports the identification of unknown compounds. The high resolution mass spectrometry became a powerful tool for identification of compounds in mixtures, biological molecules or drug characterization [71], [72], [73], [74].
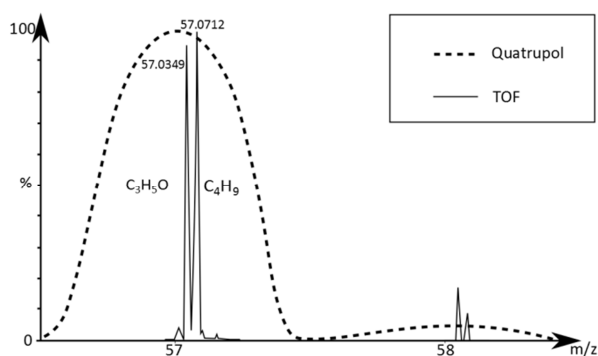

Figure 18: Effect of a higher mass resolution [from [75]]

3   Experimental Section

3.1   Chemicals

3.1.1   Starting material

➢ Petrodiesel OMV with pre-additives (Spring 2012)
➢ Rapeseed oil biodiesel (ADM) (Hamburg, Germany)

3.1.2   Solvents

➢ Acetonitrile (HPLC-grade ≥99.9%), Fischer-Scientific
➢ Diethyl ether (techn.), Institute of Chemistry, University of Graz
➢ n-Hexane (HPLC-grade ≥97%), VWR
➢ n-Hexane (techn. 95%), Carl Roth
➢ Methanol (HPLC-grade ≥99,5%), VWR
➢ Methanol (techn. >98%), VWR
➢ Petroleum ether (40-60°C bp.) puriss, Sigma-Aldrich
➢ Tetrahydrofuran (THF) (HPLC-grade ≥99,5%), VWR

3.1.3   Reference material

➢ 1,3-Diolein (≥99%), Sigma-Aldrich
➢ Linoleic acid (C18:2) (≥99%), Sigma-Aldrich
➢ Linoleic acid methyl ester (C18:2 ME) (≥99%), Fluka
➢ Linolenic acid (C18:3) (≥99%), Fluka
➢ Linolenic acid methyl ester (C18:3 ME) (≥98%), Merck
➢ 1-Monoolein (≥99%), Sigma-Aldrich
➢ Oleic acid (C18:1) (≥99%), Sigma Aldrich
➢ Oleic acid methyl ester (C18:1 ME) (≥99%), Fluka
➢ Stearic acid (C18:0) (≥99%), Sigma-Aldrich
➢ Stearic acid methyl ester (C18:0 ME) (≥99%), Sigma-Aldrich
➢ Triolein (≥99%), Sigma-Aldrich

3.1.4   Reagents

➢ Acetic acid (96%), VWR
➢ Boron trifluoride in methanol (20% BF_3-MeOH adduct), Merk
➢ Formic acid (≥98%), Sigma-Aldich
➢ Helium (5.0) and Nitrogen (5.0), Messer
➢ Hydrogen peroxide (30%), VWR
➢ Magnesium sulphate (≥97%, anhydrous), Acros
➢ Oleic acid, Institute of Chemistry, University of Graz
➢ Sand (50-70 mesh particle size, heated up to 775°C for 20 hours), Sigma-Aldrich
➢ Silicagel 60 (0,015-0,040 mm; heated up to 200°C for 24 hours), Merck
➢ Sodium chlorid, Institute of Chemistry, University of Graz
➢ Sodium hydrogen carbonate (≥99%), Riedel-de Haën
➢ Sodium hydroxide, Institute of Chemistry, University of Graz
➢ Sodium sulphate (≥99%, anhydrous), Carl Roth
➢ Sulfuric acid (≥95%), Carl Roth

3.2 Instruments

3.2.1 Sample preparation

➢ Analytical balance Sartorius BP210S, max. 210 g; d = 0.1 mg
➢ Autovortex SA6, Stuart Scientific, Staffordshire, United Kingdom
➢ Glas tubes (Pyrex®) with PTFE screw caps
➢ PetroOXY, Petrotest, Dahlewitz, Germany
➢ Rancimat 743, Metrohm, Herisau, Switzerland
➢ Rotavapor, Heidolph VV2000 with water bath Heidolph WB2000 and membrane vacuum pump ABM MZ 2C, Schwabach, Germany

3.2.2 Mass spectrometry

➢ GC-MS: Hewlett-Packard HP6890 gas chromatography system with HP7683 Autosampler and HP5973 Mass selective detector and an Agilent J&W DB-5MS UI capillary column (max. 325°C, 30 m x 250 µm x 0.25 µm (5%-Phenyl)-methylpolysiloxane ultra inert) with split/splitless injection, Helium 5.0 as carrier gas
➢ GC-TOF-MS: Agilent 7890A gas chromatography system with an Waters GCT Premier orthogonal time-of-flight mass spectrometer and J&W DB-5MS (30 m x 250 µm x 0.25 µm (5%-Phenyl)-methylpolysiloxane)
➢ MALDI-TOF-MS: Waters Micromas® MALDI micro MX™ time-of-flight mass spectrometer

3.2.3 Size-exclusion chromatography

➢ Hewlett-Packard HP1100 series high performance liquid chromatography with Degasser G1322A, Quaternary pump G1311A, Auto sampler G1313A and Column thermostat G1316A and a Knauer K2301 refractive index detector with Interface HP35900
Agilent PLgel columns (300 mm x 7.5 mm x 5 µm) 50, 100 or 500 Å

3.2.4 High performance liquid chromatography

➢ Hewlett-Packard HP1100 series high performance liquid chromatography with Degasser G1322A, Quaternary pump G1311A, Auto sampler G1313A and Column thermostat G1316A and a UV- VIS detector G1314A
Agilent Column Zorbax Eclipse XDB-C18 (4.6 x 150 mm and 5µm)

3.3 Experimental pathway

The IP of biodiesel, biodiesel blends and oleic acid methyl ester was determined by the Rancimat and PetroOxy device. The aging process in the Rancimat was stopped at certain aging time. Samples were separated by column chromatography in 3 fractions with different polarities.

The fractions were analyzed by high performance liquid chromatography and size exclusion chromatography. The measurements give information on the polarity, molecular weight and mass distribution of the fractions. The identification of aging products was performed by high resolution mass spectrometry. A saponification and methylation step was performed in order to allow a characterization of the linkage of di-and oligomers.
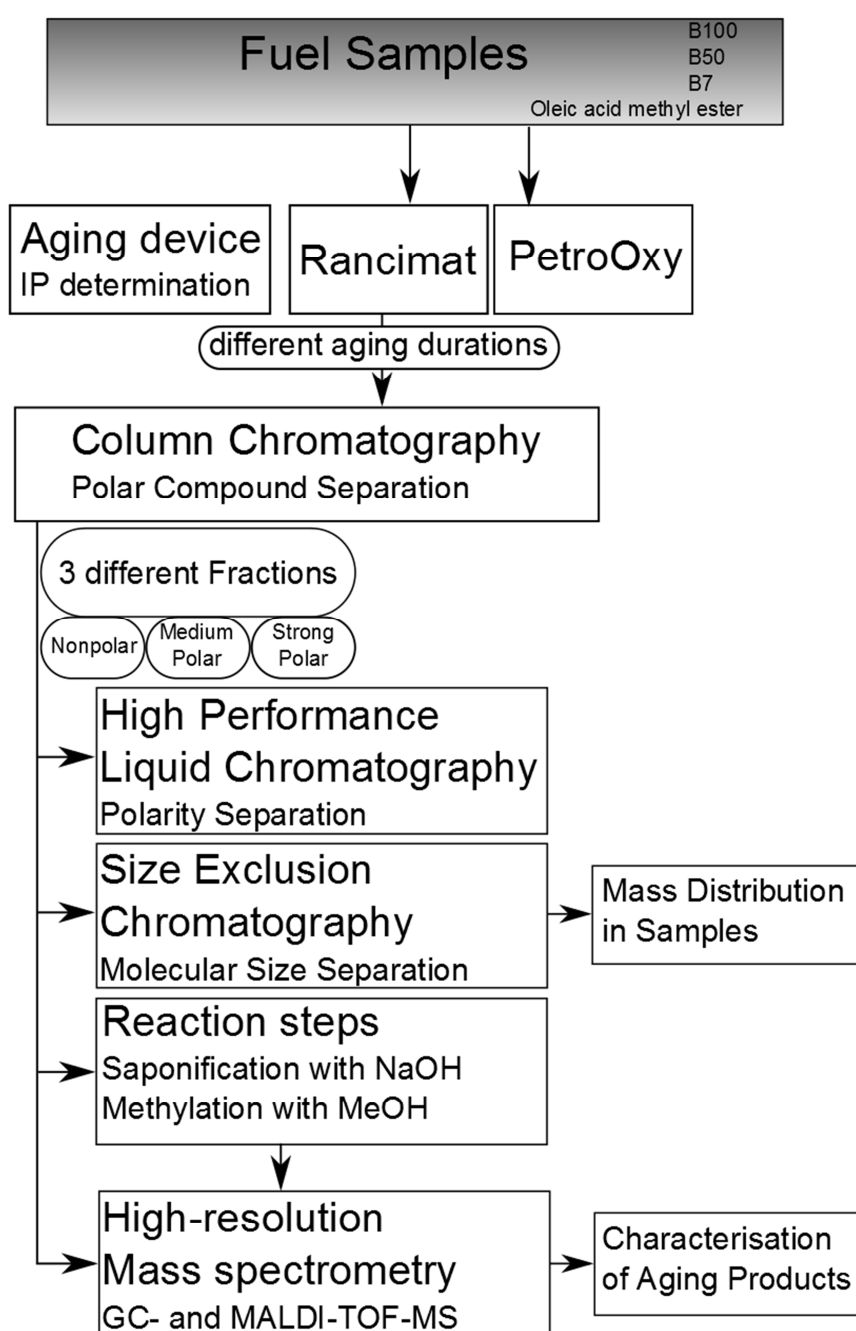
Figure 19: Experimental flow chart of the analytical procedures

3.4   Sample Preparation

The biodiesel-blends were made by mixing the biodiesel with the exact volumetric amount of petrodiesel to make B7 and B50.

Oleic- and linoleic acid methyl ester were produced by acid catalyzed methylation. The acids (oleic acid (200 g) or linoleic acid (15 g) were mixed with methanol (40 g) and sulfuric acid (0.5 g 95%) and then heated up to reflux for 4 h. Oleic acid was mixed with methanol (40 mL) again and heated up a second time. For the work up, the reaction mixtures were washed with water till the pH of the washing water was neutral. Then the organic phase was washed two times with NaCl (aq) and dried over $MgSO_4$. Analysis by GC-MS shows the purity of the products.

3.5   Accelerated Aging of Biodiesel

Two different types of devices were used for the simulated aging and oxidation of biodiesel or biodiesel blends.

3.5.1   Rancimat

The biodiesel and biodiesel blend samples (7.5 g) were aged under Rancimat conditions as specified in the standard method EN 15751 [51]. The air stream through the samples was 10 L/h and the samples were heated up to 110°C +ΔT=1.4°C. Products of the oxidation were blown out of the reaction tube and passed in a beaker with distilled water (20 mL). A measure cell analyses the increasing conductivity. The aging was stopped at certain times and the samples were stored at -20°C and under nitrogen till they were used.

3.5.2   PetroOXY

Biodiesel samples (5 mL) were filled in the PetroOxy-device. For sealing a new rubber O-ring was put in the groove before closing the screw cap. After locking the safety hood, the device was purged once with oxygen. The measurement starts when the oxygen pressure is at 700 kPa. The chamber was heated up to 140°C so the final oxygen pressure is approximately at 1,000 kPa. The measurement was stopped at a pressure drop of 10% of the maximal pressure and the samples were filled in a screw cap tube under nitrogen and stored in a fridge at -20 °C. The rubber O-ring was exchanged for every new test.

3.6   Synthesis and Reaction of Epoxides

Oleic acid methyl ester (5 mL) mixed with formic acid (98%, 2 mL) was cooled on an ice bath. Hydrogen peroxide (30%, 3.5 mL) was added dropwise to the cold solution. This reaction mixture was stirred for 16 h and washed with aqueous sat. $NaHCO_3$ to neutral and two times with sat. NaCl (aq). The product of the reaction was dried over $MgSO_4$, filtered and stored under nitrogen in the fridge at 6°C.

The stearic acid methyl ester epoxide (1 g) was dissolved in hexane (20 mL) and mixed with formic (98%) and acetic acid (96%) (0.5 mL each). This solution was heated up to reflux for 5 hours and then stirred at room temperature overnight. The solution was washed with water to neutral and two times with sat. NaCl(aq), dried over $MgSO_4$ and filtered. The solvent was removed with a nitrogen stream. The analysis of the products was performed by a GC-MS.

3.7   Quantitative and Qualitative Characterization

Different types of chromatography and mass spectrometry were used for the quantitative and qualitative characterization of aged biodiesel.

3.7.1 Column Chromatography

A silica gel-column-chromatography was used to separate the polar and the nonpolar substances in the biodiesel samples which were aged in the Rancimat device (3.5.1). The method was done according to the AOCS Cd 20-91 method [76]. The column was filled with a small amount of sand (approx. 5 g) before the anhydrous silica gel (50 g), slurried in petrol ether, was put into the column. On top of the silica layer a second layer of sand (5 g) was put into the column. Eluent 1 was a mixture of petrol ether and diethyl ether (87:13 v/v). The accurately weighed samples (2 g for B100 and B50 and 4 g for B7 samples) were dissolved in eluent 1 (2 mL) and put on the column. The samples were chromatographed with eluent 1 (160 mL). The second eluent was diethyl ether (100 mL) and a mixture of petrol ether, diethyl ether and methanol (10:70:20 v/v/v) (100 mL). The third eluent was methanol (50 mL). These three fractions were collected separately. The column was conditioned with eluent 1 (200 mL) again before the next use. The solvents were removed by the use of a rotavapor. The amount of the fractions was weighed accurately. The separated compounds were stored in the fridge at -20°C and under nitrogen. The amount of the polar content is the mass of each fraction proportional to the used sample amount (Equation 1).

$$\%_{m,f} = \frac{m_f}{m} * 100 \qquad \text{(Equation 1)}$$

Equation 1: Quantification of the polar content of an aged biodiesel sample with column chromatography; $\%_{m,f}$ is the mass proportion of a fraction; m_f is the mass of a fraction; m is the mass of the initial sample

Table 2 summarizes the composition and the used volume of the eluents for the polarity separation in the column chromatography.

Table 2: Eluent composition for column chromatography

Eluent	1	2		3	Column conditioning
Fraction	Nonpolar	Medium polar		Strong polar	-
Petrol ether [%$_{vol}$]	87	-	10	-	87
Diethyl ether[%$_{vol}$]	13	100	70	-	13
Methanol [%$_{vol}$]	-	-	20	100	-
Volume [mL]	160	100	100	50	200

3.7.2 Size-Exclusion Chromatography

The size-exclusion-chromatography (SEC) performed on HP Series 1100 was used to separate the samples by their hydrodynamic volumes. A method according to the standard method DGF-C III 3c (10) [77] was used. Therefore, 1 drop of the sample (approx. 30 mg) was dissolved in a vial with tetrahydrofuran (THF) (5 mL). The sample (50 μL) was injected via an auto sampler into the SEC-system. THF was used as eluent and the eluent flow was 1 mL/min. A 5 μm guard column (30 mm) was installed. The first separation column was a 100 Å column followed by a 500 Å column. Both columns were Agilent PLgel columns (300 mm x 7.5 mm x 5 μm). The columns were tempered at 40°C. A Knauer K2301 refractive index detector gives the signal via the Interface HP 35900 to the data analyzing software "ChemStation" A.10.02.1757 from Agilent. The peak areas reflect the content of the molecular size distribution of the aged biofuel sample. By size exclusion chromatography the samples were separated in their fragmental, monomeric, dimeric and

oligomeric content. The area proportion of each peak to all peaks gives the portion of the mass distribution for this content (Equation 2).

$$\%_{M,SEC} = \frac{A_x}{\sum A} * 100$$

(Equation 2)

Equation 2: Quantification of molecular size of the aged biodiesel samples with size-exclusion chromatography; $\%_{M,SEC}$ is the mass distribution of a peak; A_x is the area of a peak; ΣA is the sum of all peaks areas.

For the comparison of the MALDI-TOF-MS and the SEC (4.7.3) results, additionally a 50 Å column with the same dimensions were used in front of the 100 Å and 500 Å columns. The higher resolution leads to a better separation of peaks between the region of the dimeric and monomeric content. The molecular size was approximately determined with the use of standards. The used standards were oleic acid methyl ester, stearic acid, and the 1-mono-, 1,3-di- and triglycerides of oleic acid. The triglyceride of oleic acid represents trimers as aging product and the 1,3-glyceride of oleic acid dimers. Polar oxidized aging products in the monomeric molecular range are determined with the 1-mono glyceride of oleic acid.

3.7.3   Composition of a Sample

The results of the size-exclusion chromatography and the column chromatography give the content of products formed during the aging of biodiesel for each fraction in the whole sample (Equation 3).

$$\%_{M,sample} = \%_{m,f} * \%_{M,SEC}$$

(Equation 3)

Equation 3: Quantification of the molecular size for each fraction in the sample input; $\%_{M,SEC}$ is the molecular content for each fraction for the sample; $\%_{m,f}$ is the result of the column chromatography; $\%_{M,SEC}$ is result of the SEC-analysis.

3.7.4   High Performance Liquid Chromatography

An HPLC-system from HP Series 1100 was used to separate the samples by their polarity. The sample (ca. 30 mg) was dissolved in acetonitrile and injected (5 µL) into the HPLC system. A solvent gradient was performed. The start solvent mixture was 90% H_2O and 10% acetonitrile. In the next 15 minutes the polarity changed constantly to a mixture of 10% H_2O and 90% acetonitrile, which was held for the next 5 minutes. For column conditioning the start mixture was eluated for 10 minutes through the system. The solvent flow was set constant by 1 mL/min for the analysis. The used column was an Agilent Zorbax Eclipse XDB-C18 (4.6 x 150 mm and 5 µm). The UV-VIS detection was adjusted by a wavelength of 205 nm.

3.7.5   Gas Chromatography-Mass Spectrometry

The GC-MS measurements were performed on a HP6890 gas chromatograph with an HP5973 quadrupole mass detector and a capillary column (DB-5MS, max. 325°C, 30 m x 250 µm x 0.25 µm). The samples (1 µL) were injected with an HP7683 autosampler. The inlet temperature was set at 300°C. As carrier gas helium (1 mL/min, 50:1 split) was used. The oven temperature program was started from 80°C with a gradient of 30°C/min up to 280°C then with a gradient of 15°C/min to 310°C and this temperature was held for 10 minutes, till the third gradient of 15°C/min heated the oven up to 320°C for 2 minutes. A mass-spectrometer was used as detector. The GC-transfer line to the MS was heated to 300°C. The MS worked in the scan mode within a mass range of 40-800 u. The quadrupole temperature was set at 150°C and the source temperature at 230°C. The fragmentation

was performed by electron ionization with 70 eV acceleration voltage. Data analysis was performed with the Agilent "MSD ChemStation" E.02.02.1431 software and the Wiley 275 mass spectra database.

3.7.6 High Resolution Mass Spectrometry

Samples of oleic and linoleic acid methyl ester (7.5 g) were aged for 21 hours and 42 hours (just oleic acid methyl ester) in the Rancimat device (3.5.1). These samples and also an un-aged oleic acid methyl ester were chromatographed and separated in a nonpolar, medium polar and strong polar fraction by column chromatography (3.7.1). These sample fractions were stored under nitrogen and were handed to Dr. Robert Saf who analyzed these aged and fractionated samples with a MALDI-TOF-MS and GC-TOF-MS. The analysis software was "MassLynx 4.1" with the NIST MS search 2.0 and Wiley registry mass spectra 8th edition database.

3.7.6.1 GC-TOF-MS

The GC-TOF-mass spectrometry was performed on an Agilent 7890A with a Waters GCT Premier orthogonal time-of-flight mass analyser. The temperature program for the GC-method starts at 40°C for 2 minutes. The oven was heated up to 280°C with a rate of 30°C/min. The next temperature ramp was 15°C/min to 310°C. This temperature was held for 10 minutes till the oven was finally heated up to 320°C with 15°C/minutes for 2 minutes. The sample (1 µL) was injected via an auto sampler. The split/splitless (1:100 split ratio) inlet had a temperature of 320°C. The carrier gas helium had a flow of 1 mL/min through the column (DB5-MS 30 m x 250 µm x 0.25 µm). The transfer line temperature was 260°C. Electron ionization (70 eV, source 250°C) was used to produce ions. The analyzed mass range was 50 to 800 u with approx. 7000 FWHM resolution.

3.7.6.2 MALDI-TOF-MS

The MALDI-TOF-MS analyses were performed on a Waters Micromass MALDI micro MX time of flight mass spectrometer. For the MALDI-method a laser (337 nm wavelength, 5 Hz frequency) generates ions by irradiation. For sample preparation a solution of analytes (5 mg/mL in THF) was mixed with the matrix dithranol solution (10 mg/mL in THF) and CF_3COONa-solution (0.1 mg/mL in THF) in a microtube cap in a ratio of 2:10:1 (v/v/v). The resulting mixture (0.5 µL) was positioned on the sample plate (Stainless steel) and dried under air.

3.8 Esterification of aged Biodiesel and Oleic acid methyl ester

The three fractions of the 24 hours aged Biodiesel and the 21 hours aged oleic acid methyl ester were saponified and again methylated for the analysis by GC-MS. According to the official method of DGF-(C-VI11a(98)) [78] the accurately weighed samples (50-150 mg) were mixed in a 50 mL round bottom flask with NaOH/MeOH (4 mL 0.5 mol/L). This solution was stirred under reflux for 10 minutes. BF_3-MeOH (5 mL, 10%) was added with a pipette through the condenser and also stirred under reflux for further 30 min. This mixture was allowed to cool down to room temperature and hexane (5 mL) was added also through the condenser. After washing with sat. NaCl (aq) the organic phase was dried over $MgSO_4$ and stored in a screw cap tube under nitrogen before analyzed with a GC- and MALDI-TOF-MS.

4 Results and Discussion

4.1 Determination of the IP of Biodiesel

The Metrohm software of the Rancimat device determines the IP of the biofuels via the maximum of the second derivative of the conductivity trend.

The IP was also measured with the PetroOxy device. The IP is the time it takes to a pressure drop of 10% of the maximal pressure during the aging simulation.

The biofuel samples were stored under nitrogen in the dark. But the determination of the IP after six or ten months (Table 3) shows that the samples also degrade to a certain extent at room temperature over the months. They lose their oxidation reserve during the storage. So for preparing the biofuels samples for further tests, the aged samples were stored under nitrogen and in a freezer at -20°C so no further aging should happen and lead to reproducible results.

Table 3: IP determination of biodiesel and blends.

Biodiesel type	IP Rancimat [h] January 2013	IP Rancimat [h] November 2013	IP PetroOxy [min] May 2013	IP PetroOxy [min] November 2013
B100	7.5	5.6	25.0	19.5
B50	11.4	8.0	29.7	23.8
B7	31.3	27.1	62.9	60.1

As expected, samples with a lower biodiesel-content have a higher IP. The IP is increasing because the content of unsaturated fatty acid methyl esters in the mixture is lower. The aging process starts at the double bonds. First they get oxidized and fragmented. These fragments produce volatile acids which increase the conductivity of the measuring cell.

The Rancimat method EN 15751 [51] for the determination of the IP of blends, is specified for diesel fuels with a minimum content of 2%$_{vol}$ fatty acid methyl esters. The B0 petrodiesel is not included in this standard method. The software is not able to give a reproducible result for the analysis of B0 and stops the measurement at undefined times but manual determination of IP is possible.

4.2   Aging of Biodiesel

During the aging of bio- and petrodiesel in the Rancimat device the samples begin to change their chemical and physical properties. The effect of the aging time on these samples can be shown in a change of color, density and viscosity [79].
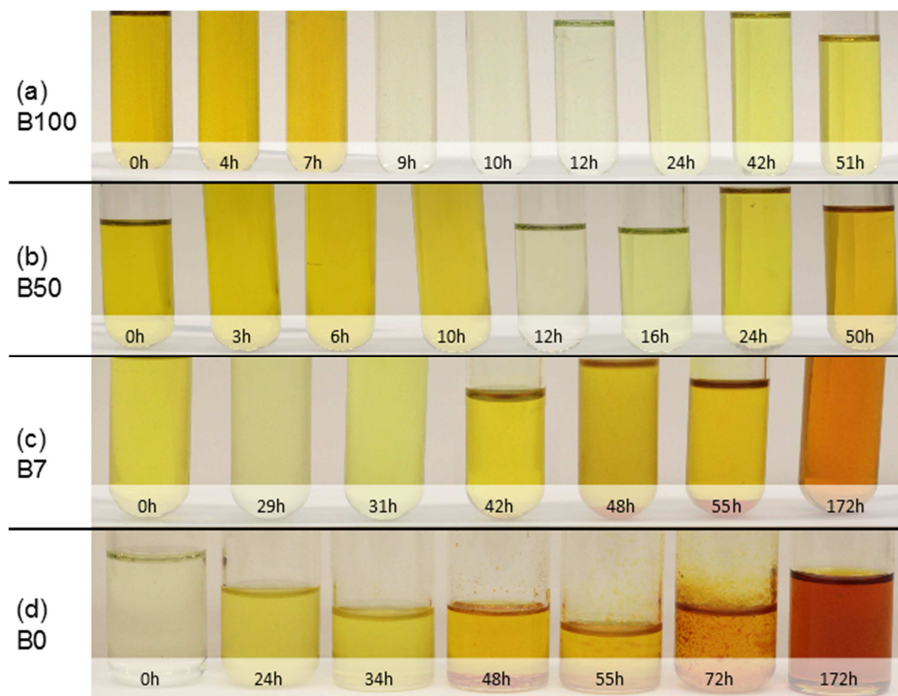
Figure 20: Color change during the aging of biofuel types ((a) B100 (b) B50 (c) B7 and petrodiesel ((d) B0) with the Rancimat device

The process of aging could easily be followed by the color change during the different aging steps of a biodiesel. The yellow color of biodiesel comes from natural antioxidants like tocopherols or carotenoids [80]. The biofuel B100 (a) does not change its yellow color in the first 7 hours in the Rancimat device. But after 9 hours of aging, the sample gets colorless and with prolonged aging the sample gets lightly yellow again. The aging of B50 (b) shows the same trend, but after a longer aging time. The change from yellow to colorless occurs between 10-12 hours and then the sample gets lightly yellow again. The time for changing from yellow to colorless corresponds to the measured IP. At this time all of the colored antioxidants are consumed and the methyl esters get oxidized. The lightly yellow color could come from aging products like epoxides or oligomers. The sample of B50 aged for 50 hours has a more intensive color than the B100 sample at 51 hours. The high petrodiesel content in the B7 biofuel leads to quite different results. The antioxidants have a lower concentration and the un-aged sample has a lighter yellow than B100. After 29 hours of aging, the sample was colorless but cloudy. The cloudiness disappears with a longer aging and the 42 hours sample was clear again. After 48 hours the color changes to orange and a brown residue occurs. After a long aging of 172 hours the sample became red-orange. The residue occurs because of the polarity difference from the almost nonpolar sample to the polar oxidized products. Also, the color of petrodiesel B0 changes during the aging. First, the petrodiesel is colorless and gets yellow to orange and after a long time in the Rancimat device the color of the sample was red. After 55 hours aging time a brown-red residue occurs. The sample which was 172 hours in the Rancimat device had an intensive red color that could be caused by aging products like oxidized aromatic systems or oligomers. The red- brown color of the petrodiesel comes from oxidation products like oligomers.

4.3   Content of polar Compounds

The quantification of the polar content in Biodiesel during the aging was done by column chromatography (3.7.1). The aging time versus the amount of the fractions gives the time resolved polarity trend of the aged biodiesel samples.

4.3.1   Aging of B100 Biodiesel

Table 4 and Figure 21 show the formation of polar compounds during the aging of B100.

The nonpolar fraction elutes with a mixture of petrol ether: diethyl ether 87:13 (160 mL). The medium polar content was the collected fractions of diethyl ether (100 mL) and a mixture of petrol ether: diethyl ether: methanol 10:70:20 (100 mL) and the strong polar fraction elutes with methanol (50 mL).

Table 4: Polar content of aged B100 biodiesel

B100	Nonpolar (I)	Medium Polar (II)	Strong Polar (III)	
Aging time [h]	[% m/m]	[% m/m]	[% m/m]	
0	97.2	2.6	1.2	
2	97.7	2.0	1.1	
4	98.5	1.7	1.2	
7	95.8	2.8	1.4	
9	86.2	12.6	3.7	IP
10	84.1	12.3	3.6	
12	64.8	27.6	8.2	
17	49.7	31.6	17.2	
24	42.1	42.2	17.3	
42	36.3	45.3	20.4	
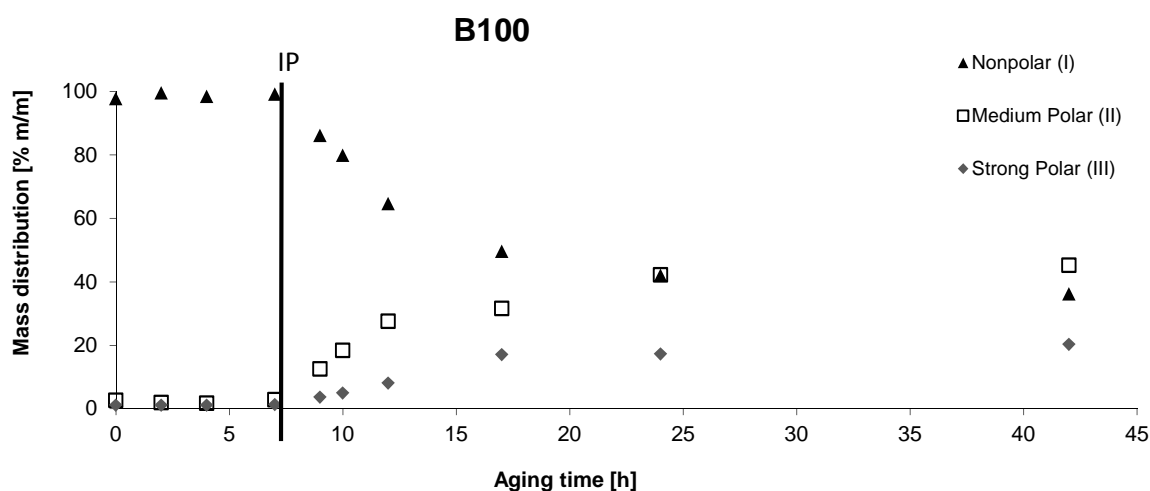
Figure 21: Column chromatography of time resolved biodiesel aging

Before reaching the IP of biodiesel at 8 hours, the content of nonpolar and polar compounds was constant and almost the whole sample consists of the nonpolar fatty acid methyl esters. After reaching the IP of biodiesel at 8 hours, Figure 21 shows the decreasing amount of the nonpolar and the increasing amount of the two polar fractions. First, the slope of the aging process is high and gets

lower by the length of the aging time. The sample which was in the Rancimat device for 42 hours has a content of 65% of medium or strong polar compounds. GC-MS analyses show the presence of epoxides, alcohols, aldehydes and ketones in these polar fractions.

4.3.2 Aging of B50 Biodiesel

The formation of polar aging products during the aging of B50 biodiesel out of rape seed oil is shown in Table 5 and Figure 22.

Table 5: Polar content of aged B50 biodiesel

B50	Nonpolar (I)	Medium Polar (II)	Strong Polar (III)	
Aging time [h]	[% m/m]	[% m/m]	[% m/m]	
0	94.2	1.6	0.5	
3	99.5	1.6	0.7	
6	98.8	1.8	0.9	
10	88.4	11.1	1.5	IP
12	90.0	7.4	3.1	
16	75.4	19.8	6.7	
24	54.4	33.2	12.8	
50	41.9	51.1	7.3	
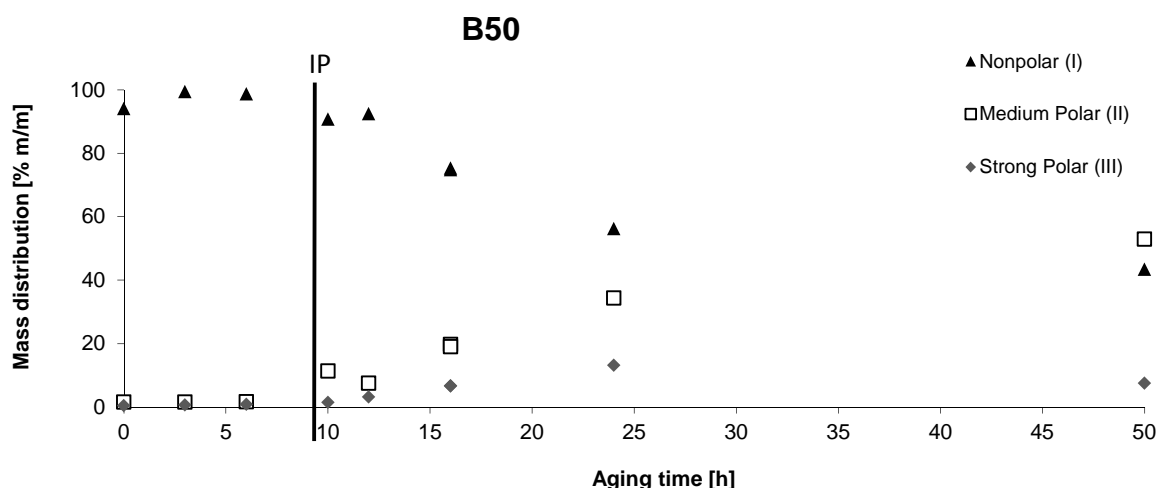
Figure 22: Column chromatography of time resolved B50 biodiesel/petrodiesel blend aging

As shown for the aging of B100, the amounts of polar compounds in the B50 blend increase after reaching the IP of 9.5 hours. The lower slope after this point indicates that the formation of polar aging products is slower compared to the B100 samples. The unaged sample (0 hours) sums up to just 96%, the missing 4% of the sample were volatiles and were removed with the solvent in the rotavapor. During the aging with the Rancimat device these volatile molecules were blown out of the system and were not inserted in the column.

An amount of 58% of polar compounds was formed after an aging time of 50 hours. This is almost as high as the polar content in B100 biodiesel with an amount of 65% polar compounds in total. The prolonged aging time and the continuous oxygen supply leads to this high polar content. Previous work shows, that some molecules in the petrodiesel can also get oxidized and form polar cyclo-aromatic systems like tetralin-1-ol or tetralon [81].

4.3.3 Aging of B7 Biodiesel

The polar content of B7 biodiesel aged different long is shown in Figure 23 and Table 6. The separation of the polar compounds was performed by column chromatography.

Table 6: Polar content of aged B7 biodiesel

B7	Nonpolar (I)	Medium Polar (II)	Strong Polar (III)	
Aging time [h]	[% m/m]	[% m/m]	[% m/m]	
0	95.1	0.3	0.4	
24	98.2	0.4	0.3	
29	96.9	2.3	1.0	
31	95.6	4.7	1.0	IP
34	95.8	4.0	1.1	
42	88.9	10.1	3.1	
51	84.3	13.4	3.9	
97	78.5	17.1	5.4	
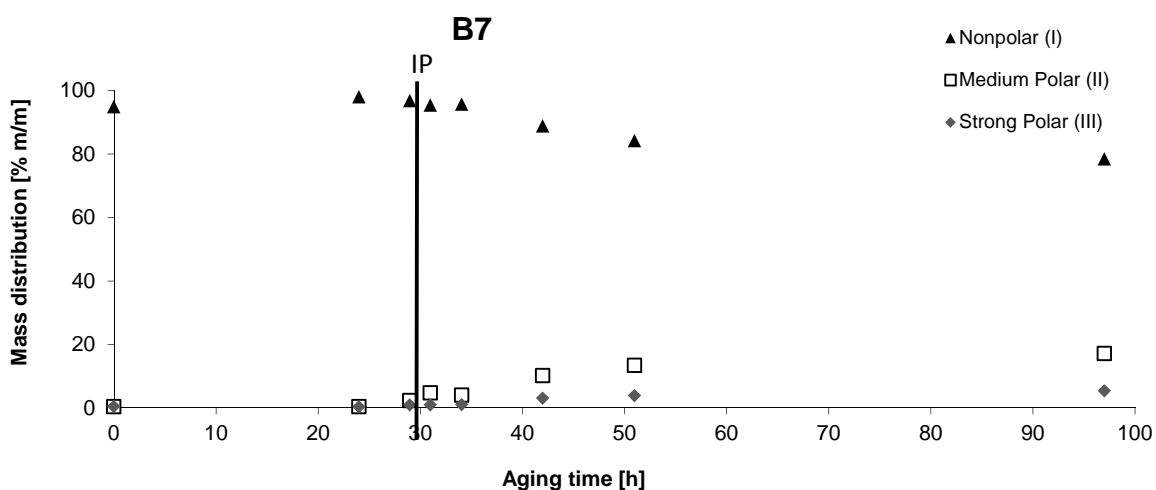
Figure 23: Column chromatography of time resolved B7 biodiesel/petrodiesel blend aging

Because of the high content of petrodiesel in the B7 blend, the slope of the increasing polar compounds which is formed during aging is much lower than in B100 biodiesel or B50 biodiesel blend. The petrodiesel in the blend gives a higher IP and also the aging reaction occurs slower. After an aging procedure of 97 hours, the B7 biodiesel blend contains in total 22% polar products.

4.4 High Performance Liquid Chromatography (HPLC)

Both polar fractions of a B100 biodiesel which was aged for 17 hours in the Rancimat device (3.2.4) were analyzed by HPLC (3.7.4). This analysis should show the polarity trend of the polar fractions and also the quality of the column chromatography separation.
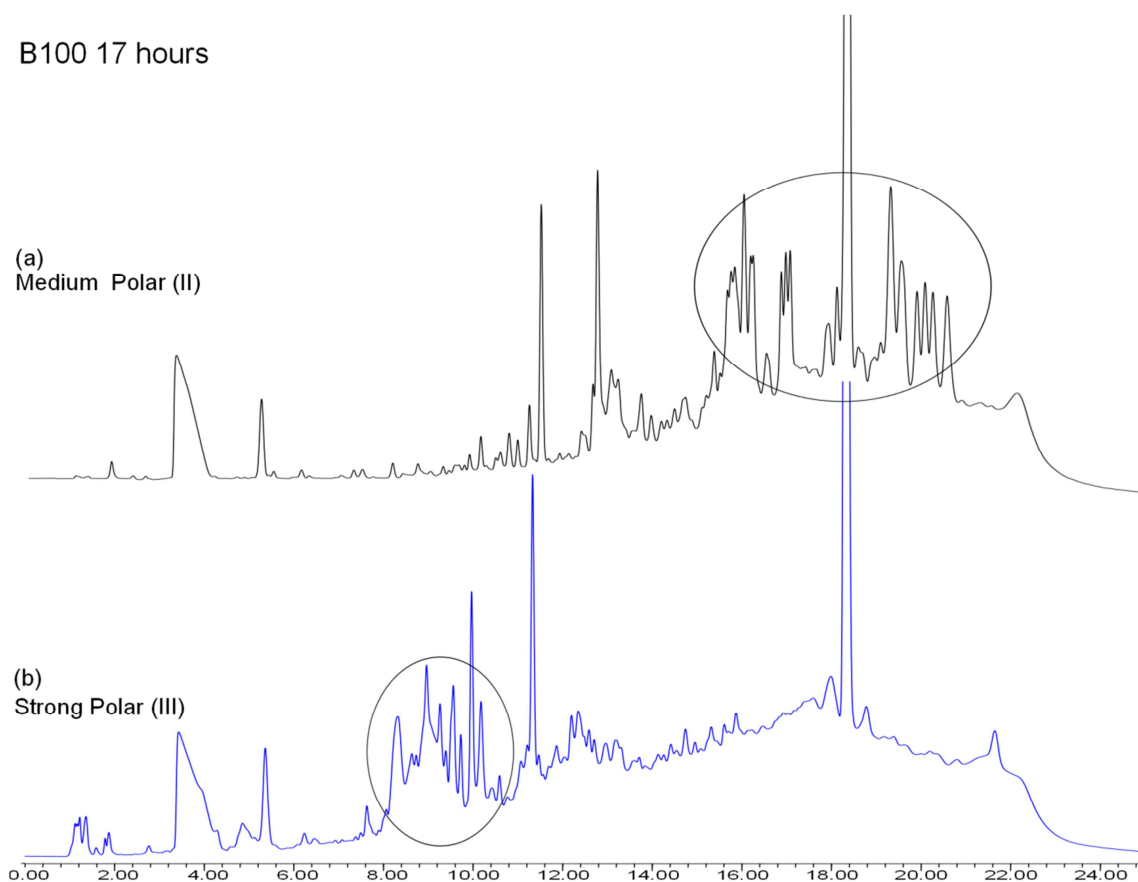
Figure 24: HPLC-analysis of the polar fractions of a B100 aged for 17 hours in the Rancimat device

The HPLC-analysis of an aged B100 biodiesel is shown in Figure 24. Several different aging products are formed during the aging reaction in the Rancimat device and a lot of peaks occur in the chromatograms.

A nonpolar C18-HPLC-column separates the aging products according to their polarity. The polarity of the analyzed molecules is decreasing with higher retention times. This can be shown in Figure 24, where the marked aging products in the medium polar fraction (a) occur at higher retention times than in the strong polar fraction. The aging products found in the strong polar fraction (b) have a lower retention time. Some peaks, especially in the retention time region of 12-16 minutes between the marked aging products, can be found in both fractions. The column chromatography was not efficient enough for the separation of all the aging products in one of the fractions. But because of consistently performing the same method, the results for the column chromatography are reproducible and should not influence further analyses.

The detector was a UV-VIS spectrometer, which gives no further information of the analyzed aging products. A further identification of the aging products was not possible in this case. The use of a mass spectrometer with an APC or ES ionization as detector could produce more information of the aging products.

35

4.5 Size-Exclusion-Chromatography

The content of the aged and fractionated biodiesel samples was analyzed by size exclusion chromatography (3.7.2). The peak areas divided by the sum of all areas give the mass fraction of this peak. The higher the retention times, the smaller is the molecular weight.

For an example, Figure 25 shows a typical size exclusion chromatogram of the strong polar fraction of B100 biodiesel aged for 10 hours in the Rancimat device.
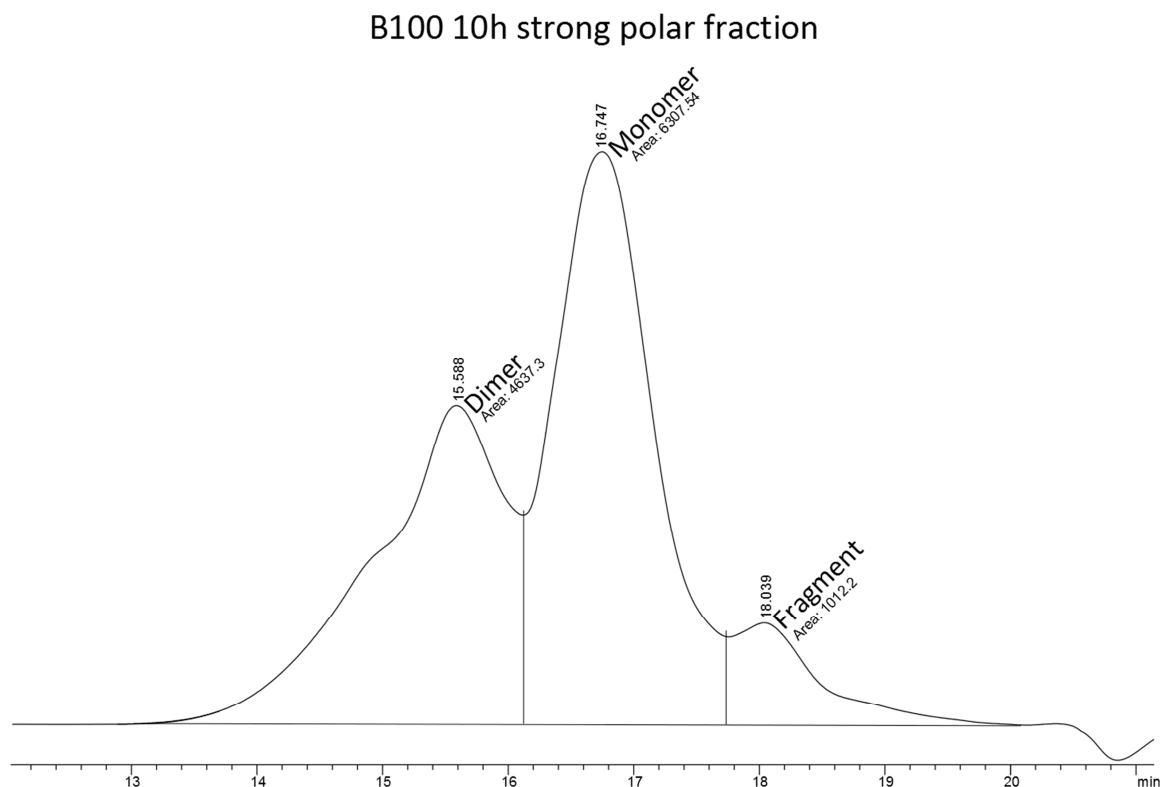
Figure 25: Example SEC-analysis of the strong polar fraction of a B100 biodiesel aged for 10 hours in the Rancimat device

The peak at a retention time of 15.6 minutes in Figure 25 represents the dimeric content. Further peaks are, with a retention time of 16.7 minutes, the monomeric content and with 18.0 minutes the amount of fragments. In this example of the strong polar fraction the dimeric content was 39%, the monomeric content 52% and the fragmental content was 8% of the sample. A shoulder at the dimeric peak (approx. 15 minutes) can be observed at higher aging time. This shoulder suggests the existence of some molecules with a higher mass, probably between a dimer and trimer, what is also shown in further analysis.

4.5.1 SEC-analysis of B100 Biodiesel

The B100 biodiesel were aged for different times in a Rancimat device and fractionated by the use of column chromatography. A SEC analysis shows the mass distribution of the samples.

Table 7: SEC-analysis of the nonpolar fraction of aged B100 biodiesel

Aging time [h]	Nonpolar Fraction (I)		
	Monomer [%]	Dimer [%]	Fragment [%]
0	96.1	1.6	2.2
2	95.0	1.7	3.3
4	95.6	1.7	2.7
7	95.9	1.9	2.2
9	95.1	1.9	3.0
10	95.1	2.4	2.5
12	94.3	3.2	2.5
17	97.0	0.7	2.4
24	93.6	1.4	3.2
42	71.5	27.5	1.0
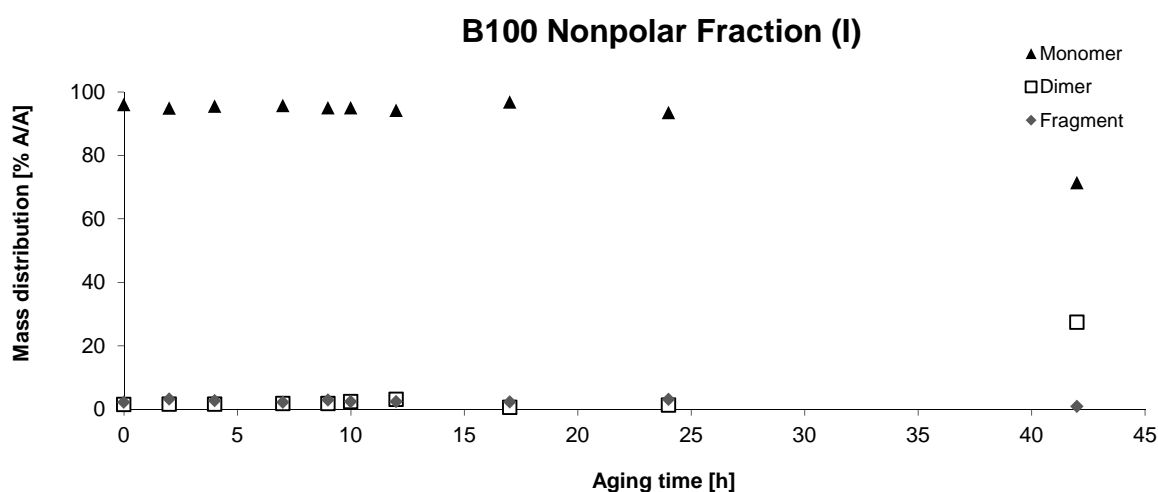
Figure 26: Time resolved SEC-analysis of the nonpolar fraction of aged B100 biodiesel

The content of the nonpolar fraction during the aging does not change significantly. Almost all samples were in the region of monomer. Just after a long aging time of 42 hours, the dimeric content increased to 25% in this fraction.

Table 8: SEC-analysis of the medium polar fraction of aged B100 biodiesel

Aging time [h]	Medium Polar Fraction (II)		
	Monomer [%]	Dimer [%]	Fragment [%]
0	77.6	8.4	8.9
2	78.9	13.6	6.1
4	82.2	11.0	6.8
7	75.4	19.8	4.9
9	56.0	36.8	7.2
10	63.7	27.1	6.7
12	60.4	19.1	9.8
17	59.3	31.3	5.1
24	36.8	50.6	12.6
42	20.5	64.1	15.4
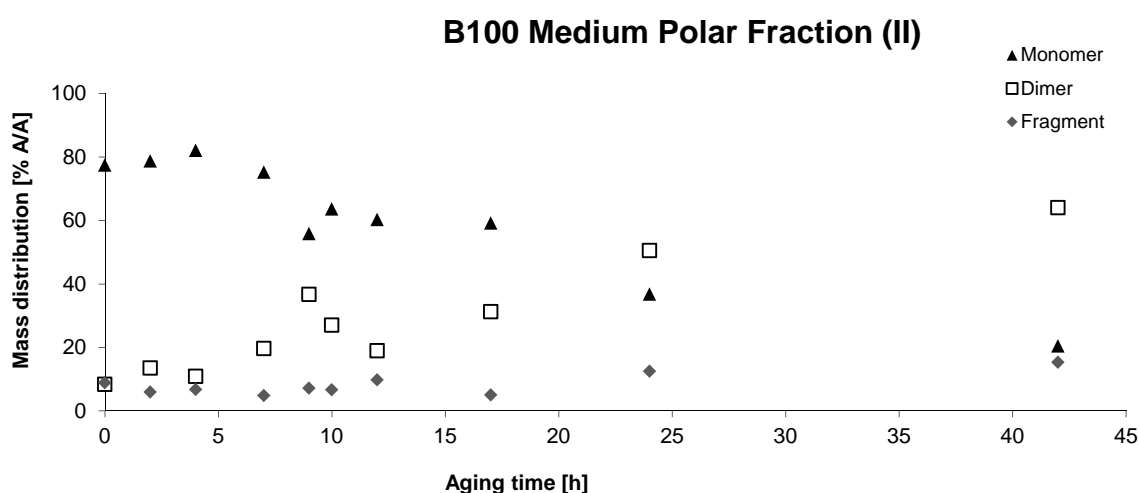
Figure 27: Time resolved SEC-analysis of the medium polar fraction of aged B100 biodiesel

Differently to the nonpolar fraction, the medium polar fraction shows a big increase of the dimer content and also fragments of the fatty acid methyl esters were produced after reaching the IP. The polar monomer content is decreasing during the whole aging process. Therefore, the dimers are probably produced out of these oxidized monomers.

Table 9: SEC-analysis of the strong polar fraction of aged B100 biodiesel

Aging time [h]	Strong Polar Fraction (III)		
	Monomer [%]	Dimer [%]	Fragment [%]
0	95.5	1.3	3.1
2	85.8	7.0	7.2
4	78.0	12.7	7.4
7	72.0	21.0	5.2
9	65.2	23.9	7.0
10	52.8	38.8	8.5
12	41.9	46.1	12.0
17	38.2	48.5	13.3
24	26.6	66.8	6.6
42	13.1	77.4	9.5
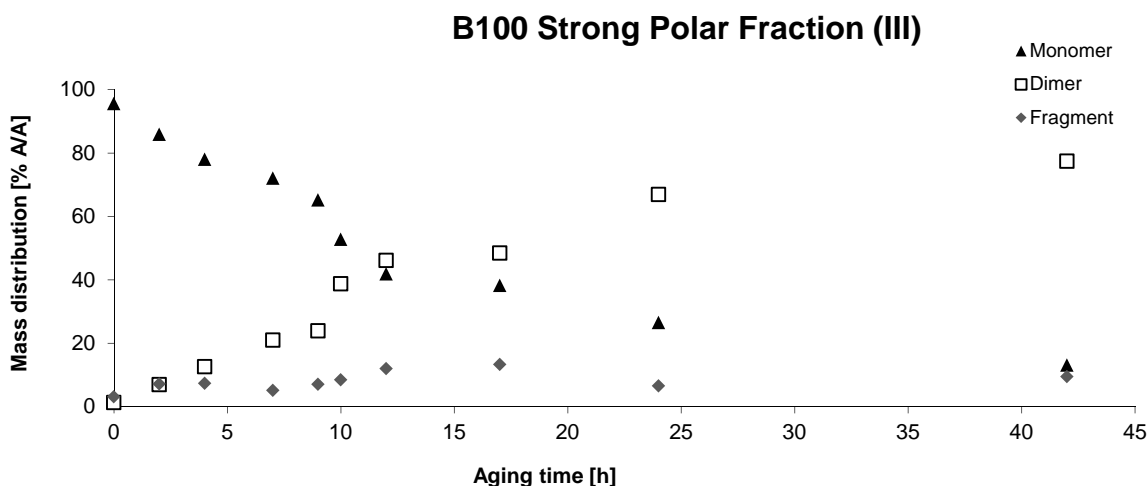
Figure 28: Time resolved SEC-analysis of the strong polar fraction of aged B100 biodiesel

The content of dimers and also fragments increases immediately when the B100 gets aged and not after reaching the IP like in the other fractions. The decreasing polar monomer content might show that these polar monomers are dimerizing or breaking to fragments.

4.5.2   SEC-analysis of B50 Biodiesel blend

Also the B50 biodiesel blend was aged in a Rancimat device. The aging was stopped at certain aging intervals and the samples were chromatographed in three different fractions. The SEC analyses of these samples give the mass distribution of the fraction.

Table 10: SEC-analysis of the nonpolar fraction of aged B50 biodiesel

Aging time [h]	Nonpolar Fraction (I)		
	Monomer [%]	Dimer [%]	Fragment and Petrodiesel[%]
0	58.9	0.8	33.7
3	65.3	1.2	33.5
6	63.7	0.8	33.5
10	60.4	0.9	38.7
12	59.0	0.7	40.3
16	58.6	0.6	40.8
24	67.7	0.3	32.0
50	50.4	6.4	43.3

B50 Nonpolar Fraction (I)
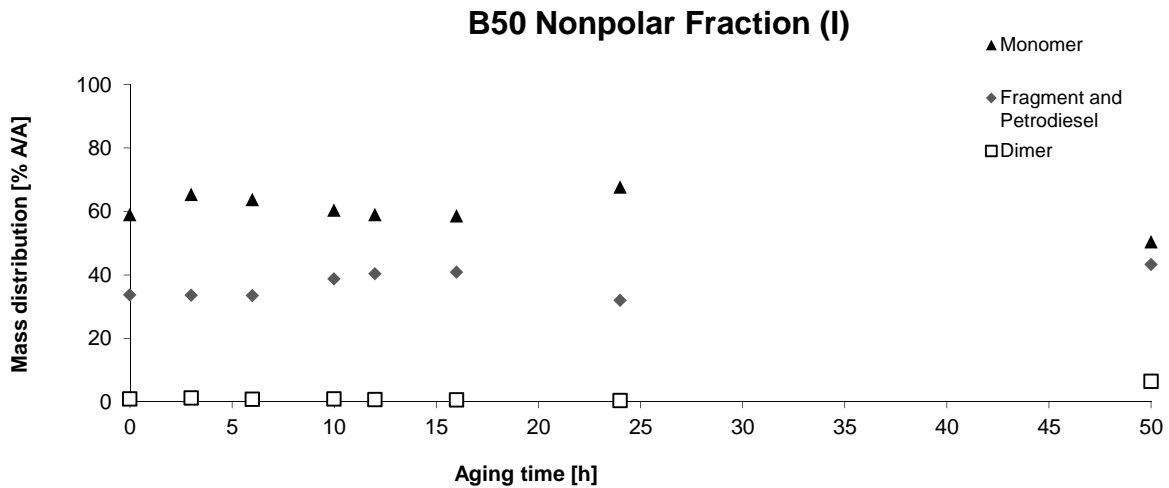
Figure 29: Time resolved SEC-analysis of the nonpolar fraction of aged B50 biodiesel

The aging of the nonpolar fraction of B50 biodiesel shows similar results to the aging of the nonpolar fraction of B100. The content of this fraction versus aging time is quite constant and no significant change occurs. Because of the petrodiesel in the mixture the integration of the peaks was difficult (shown in Figure 30). The petrodiesel gives, because it is composed of molecules with a broad molecular mass range, a broad peak over a long time which also overlays with the monomer peak and has the same retention time as the fragments, which explains the inconsistent results. There is no significant dimeric content in the nonpolar faction until 24 hours of aging, but after a longer aging time the dimeric content was about 6%. The amount of the "fragment and petrodiesel" content was about 35% instead of the expected 50% in the un-aged B50 blend. Peak overlapping (Figure 30) leads to this lower amount.
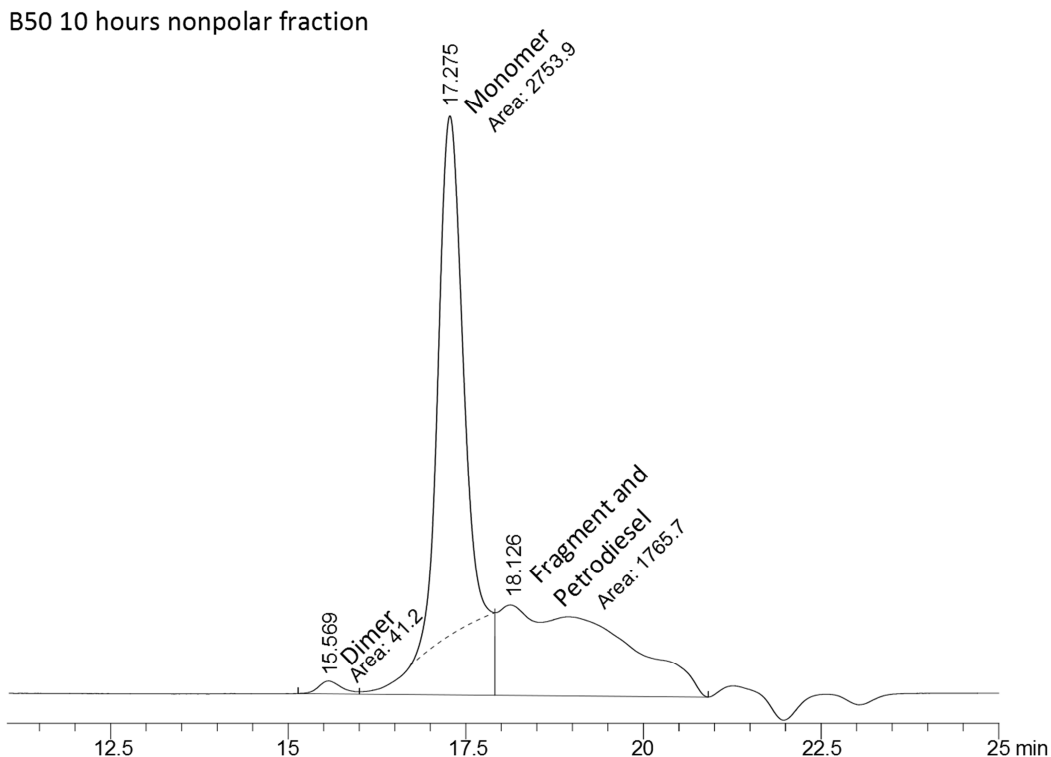
Figure 30: Example of a size exclusion chromatogram of the nonpolar fraction of B50 biodiesel aged for 10 hours

40

Figure 30 shows the nonpolar fraction of a B50 biodiesel aged for 10 hours in the Rancimat device. The broad "fragment and petrodiesel" peak (estimated 16.5-21 minutes) overlays with the monomer peak (17.3 minutes). The overlapping part of the "fragment and petrodiesel" peak has the same molecular mass as the monomeric content.

Table 11: SEC-analysis of the medium polar fraction of aged B50 biodiesel

Aging time [h]	Medium Polar Fraction (II)		
	Monomer [%]	Dimer [%]	Fragment [%]
0	87.9	1.1	4.9
3	60.0	12.9	16.7
6	71.0	13.3	12.5
10	83.8	1.0	3.5
12	58.9	32.7	7.1
16	53.3	25.5	21.2
24	46.1	29.5	23.6
50	23.3	54.5	22.2
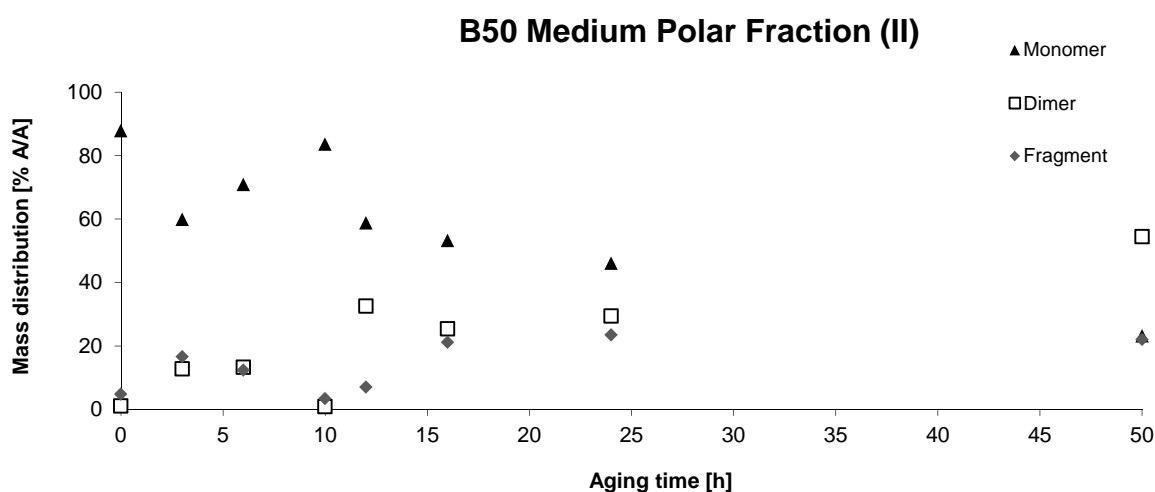
Figure 31: Time resolved SEC-analysis of the medium polar fraction of aged B50 biodiesel

The SEC-results of the medium polar fraction after the aging of B50 shows a fluctuating composition. The amount of this fraction with an aging time less than 10 hours is, with 1.6% of the whole sample, very low. Therefore, errors like peak overlapping or inaccurate integration have a bigger influence to the results. The IP of B50 determined with the Rancimat method is about 10 hours and here the drop of the monomer content and the increasing of the dimer and also the fragment content becomes visible. After an aging time of 50 hours a dimeric content of more than 50% occurs.

Table 12: SEC-analysis of the strong polar fraction of aged B50 biodiesel

Aging time [h]	Strong Polar Fraction (III)		
	Monomer [%]	Dimer [%]	Fragment [%]
0	75.9	8.5	11.8
3	66.6	5.3	21.2
6	69.9	10.6	15.9
10	69.4	19.4	9.5
12	55.2	30.9	12.5
16	38.6	42.7	18.7
24	25.8	53.3	20.9
50	22.0	66.9	11.0
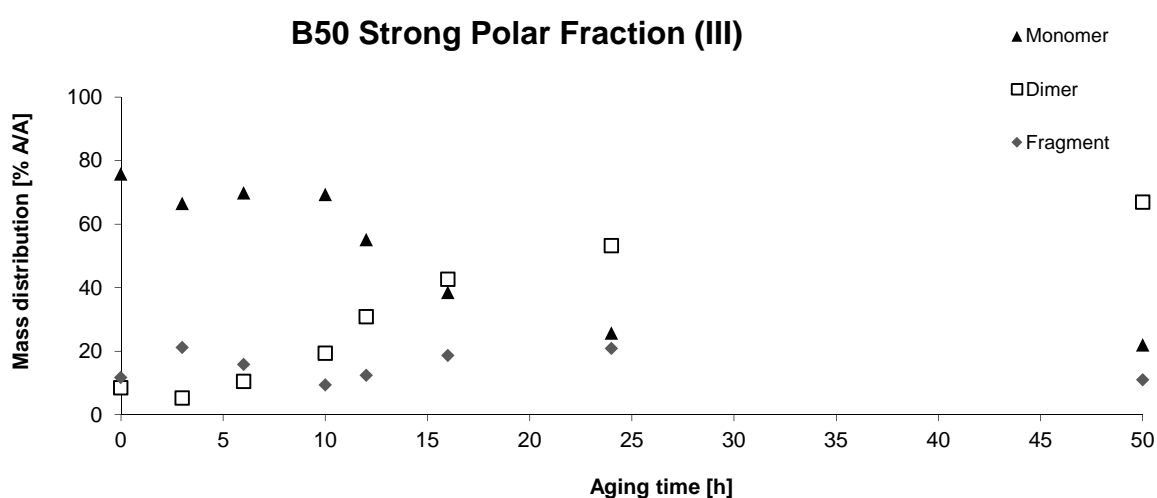
Figure 32: Time resolved SEC-analysis of the strong polar fraction of aged B50 biodiesel

The un-aged (0 hours) strong polar fraction of B50 biodiesel blend consists 75% of polar monomers. During the aging the monomeric content starts to decrease after reaching the IP while the content of dimers is increasing. The fragment content shows an unclear trend.

4.5.3   SEC-analysis of B7 Biodiesel
The different polar fractions of the aged B7 samples were analyzed by SEC.

Table 13: SEC-analysis of the nonpolar fraction of aged B7 biodiesel

Aging time [h]	Nonpolar Fraction (I)		
	Monomer [%]	Dimer [%]	Fragment and Petrodiesel [%]
0	22.7	0.3	77.1
24	24.3	0.2	75.5
29	23.8	0.2	76.0
31	24.3	0.2	75.5
34	23.1	0.2	76.8
42	25.9	n.d.	74.1
51	26.0	n.d.	74.0
97	31.8	n.d.	68.2
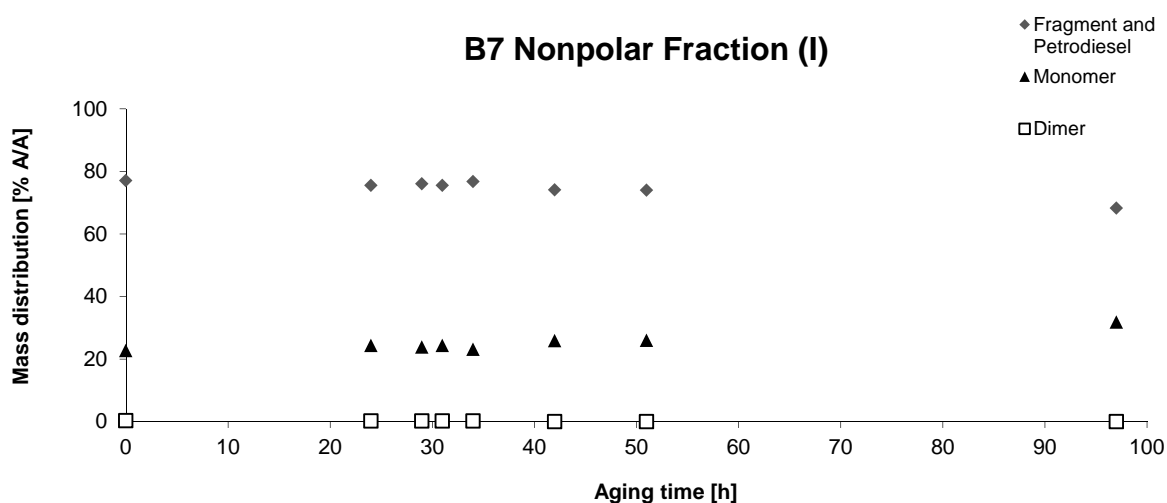
Figure 33: Time resolved SEC-analysis of the nonpolar fraction of aged B7 biodiesel

The SEC-analyses of the nonpolar fraction show constant results during the aging of B7 Biodiesel. The amount of 20% monomers instead of the expected 7% is a result of peak overlapping (discussed in Figure 30 for B50 biodiesel). Furthermore, different response factors of the petrodiesel and biodiesel for the refraction index detector can also lead to this higher monomeric content.

No dimers could be found in the nonpolar fraction, even after a prolonged aging time. Therefore, the aging process of B7 produces only polar dimers. The petrodiesel gives wide peaks with a high retention time and overlay the peaks of formed fragments (see Figure 30 for B50). A separation of the fragment peaks and the wide petrodiesel peak without manipulating the result is not possible.

Table 14: SEC-analysis of the medium polar fraction of aged B7 biodiesel

Aging time [h]	Medium Polar Fraction (II)		
	Monomer [%]	Dimer [%]	Fragment [%]
0	58.0	26.2	9.9
24	49.2	11.7	37.2
29	39.6	9.7	50.4
31	38.4	9.1	52.2
34	33.1	9.9	56.7
42	30.3	16.6	53.0
51	28.5	21.7	49.6
97	21.0	35.1	43.9
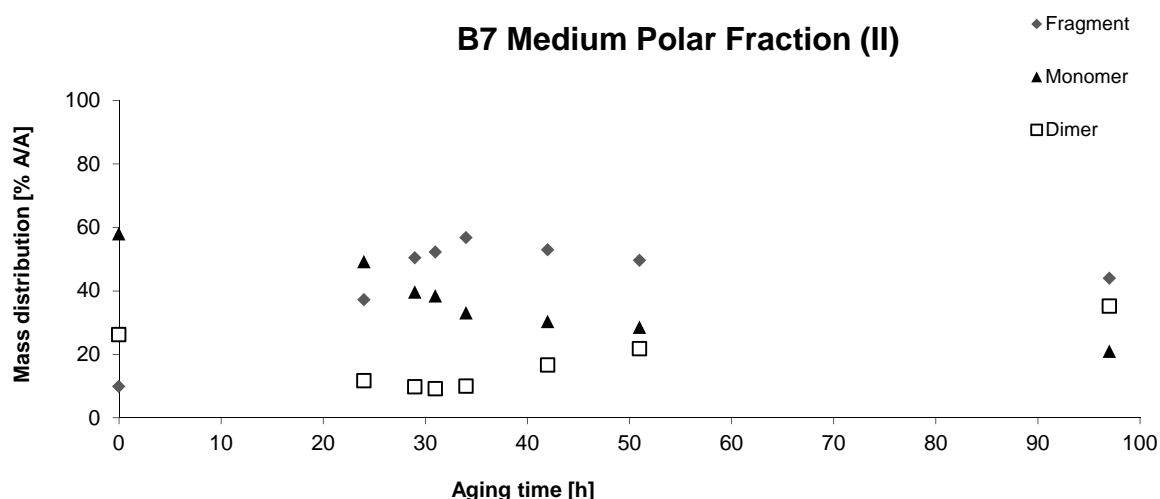
Figure 34: Time resolved SEC-analysis of the medium polar fraction of aged B7 biodiesel

In the chromatogram of the un-aged sample (0 hours) a peak occurs at shorter retention time than the dimer peak. This peak represents 6% of the sample. Because of the shorter retention time the molecules of this peak must have a bigger size than a dimer. These molecules could be trimers or dimers with an attached fragment what give a higher mass. After an aging procedure of 24 hours, this peak reflects just 1% of all areas and with longer aging time this peak disappears from the chromatograms. By aging, polar monomers, dimers and fragments occur in a higher amount or maybe these big molecules break down to smaller molecules. The increase of the fragments might come from the fragmentation of the polar monomers, which are decreasing during the aging before reaching the IP, but also from the oxidation of the petrodiesel.

Table 15: SEC-analysis of the strong polar fraction of aged B7 biodiesel

Aging time [h]	Strong Polar Fraction (III)		
	Monomer [%]	Dimer [%]	Fragment [%]
0	n.d.	n.d.	n.d.
24	61.5	25.4	9.8
29	59.0	17.5	22.4
31	46.8	21.2	31.0
34	47.0	27.8	24.9
42	31.5	34.9	33.4
51	31.0	42.2	26.7
97	24.5	55.8	18.6
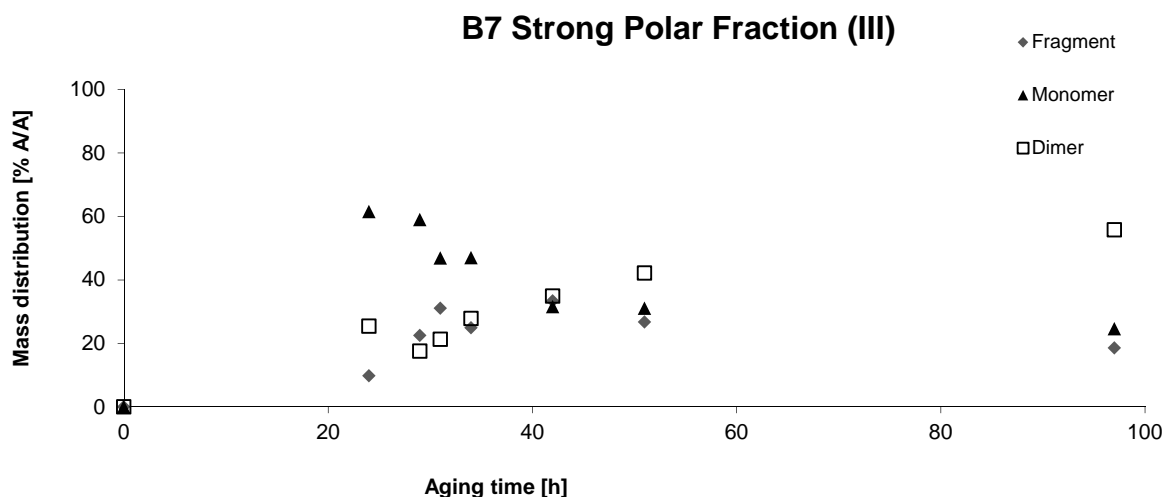
Figure 35: Time resolved SEC-analysis of the strong polar fraction of aged B7 biodiesel

The amount of the un-aged (0 hours) strong polar fraction was too small to create a SEC-chromatogram. During the aging of B7 biodiesel the strong polar fraction is produced in sufficient amount for the SEC analysis.

During the aging procedure the polar monomer content is decreasing. These polar molecules break up to fragments whose content is increasing. With a longer aging time the dimeric content is increasing up to 56%. These dimers might be formed from the reaction of polar monomers and their fractions.

4.6   Component Distribution of Biodiesel and –blends after aging

The combination of the content of polar compounds (column chromatography 4.3) and the results of the size exclusion chromatography (4.5) for all fractions give the absolute mass fraction of the components of the aged biodiesel in the samples.

4.6.1   Component Distribution of a B100 Sample during the Rancimat aging

The absolute amount of the aging products which are formed during the aging of B100 biodiesel is shown in the following tables and figures.

Table 16: Content analysis of the nonpolar fraction of aged B100 Biodiesel

Aging time [h]	Nonpolar Fraction (I)		
	Monomer [%]	Dimer [%]	Fragment [%]
0	94.1	1.6	2.2
2	94.7	1.7	3.3
4	94.2	1.7	2.7
7	95.2	1.9	2.2
9	82.0	1.6	2.6
10	76.1	1.9	2.0
12	61.1	2.1	1.6
17	48.2	0.3	1.2
24	39.5	0.6	1.4
42	25.9	10.0	0.4
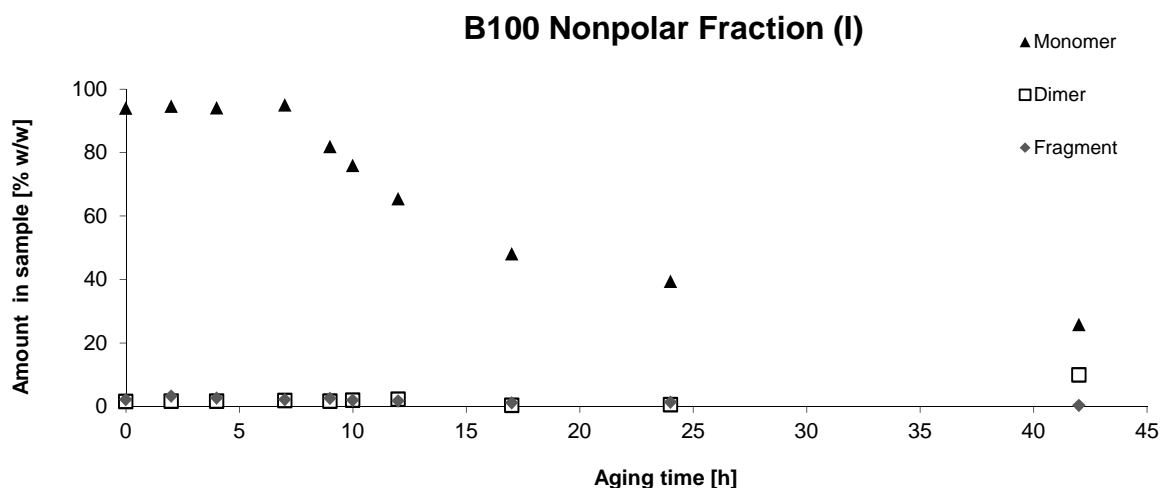
Figure 36: Time resolved analysis of the nonpolar fraction of aged B100

The Rancimat-IP of B100 was at 8 hours. After reaching the IP of B100 the monomeric content in the nonpolar fraction decreases, because the monomers in this fraction are oxidized and get a higher polarity. These oxidized products of the monomers can be found in the two polar fractions. After an aging time of 42 hours, nonpolar dimers were formed in an amount of 10% of the aged sample.

Table 17: Content analysis of the medium polar fraction of aged B100 Biodiesel

Aging time [h]	Medium Polar Fraction (II)		
	Monomer [%]	Dimer [%]	Fragment [%]
0	2.0	0.2	0.2
2	1.6	0.3	0.1
4	1.4	0.2	0.1
7	2.2	0.6	0.1
9	7.1	4.6	0.9
10	11.7	5.0	1.2
12	16.7	5.3	2.7
17	18.8	9.9	1.6
24	15.6	21.4	5.3
42	9.3	29.0	7.0
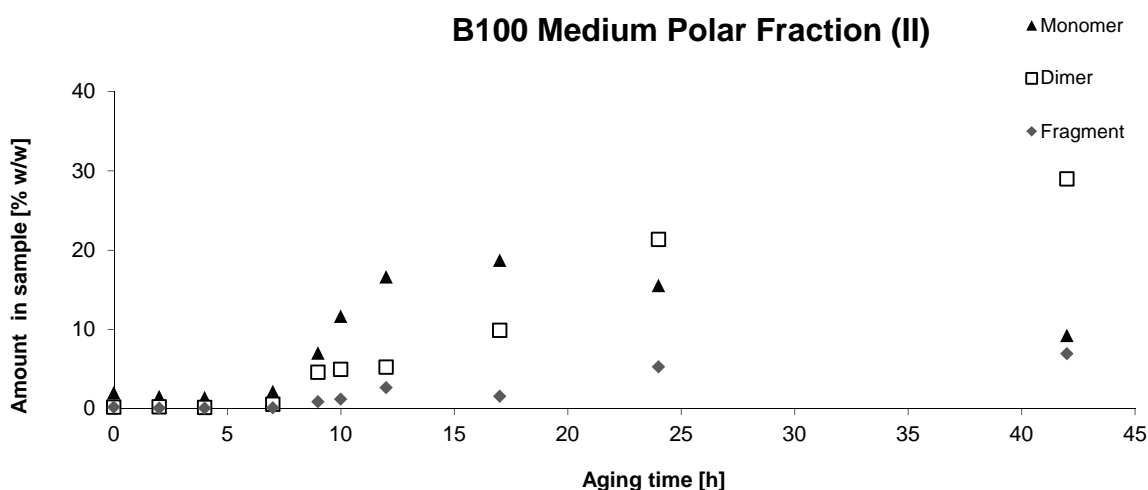
Figure 37: Time resolved analysis of the polar fraction of aged B100

First, after reaching the IP of B100 the amount of dimers, polar monomers and fragments is increasing. The monomers in the nonpolar fraction are getting oxidized and can be found in this polar fraction. At first, the content of polar monomers increases very fast, but after a longer aging time the polar monomers decrease and more dimers were formed out of these polar molecules. So the formation of dimers is obviously directly linked to the production of polar monomers. The amount of the dimers found in this polar fraction of the inserted sample is 29% after an aging time of 42 hours.

Table 18: Content analysis of the strong polar fraction of aged B100 Biodiesel

Aging time [h]	Strong Polar Fraction (III)		
	Monomer [%]	Dimer [%]	Fragment [%]
0	1.1	n.d.	n.d.
2	1.0	0.1	0.1
4	0.9	0.1	0.1
7	1.0	0.3	0.1
9	2.4	0.9	0.3
10	2.7	2.0	0.4
12	3.4	3.8	1.0
17	6.6	8.3	2.3
24	4.6	11.6	1.1
42	2.7	15.8	1.9
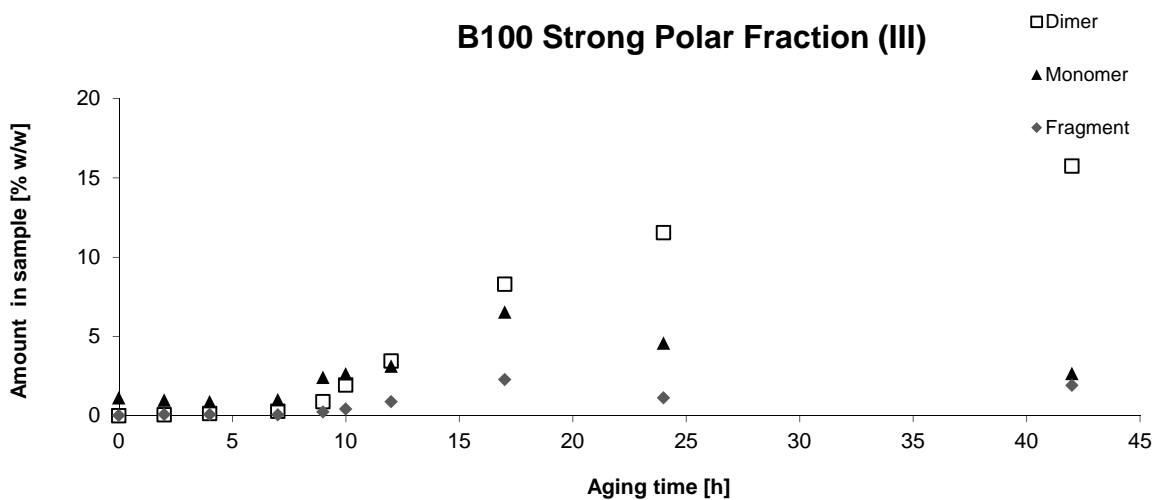
Figure 38: Time resolved analysis of the strong polar fraction of aged B100

Also, as the medium polar fraction of B100, the strong polar fraction shows an increase of the content of fragments, polar monomers and dimers after reaching the IP. Furthermore, the content of polar monomers is increasing first and then decreasing while the dimer content increases. The dimeric content in this fraction after the aging time of 42 hours is 16% of the starting sample.

The total dimeric content of B100 biodiesel after an aging time of 42 hours is 55% of the starting sample. This amount of dimers can explain the increasing viscosity during the aging.

4.6.2 Component Distribution of a B50 Sample during the Rancimat aging

Table 19: Content analysis of the nonpolar fraction of aged B50 Biodiesel

Aging time [h]	Nonpolar Fraction (I)		
	Monomer [%]	Dimer [%]	Fragment and Petrodiesel [%]
0	55.5	0.8	31.7
3	65.0	1.2	33.4
6	62.9	0.8	33.1
10	54.9	0.8	35.2
12	54.6	0.7	37.3
16	43.9	0.4	30.6
24	38.1	0.2	18.0
50	21.9	2.8	18.8
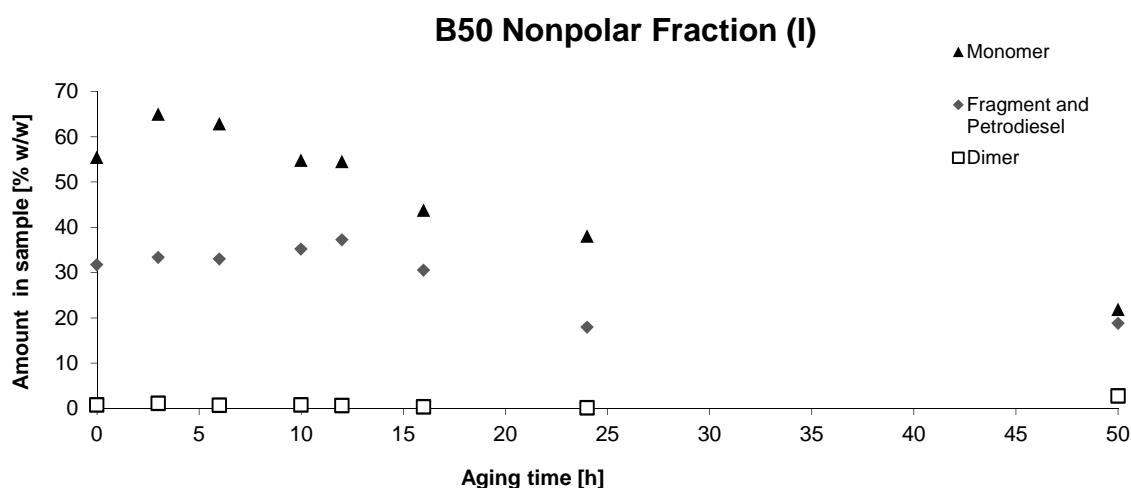
Figure 39: Time resolved analysis of the nonpolar fraction of aged B50

The amount of monomers in the B50 biodiesel blend is constantly decreasing during the aging process. It starts with an amount of 65% monomeric content after 3 hours in the Rancimat device and falls to an amount of 22% after an aging time of 50 hours. These monomers are getting oxidized and can be found in the polar fractions. Also the fragment and petrodiesel content is decreasing but not as strong as the monomeric content. Just a small amount of dimers (3%) can be found in the nonpolar fraction after an aging time of 50 hours.

Table 20: Content analysis of the medium polar fraction of aged B50 Biodiesel

Aging time [h]	Medium Polar Fraction (II)		
	Monomer [%]	Dimer [%]	Fragment [%]
0	1.4	n.d.	0.1
3	1.0	0.2	0.3
6	1.3	0.2	0.2
10	9.6	0.1	0.4
12	4.5	2.5	0.5
16	10.2	4.9	4.1
24	15.9	10.2	8.1
50	12.3	28.9	11.8
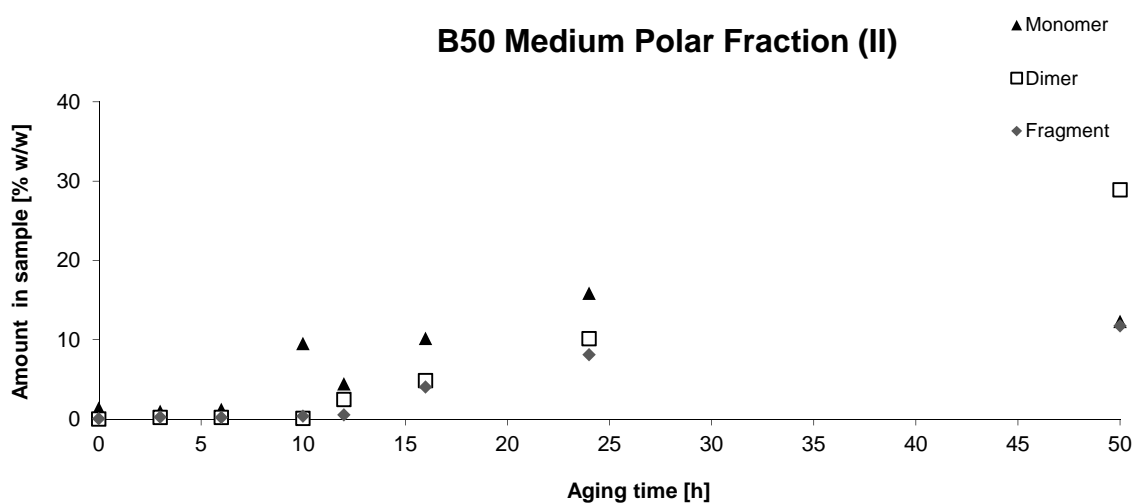
Figure 40: Time resolved analysis of the medium polar fraction of aged B50

After reaching the IP of B50 biodiesel, the content of polar monomers, fragments and dimers start to increase. Like the aging of B100 Biodiesel (Figure 37) the polar fraction shows that the polar monomer content is higher than the content of dimers first, but after higher aging times these polar monomers are dimerizing or fragmenting. The dimeric content after 50 hours was 30% of the total sample.

Table 21: Content analysis of the strong polar fraction of aged B50 Biodiesel

Aging time [h]	Strong Polar Fraction (III)		
	Monomer [%]	Dimer [%]	Fragment [%]
0	0.4	n.d.	0.1
3	0.5	n.d.	0.1
6	0.6	0.1	0.1
10	1.0	0.3	0.1
12	1.8	1.0	0.4
16	2.6	2.9	1.3
24	3.4	7.1	2.8
50	1.7	5.1	0.8
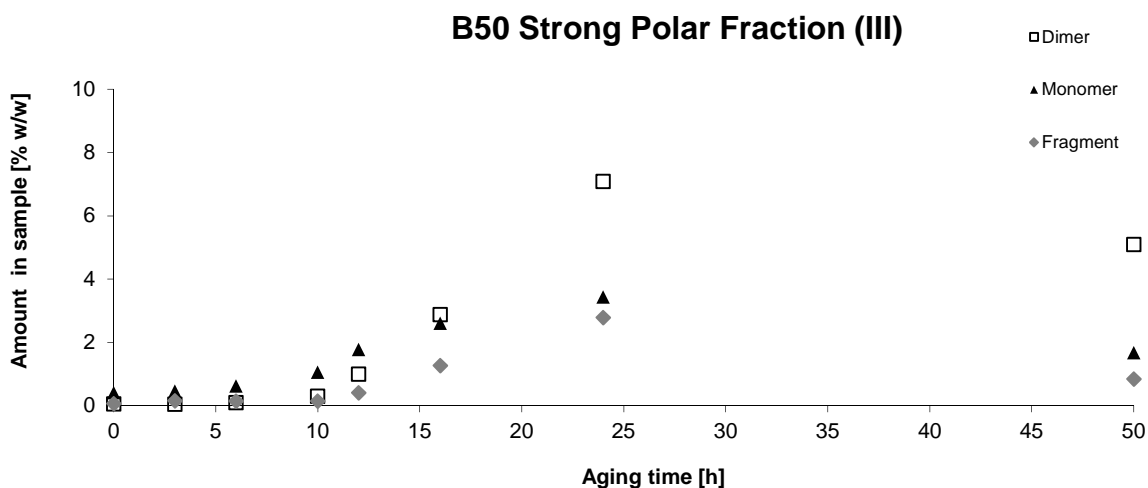
Figure 41: Time resolved analysis of the strong polar fraction of aged B50

The oxidation process of the strong polar fraction of B50 biodiesel shows an increase of the polar content after reaching the IP, like the medium polar fraction (Figure 40). The strong polar fraction of B50 is in a much lower concentration than the medium polar fraction (Figure 22 and Table 5). The strong polar dimeric content reached a maximum of 7% of the B50 sample at 24 hours of aging.

The dimeric content in total is 38% of the starting B50 biodiesel-blend sample after an aging time of 50 hours.

4.6.3   Component Distribution of a B7 Sample during the Rancimat aging

Table 22: Content analysis of the nonpolar fraction of aged B7 Biodiesel

Aging time [h]	Nonpolar Fraction (I)		
	Monomer [%]	Dimer [%]	Fragment and Petrodiesel [%]
0	21.5	0.3	73.3
24	23.9	0.2	74.2
29	23.1	0.2	73.6
31	23.2	0.2	72.1
34	22.1	0.1	73.5
42	23.0	n.d.	65.9
51	21.9	n.d.	62.4
97	26.8	n.d.	57.5
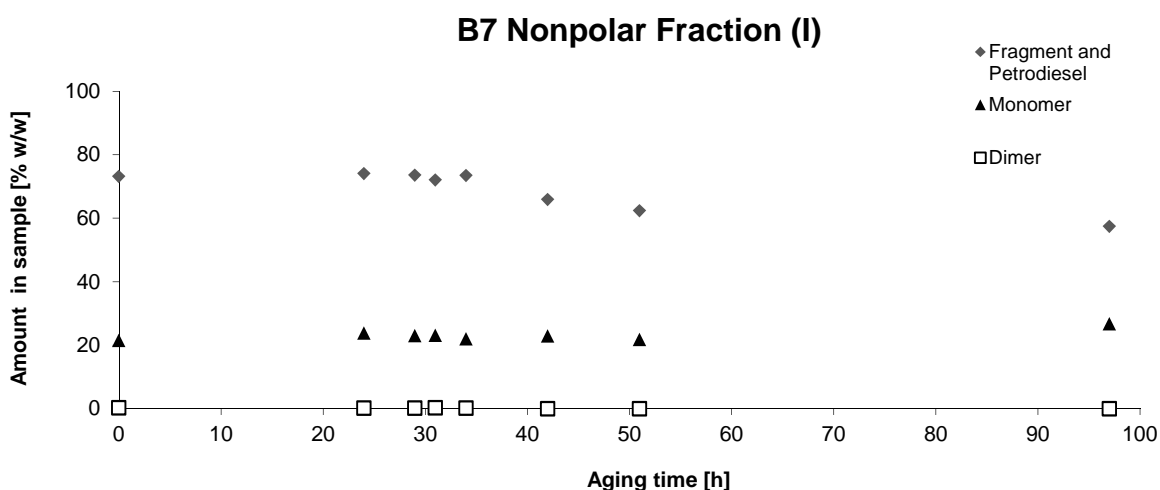
Figure 42: Time resolved analysis of the nonpolar fraction of aged B7

Because of the high content of petrodiesel in the blend, the amount of compounds in the nonpolar fraction during the aging stays nearly unchanged.

Table 23: Content analysis of the medium polar fraction of aged B7 Biodiesel

Aging time [h]	Medium Polar Fraction (II)		
	Monomer [%]	Dimer [%]	Fragment [%]
0	0.2	0.1	n.d.
24	0.2	n.d.	0.1
29	0.9	0.2	1.2
31	1.8	0.4	2.4
34	1.3	0.4	2.3
42	3.1	1.7	5.4
51	3.8	2.9	6.6
97	3.6	6.0	7.5
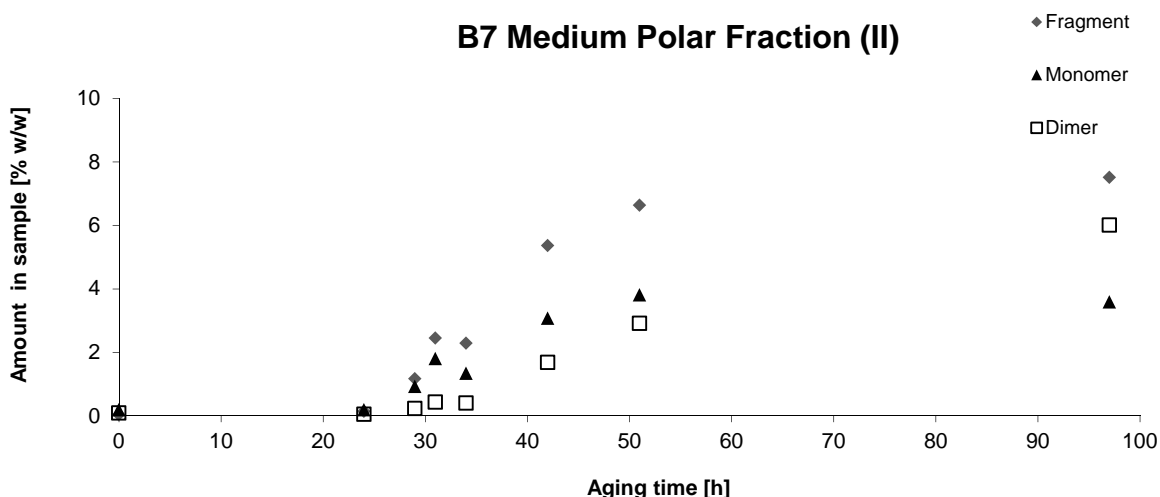
Figure 43: Time resolved analysis of the medium polar fraction of aged B7

Like in the aging of B100 and B50 biodiesel, the content of polar monomers, dimers and fragments starts to increase after reaching the IP. In the beginning the polar monomeric content is higher than the dimer content and just after the aging time of 97 hours the dimeric content was, with 6% of the total sample, higher. But on the contrary to the others, the highest amount was the polar fragment content. These molecules originate from splitting the monomers and by oxidizing some of the petrodiesel substances. Because of the high petrodiesel content in the blend the amounts of the polar aging products are smaller than in the B100 biodiesel.

Table 24: Content analysis of the strong polar fraction of aged B7 Biodiesel

Aging time [h]	Strong Polar Fraction (III)		
	Monomer [%]	Dimer [%]	Fragment [%]
0	n.d.	n.d.	n.d.
24	0.2	0.1	n.d.
29	0.6	0.2	0.2
31	0.5	0.2	0.3
34	0.5	0.3	0.3
42	1.0	1.1	1.0
51	1.2	1.6	1.0
97	1.3	3.0	1.0

B7 Strong Polar Fraction (III)

◆ Fragmente
▲ Monomere
□ Dimer

(Y-axis: Amount in sample [% w/w], 0 to 4; X-axis: Aging time [h], 0 to 100)
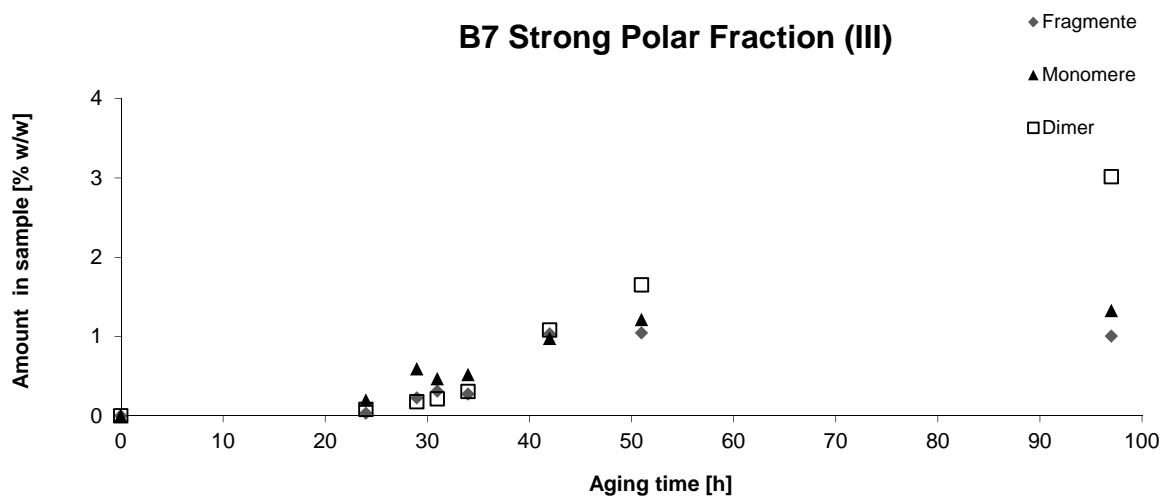
Figure 44: Time resolved analysis of the strong polar fraction of aged B7

The amount of the strong polar content formed during the aging of B7 Biodiesel is very low because of the blending ratio (Figure 23 and Table 6). The dimeric content was about 3% of the whole sample in the strong polar fraction after the aging time of 97 hours.

4.7 Identification of aging Products

The identification of oxidized products during the aging of Biofuel was performed by high resolution time of flight mass spectrometry with gas chromatography (GC-TOF-MS) and matrix associated laser desorption/ionization (MALDI-TOF-MS).

For an easier identification, oleic acid methyl ester was investigated instead of B100 biodiesel. Oleic acid methyl ester is the major component of B100 biodiesel derived from rape seed oil (50-70%). Also, oleic acid methyl ester is, because of its double bond, more sensitive towards oxidation than saturated fatty acid methyl esters. Linoleic acid methyl ester, which also occurs in a relatively high amount in rape seed oil biodiesel (15-30%), on the other hand has, because of the two double bonds, a higher possibility for the forming of isomer aging products [30]. These multitudes of isomers are causing peak overlapping and a more difficult identification of the aging products.

4.7.1 GC-TOF-MS

The identification of products formed during the accelerated aging of oleic acid methyl ester was performed with an Agilent GC-TOF-MS. These measurements were done by Prof. Saf at the Graz University of Technology, Institute for Chemistry and Technology of Materials.

The analyzed samples were the three fractions of oleic acid methyl ester which has been aged for 21 hours in the Rancimat device. This aged methyl ester was separated by column chromatography in a nonpolar, medium polar, and strong polar fraction (3.7.1).

The data analysis was performed with the MassLynx 4.1 software. The identification of the substances was done by comparison of the mass spectra and the Wiley database, reference substances or literature.

The results for the analysis of the aged linoleic acid methyl ester were more complex with more overlapping peaks. Furthermore, many identical molecules could be identified compared to the analyzed aged oleic acid methyl ester, especially in the fragmental mass region.
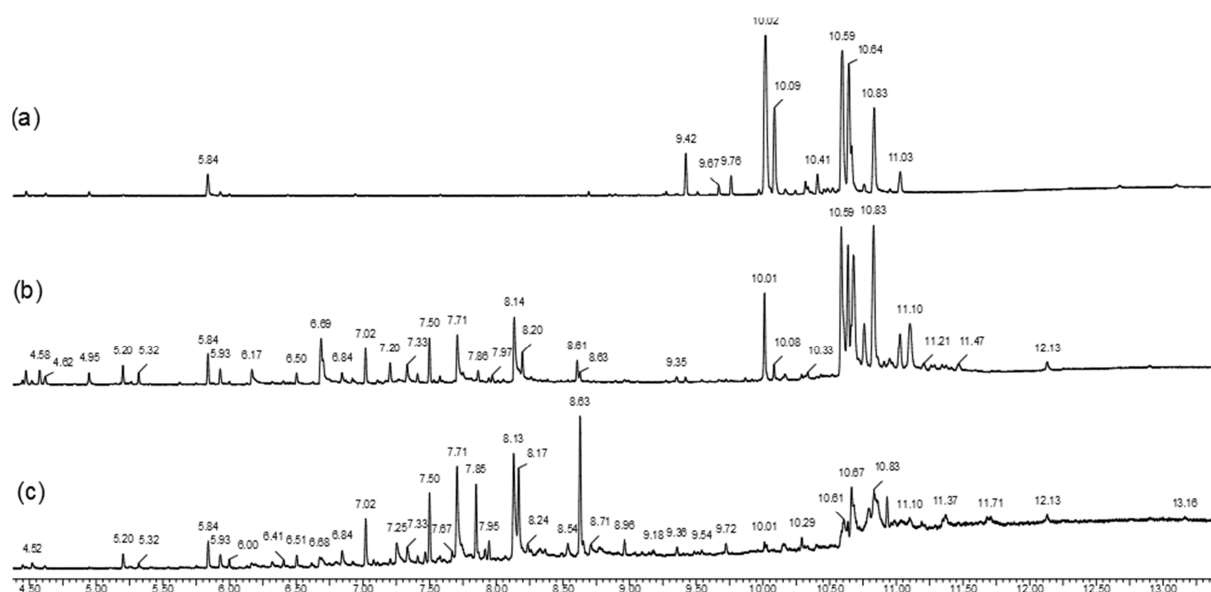
Figure 45: Gas chromatogram of oleic acid methyl ester aged for 21 hours, (a) nonpolar fraction, (b) medium polar fraction and (c) strong polar fraction

Formed fragments could be identified in the medium and strong polar but not in the nonpolar fraction (Figure 45). This correlates to the results of the SEC-analysis of the aged B100 sample (Figure 36 -Figure 38). Here, also both of the polar fractions contain fragments after the aging with the Rancimat, while the nonpolar fraction shows no fragmental content. Some peaks occur in more than one of the fractions. This is a result of inaccurate separation of the column chromatography and is also shown in the HPLC analysis (4.4).

4.7.1.1   Nonpolar fraction of oleic acid methyl ester aged for 21 hours

The following figures show the gas chromatogram of the nonpolar fraction of oleic acid methyl ester, which was aged for 21 hours in the Rancimat device and fractionated by column chromatography. In the following, the identified molecules are summarized in Table 25 - Table 32.
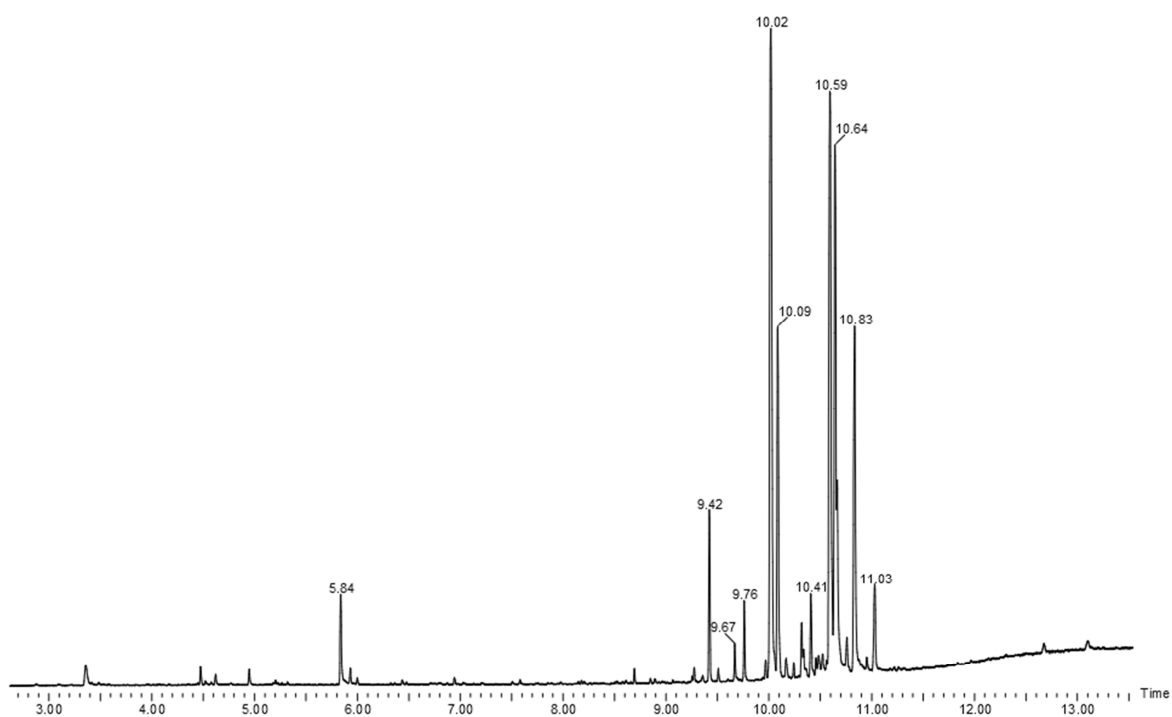
Figure 46: Gas chromatogram of the nonpolar fraction of oleic acid methyl ester aged for 21 hours (3-13 min)
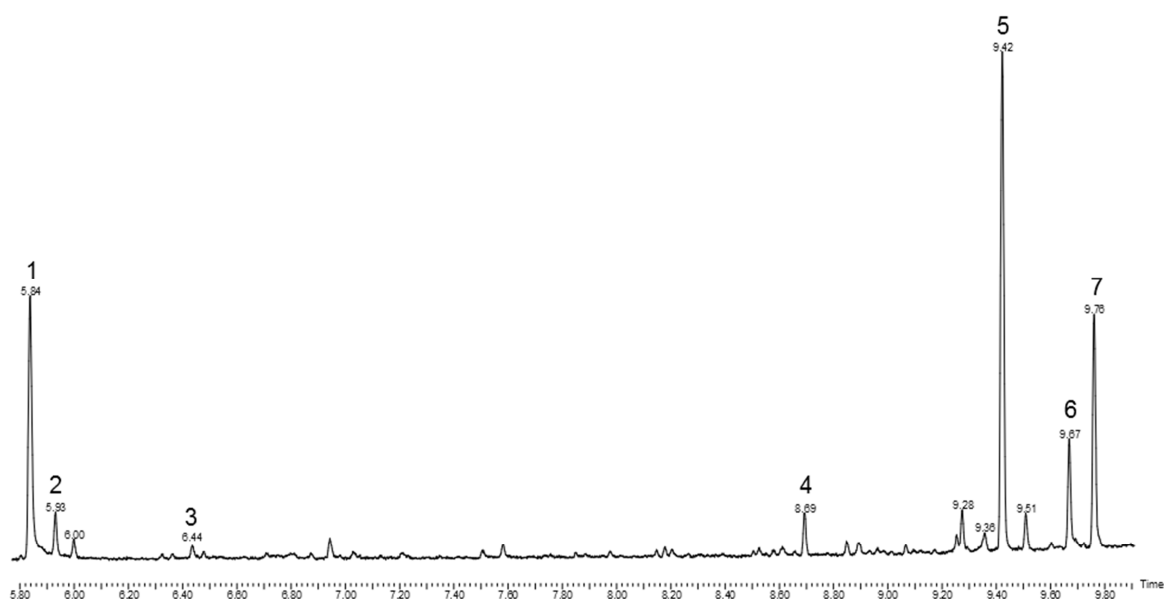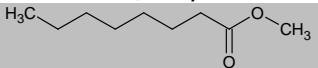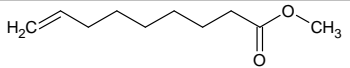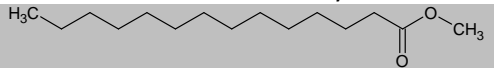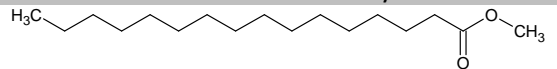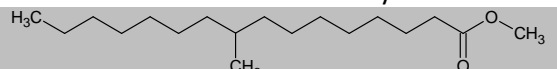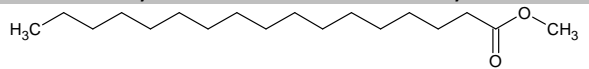
Figure 47: Gas chromatogram of the nonpolar fraction of oleic acid methyl ester aged for 21 hours (5-10 min)

Table 25: Identified peaks of the chromatogram in Figure 47

No.	Retention time [min]	Estimated Structure	Chemical Formula	Mass
1	5.838	Not identified (occurs in all fractions, maybe solvent impurity)		
2	5.931	octanoic acid methyl ester	$C_9H_{18}O_2$	158.1
3	6.435	8-nonenoic acid methyl ester	$C_{10}H_{18}O_2$	170.2
4	8.693	tetradecanoic acid methyl ester	$C_{15}H_{30}O_2$	242.2
5	9.422	hexadecanoic acid methyl ester	$C_{17}H_{34}O_2$	270.5
6	9.669	9-methyl hexadecanoic acid methyl ester	$C_{18}H_{36}O_2$	284.5
7	9.761	heptadecanoic acid methyl ester	$C_{18}H_{36}O_2$	284.5

Table 26: Difference of the analyzed molecular ions to the calculated molecular masses of the peaks found in the chromatogram in Figure 47 and the characteristic mass fragments of the peak with their relative abundance

No.	Retention time [min]	Chemical Formula	Molecular Mass		Difference		Characteristic Mass in Spectra
			Found	Calculated	Abs [mDa]	ppm	
1	5.838	Not identified	No molecular ion observable				84.0351 (100); 129.0730 (60); 57.0557 (45)
2	5.931	$C_9H_{18}O_2$	158.1305	158.1307	-0.2	-1.3	74.0357 (100); 71.0490 (85); 87.0446 (40)
3	6.435	$C_{10}H_{18}O_2$	No molecular ion observable				74.0368 (100); 69.0695 (37); 87.0454 (35); 138.1057 (25)
4	8.693	$C_{15}H_{30}O_2$	242.2262	242.2246	1.6	6.6	74.0359 (100); 87.0442 (64); 143.1078 (20)
5	9.422	$C_{17}H_{34}O_2$	270.2583	270.2559	2.4	8.9	74.0263 (100); 87.0356 (87); 143.1051 (32); 270.2540 (25)
6	9.669	$C_{18}H_{36}O_2$	284.2723	284.2715	0.8	2.8	74.0353 (100); 87.0437 (62); 143.1074 (18); 284.2725 (17)
7	9.761	$C_{18}H_{36}O_2$	284.2743	284.2715	2.8	9.8	74.0311 (100); 87.0411 (70); 143.1071 (18); 284.2719 (16)

Table 25 and Table 26 show the substances found in the nonpolar fraction of an oleic acid methyl ester sample aged for 21 hours. While Table 25 shows the structure of the molecule, Table 26 gives the difference of the measured mass peak to the calculated mass peak. The smaller this difference is, the better the probability of the estimation of the chemical formula and so the structure is. A difference of 5-10 ppm should be acceptable for the identification of the aging molecules. Higher differences can occur because of an oversaturation of the detector, when the analyte is too highly concentrated and the mass accuracy deteriorates. A completely wrong estimated chemical formula also has a big difference.

Different methyl esters with chain lengths from 8 to 17 carbon atoms occur in the first 5-10 minutes of the chromatogram of the nonpolar fraction of aged oleic acid methyl ester (Figure 47).

The not identified molecule no.1 occurs with the same retention time in all fractions (no. 6 in the medium and no. 1 in the strong polar fraction), so maybe this molecule is a solvent impurity. But in the polar fractions the fragmentation pattern is completely different and this molecule in the polar fractions could be identified as nonanal.
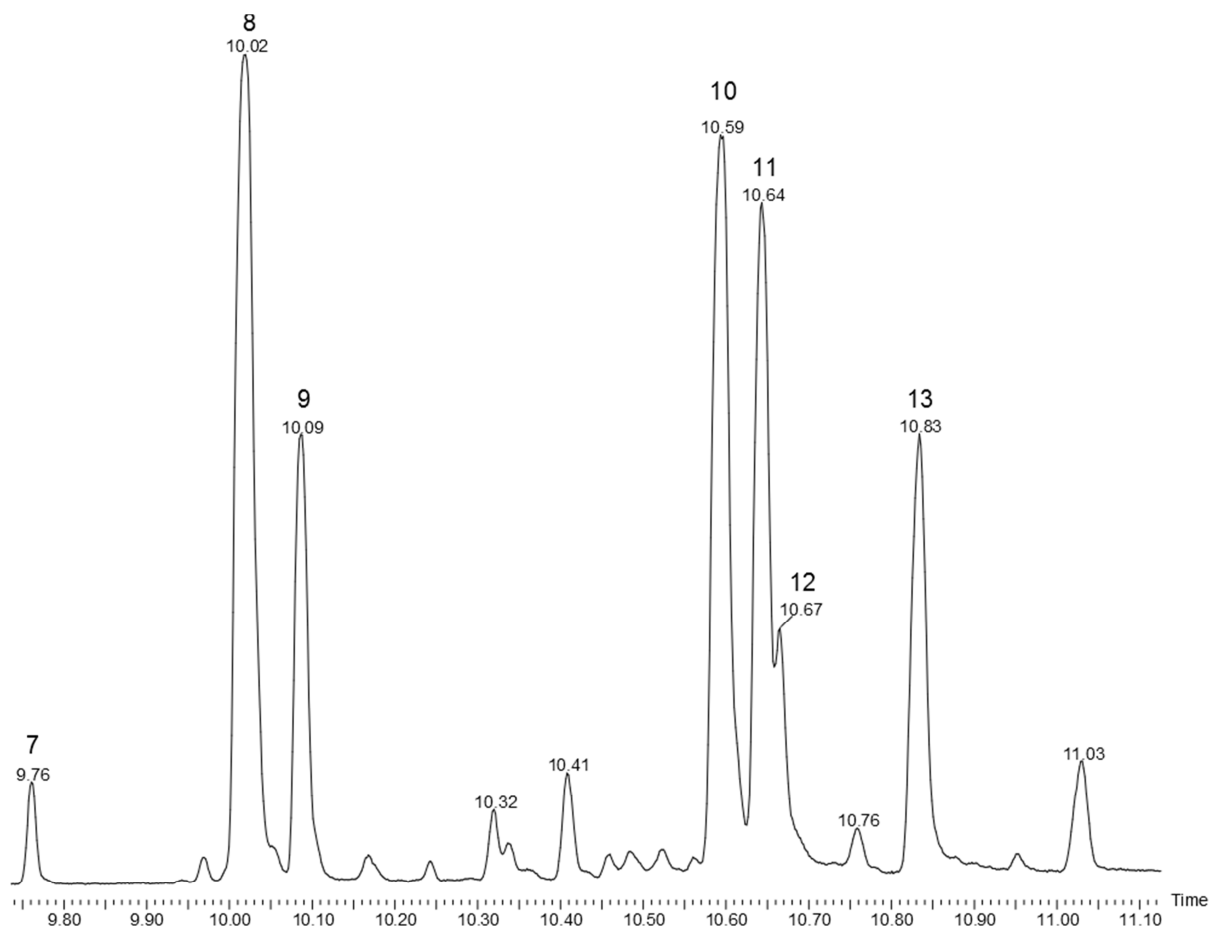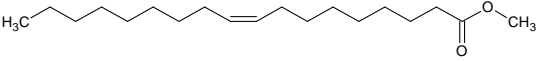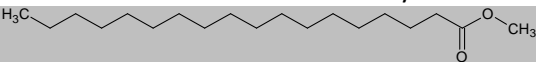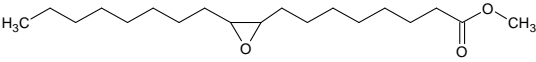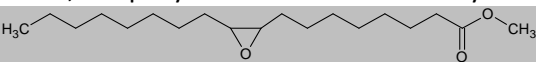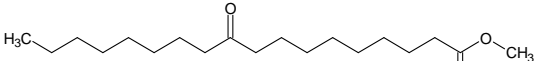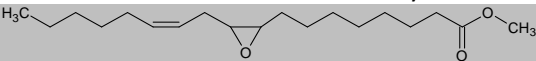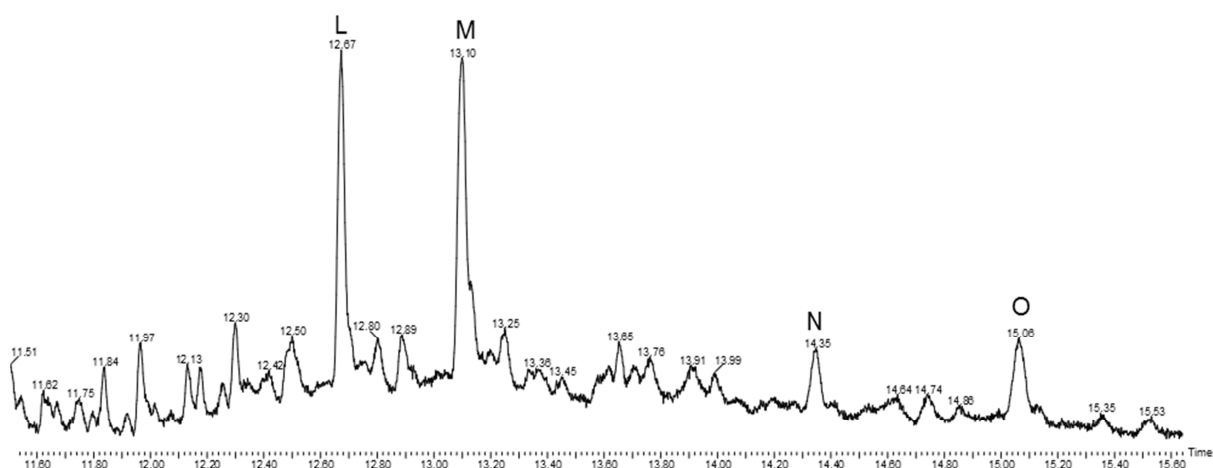
Figure 48: Gas chromatogram of the nonpolar fraction of oleic acid methyl ester aged for 21 hours (10-11 min)

Table 27: Identified peaks of the chromatogram in Figure 48

No.	Retention time [min]	Estimated Structure	Chemical Formula	Mass
8	10.019	cis-9-octadecenoic acid methyl ester	$C_{19}H_{36}O_2$	296.3
9	10.086	octadecanoic acid methyl ester	$C_{19}H_{38}O_2$	298.3
10	10.593	trans-9,10-epoxyoctadecanoic acid methyl ester	$C_{19}H_{36}O_3$	312.3
11	10.643	cis-9,10-epoxyoctadecanoic acid methyl ester	$C_{19}H_{36}O_3$	312.3
12	10.665	10-oxooctadecanoic acid methyl ester	$C_{19}H_{36}O_3$	312.3
13	10.834	9,10-epoxy-12-octadecenoic acid methyl ester	$C_{19}H_{34}O_3$	310.3

Table 28: Difference of the analyzed molecular ions to the calculated molecular masses of the peaks found in the chromatogram in Figure 48 and the characteristic mass fragments of the peak with rel. abundance

No.	Retention time [min]	Chemical Formula	Molecular Mass		Difference		Characteristic Mass in spectra
			Found	Calculated	Abs [mDa]	ppm	
8	10.019	$C_{19}H_{36}O_2$	296.2736	296.2715	2.1	7.1	69.0678 (100); 264.251 (65); 55.0551 (65); 84.0564 (55)
9	10.086	$C_{19}H_{38}O_2$	298.2867	298.2872	-0.5	-1.7	74.0319 (100); 87.0411 (75); 69.0690 (32); 143.1066 (20)
10	10.593	$C_{19}H_{36}O_3$	No molecular ion observable				74.0285 (100); 155.0983 (91); 87.0392 (65); 67.0501 (58)
11	10.643	$C_{19}H_{36}O_3$	No molecular ion observable				155.0948 (100); 74.0261 (95); 87.0375 (75); 69.0620 (70)
12	10.665	$C_{19}H_{36}O_3$	312.2718	312.2664	5.4	17.3	125.0950 (100); 156.1467 (75); 58.0421 (74); 281.2489 (29)
13	10.834	$C_{19}H_{34}O_3$	310.2522	310.2508	1.4	4.5	153.1171 (100); 97.0589 (95); 167.1335 (90); 55.0159 (85)

Different methyl esters are identified in the chromatogram (Figure 48) with a retention time of 10-11 minutes. Here, the educt oleic acid methyl ester and also stearic acid methyl ester can be found. Also oxidized species like epoxides and ketones could be found in high amounts in this fraction.
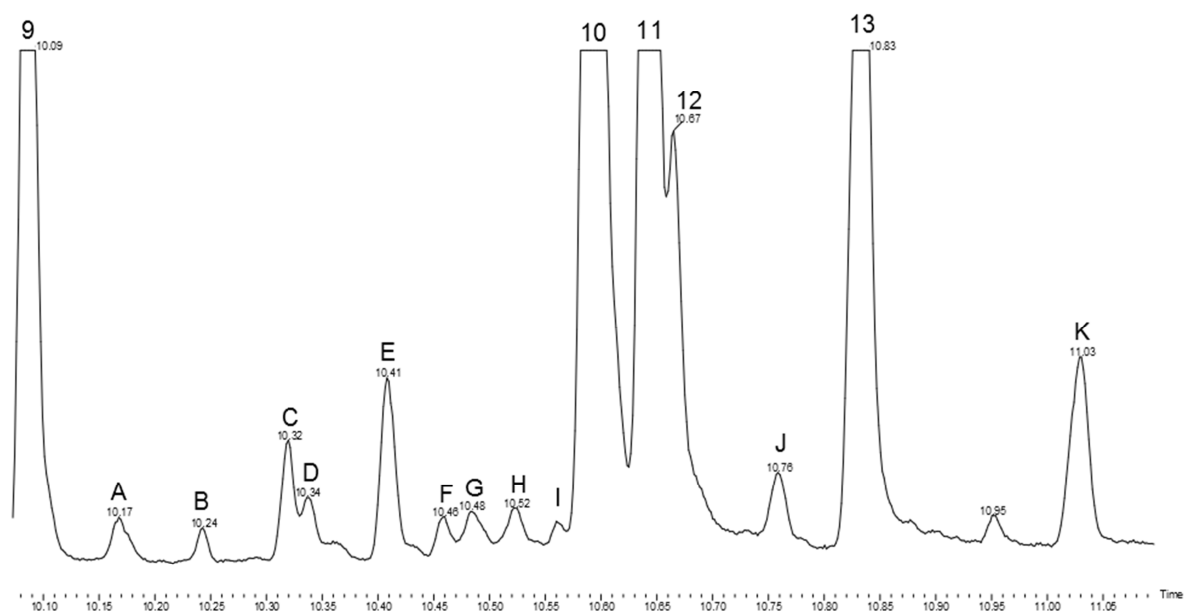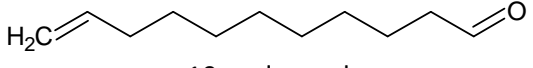
Figure 49: Gas chromatogram of the nonpolar fraction of oleic acid methyl ester aged for 21 hours (10-11 min)

Figure 49 shows the zoomed chromatogram of the nonpolar fraction of oleic acid methyl ester which was aged for 21 hours with a retention time of 10-11 minutes.

Table 29: Identified peaks of the chromatogram in Figure 49
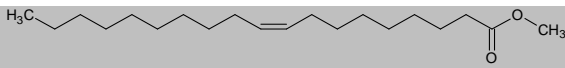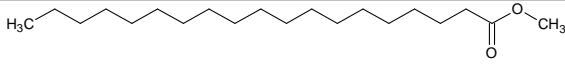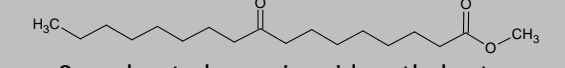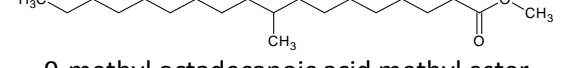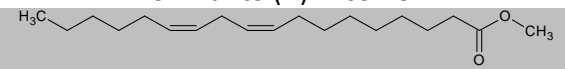
No.	Retention time [min]	Estimated Structure	Chemical Formula	Mass
A	10.168	Not identified	$C_{19}H_{32}O_3$	308
B	10.243	9-nonadecenoic acid methyl ester	$C_{20}H_{38}O_2$	310
C	10.320	nonadecanoic acid methyl ester	$C_{20}H_{40}O_2$	312
D	10.336	9-oxoheptadecanoic acid methyl ester	$C_{18}H_{34}O_3$	298
E	10.408	9-methyl octadecanoic acid methyl ester	$C_{20}H_{40}O_2$	312
F	10.460	Not identified	$C_{19}H_{34}O_3$	310
G	10.483	Similar to (F) ->isomer	$C_{19}H_{34}O_3$	310
H	10.523	Not identified	$C_{19}H_{34}O_3$	310
I	10.560	Similar to (H) ->isomer	$C_{19}H_{34}O_3$	310
J	10.759	9,12-octadecadienoic acid methyl ester	$C_{19}H_{34}O_2$	294
K	11.031	Not identified	$C_{19}H_{34}O_4$	326

Table 30: Difference of the analyzed molecular ions to the calculated molecular masses of the peaks found in the chromatogram in Figure 49 and the characteristic mass fragments of the peak with rel. abundance

No.	Retention time [min]	Chemical Formula	Molecular Mass Found	Molecular Mass Calculated	Difference Abs [mDa]	Difference ppm	Characteristic Mass in Spectra
A	10.168	$C_{19}H_{32}O_3$	308.2370	308.2351	1.9	6.2	95.0498 (100); 179.1440 (95); 165.1284 (58); 107.0500 (50)
B	10.243	$C_{20}H_{38}O_2$	310.2873	310.2872	0.1	0.3	70.0782 (100); 83.0858 (37); 98.0725 (20); 278.2623 (18)
C	10.320	$C_{20}H_{40}O_2$	312.3041	312.3028	1.3	4.2	74.0346 (100); 87.0435 (67); 143.1076 (20); 69.0694 (20)
D	10.336	$C_{18}H_{34}O_3$	298.2572	298.2508	6.4	21.5	111.0819 (100); 156.1512 (80); 71.0499 (80); 267.2340 (20)
E	10.408	$C_{20}H_{40}O_2$	312.3033	312.3028	0.5	1.6	74.0339 (100); 87.0432 (78); 71.0485 (57); 169.1582 (30)
F	10.460	$C_{19}H_{34}O_3$	310.2526	310.2508	1.8	5.8	137.0975 (100); 129.0554 (85); 95.0858 (55); 119.0873 (50)
G	10.483	$C_{19}H_{34}O_3$	310.2543	310.2508	3.5	11.3	137.0982 (100); 141.1290 (70); 119.0878 (55); 169.1258 (40)
H	10.523	$C_{19}H_{34}O_3$	310.2560	310.2508	5.2	16.8	111.0817 (100); 83.0862 (75); 168.1514 (60); 125.1338 (35);
I	10.560	$C_{19}H_{34}O_3$	310.2480	310.2508	-1.9	-6.1	83.0859 (100); 125.1326 (90); 129.0553 (90); 111.0816 (50)
J	10.759	$C_{19}H_{34}O_2$	294.2568	294.2559	0.9	3.1	67.0546 (100); 127.1126 (80); 185.1196 (70); 171.1035 (60)
K	11.031	$C_{19}H_{34}O_4$	326.2469	326.2457	1.2	3.7	57.0699 (100); 83.0851 (80); 111.0814 (60); 125.0974 (59)

In the zoomed chromatogram in Figure 49 of the nonpolar fraction of oleic acid methyl ester aged for 21 hours with a retention time of 10-11 minutes, the methyl esters of the unsaturated, saturated and branched C19 fatty acids can be found. The keto-C17 fatty acid methyl ester occur in small amounts.

Figure 50 shows the chromatogram of the nonpolar fraction of oleic acid methyl ester aged for 21 hours with a retention time of 11-15 min.

Figure 50: Gas chromatogram of the nonpolar fraction of oleic acid methyl ester aged for 21 hours (11-15 min)

Table 31: Identified peaks of the chromatogram in Figure 50

No.	Retention time [min]	Estimated Structure	Chemical Formula	Mass
L	12.673		$C_{27}H_{50}O_4$	438
M	13.098	or	$C_{28}H_{52}O_4$	452
N	14.348	Not identified	$C_{29}H_{52}O_3$	448
O	15.064	Not identified	$C_{29}H_{52}O_6$	496

Table 32: Difference of the analyzed molecular ions to the calculated molecular masses of the peaks found in the chromatogram in Figure 50 and the characteristic mass fragments of the peak with rel. abundance

No.	Retention time [min]	Chemical Formula	Molecular Mass		Difference		Characteristic Mass in Spectra
			Found	Calculated	Abs [mDa]	ppm	
L	12.673	$C_{27}H_{50}O_4$	438.3744	438.3709	3.5	8.0	127.1104 (100); 311.2584 (60); 279.2343 (45); 294.2558 (30)
M	13.098	$C_{28}H_{52}O_4$	452.3940	452.3866	7.4	16.4	141.1261 (100); 311.2583 (50); 279.2341 (45); 294.2557 (40)
N	14.348	$C_{29}H_{52}O_3$	448.4003	448.3916	8.7	19.4	171.1032 (100); 311.2625 (66); 279.2367 (50); 139.0789 (50)
O	15.064	$C_{29}H_{52}O_6$	496.3756	496.3764	-0.8	-1.6	185.1189 (100); 311.2612 (70); 294.2581 (60); 279.2363 (50)

With higher retention times the molecular mass increases, so compounds with a molecular mass of more than 400 g/mol can be found in the chromatogram at retention times from 12 to 15 minutes. A linkage from an oleic acid methyl ester to a formed fragment is plausible for this mass range like molecule M or L in Table 31. Just small peaks of these molecules are found in the chromatogram. The peaks are small because of the small concentrations in the sample, or the molecules are not sufficiently volatile or are bad to ionize. Therefore, they are not really suitable for the analysis by GC-MS. The exact linkage like a C-C bond or via an oxo- or dioxo bridge or via an ester could not be identified.

4.7.1.2   Medium polar fraction of oleic acid methyl ester aged for 21 hours

The following figures show the aged and fractionated sample of the medium polar fraction of oleic acid methyl ester.
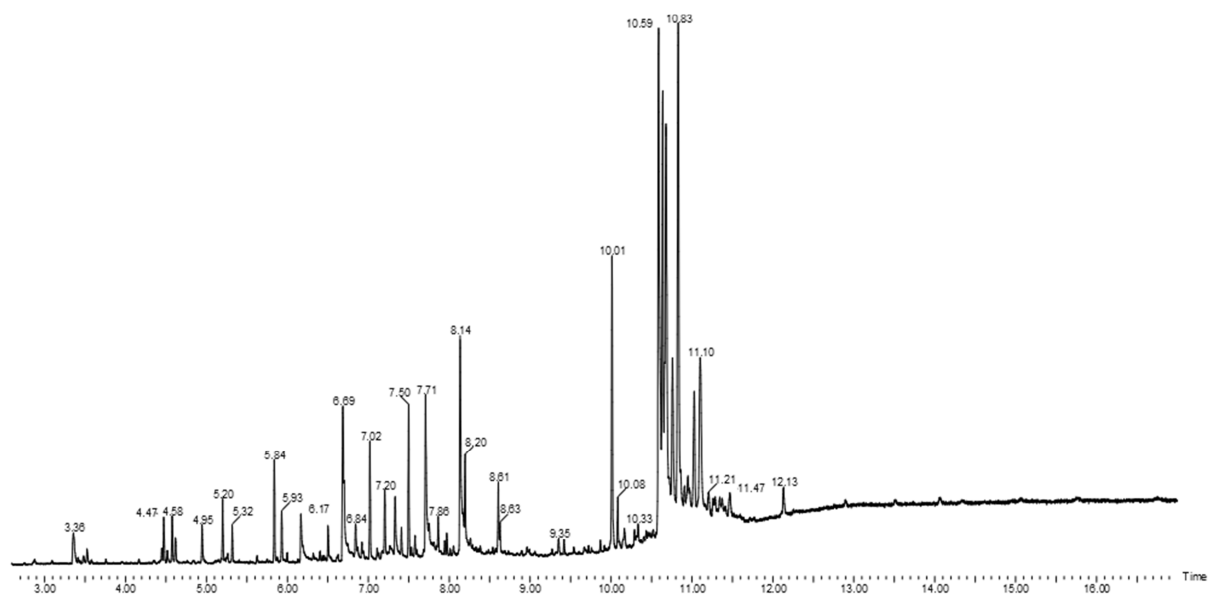
Figure 51: Gas chromatogram of the medium polar fraction of oleic acid methyl ester aged for 21 hours (3-17 min)

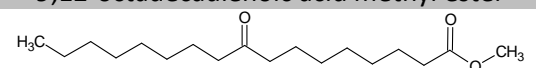In Figure 52 the part of the chromatogram of the medium polar fraction of the aged oleic acid methyl ester is shown, in which the fragments occur as aging products.
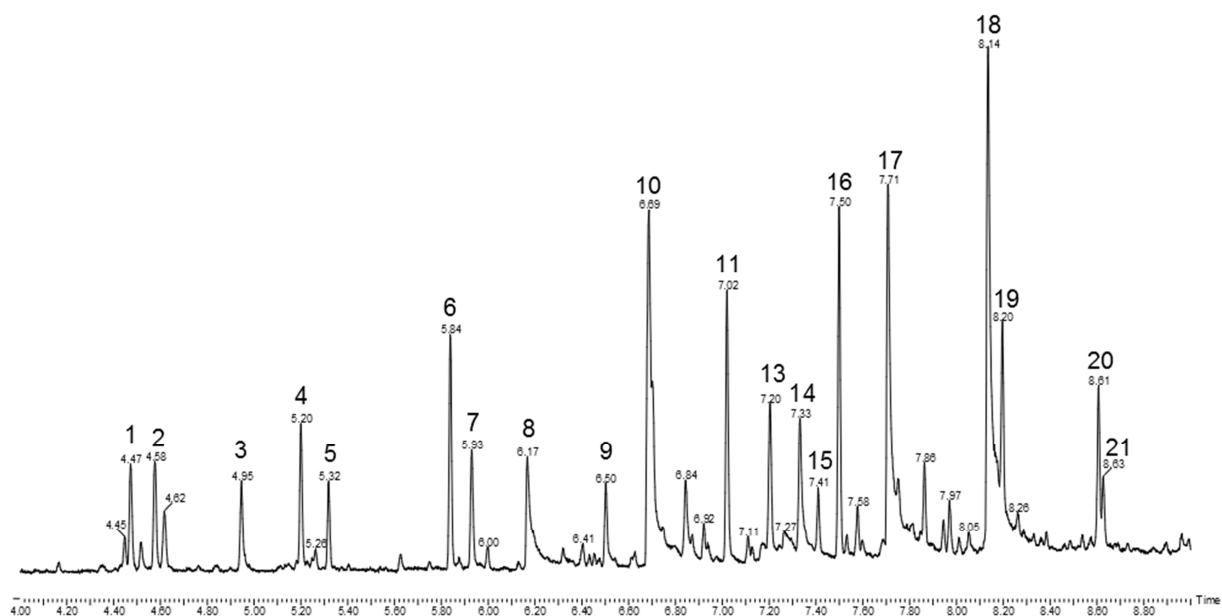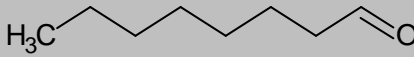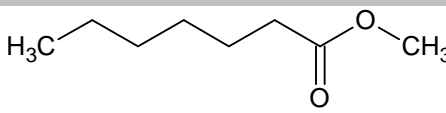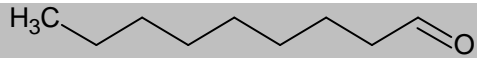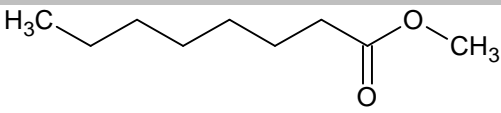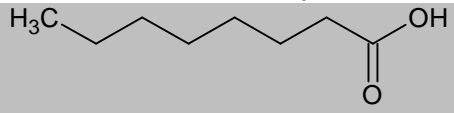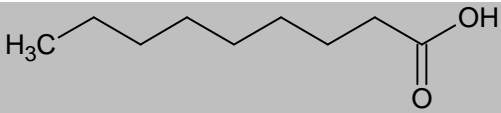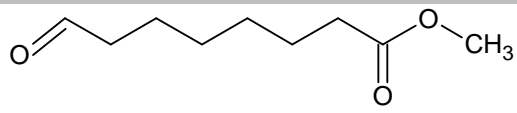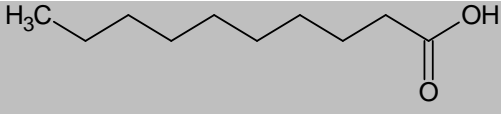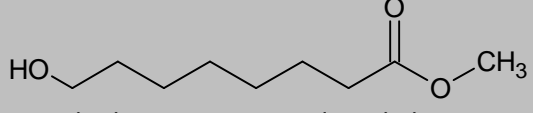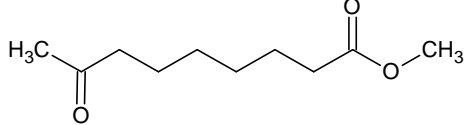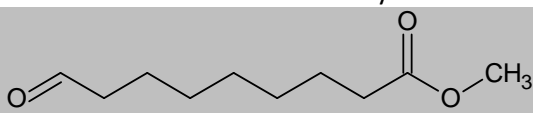
Figure 52: Gas chromatogram of the medium polar fraction of oleic acid methyl ester aged for 21 hours (4-9 min)

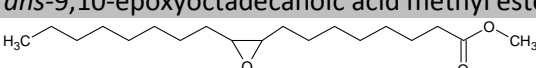Table 33: Identified peaks of the chromatogram in Figure 52

No.	Retention time [min]	Estimated Structure	Chemical Formula	Mass
1	4.473	Not identified	$C_7H_{14}O_1$	114
2	4.576	Not identified		
3	4.947	Not identified	$C_6H_{12}O_2$	116
4	5.200	octanal	$C_8H_{16}O$	128
5	5.319	heptanoic acid methyl ester	$C_8H_{16}O_2$	144
6	5.838	nonanal	$C_9H_{18}O$	142
7	5.930	octanoic acid methyl ester	$C_9H_{18}O_2$	158
8	6.168	octanoic acid	$C_8H_{16}O_2$	144
9	6.502	Not identified	$C_8H_{12}O_2$	140
10	6.687	nonanoic acid	$C_9H_{18}O_2$	158
11	7.021	8-oxooctanoic acid	$C_9H_{16}O_3$	172
12	7.111	decanoic acid	$C_{10}H_{20}O_2$	172
13	7.204	10-undecenal	$C_{11}H_{20}O$	168
14	7.333	8-hydroxyoctanoic acid methyl ester	$C_9H_{18}O_3$	174
15	7.410	8-oxononanoic acid methyl ester	$C_{10}H_{18}O_3$	186
16	7.500		$C_{10}H_{18}O_3$	186

	9-oxononanoic acid methyl ester			
17	7.708	(structure: HO–C(=O)–...–C(=O)–O–CH₃)	C₉H₁₆O₄	188
	octanedioic acid monomethyl ester			
18	8.135	(structure: HO–C(=O)–...–C(=O)–O–CH₃)	C₁₀H₁₈O₄	202
	nonanedioic acid monomethyl ester			
19	8.197	Not identified	C₁₁H₁₆O₂	180
20	8.608	Not identified	C₁₁H₁₆O₂	180
21	8.628	(structure: H₃C–O–C(=O)–...–lactone)	C₁₀H₁₆O₄	200
	5-(5-oxotetrahydrofuran-2-yl)pentanoic acid methyl ester			

Table 34: Difference of the analyzed molecular ions to the calculated molecular masses of the peaks found in the chromatogram in Figure 52 and the characteristic mass fragments of the peak with rel. abundance

No.	Retention time [min]	Chemical Formula	Molecular Mass		Difference		Characteristic Mass in Spectra
			Found	Calculated	Abs [mDa]	ppm	
1	4.473	C₇H₁₄O₁	114.1047	114.1045	0.2	1.8	85.1009 (100); 75.0438 (60); 59.0494 (58); 69.0694 (50)
2	4.576	No molecular ion observable					71.0443 (100); 57.0344 (10)
3	4.947	C₆H₁₂O₂	116.0849	116.0837	1.2	10.3	83.0837 (100); 55.0556 (32); 71.0494 (20)
4	5.200	C₈H₁₆O₁	128.1192	128.1201	-0.7	-5.5	84.0929 (100); 56.0627 (53); 69.0692 (50); 82.0779 (47)
5	5.319	C₈H₁₆O₂	144.1151	144.1150	0.1	0.7	74.0344 (100); 87.0439 (25); 101.0605 (15); 113.0971 (15)
6	5.838	C₉H₁₈O₁	142.1357	142.1358	-0.1	-0.7	98.1082 (100); 70.0773 (95); 82.0772 (85); 56.0625 (80)
7	5.930	C₉H₁₈O₂	158.1304	158.1307	-0.3	-1.9	74.0342 (100); 87.0437 (48); 71.0489 (26); 127.1125 (10)
8	6.168	C₈H₁₆O₂	144.1152	144.1150	0.2	1.4	60.0202 (100); 73.0276 (95); 101.0602 (30);

							85.1010 (30)
9	6.502	C₈H₁₂O₂	140.0826	140.0837	-1.1	-7.9	87.0442 (100); 115.0758 (75); 74.0364 (70); 81.0707 (45)
10	6.687	C₉H₁₈O₂	158.1315	158.1307	0.8	5.1	73.0241 (100); 60.0185 (90); 57.0696 (42); 115.0752 (40)
11	7.021	C₉H₁₆O₃	No molecular ion observable				74.0339 (100); 87.0422 (95); 69.0680 (60); 129.0895 (50)
12	7.111	C₁₀H₂₀O₂	No molecular ion observable				74.0363 (100); 84.0216 (40); 110.0746 (20); 125.0975 (15)
13	7.204	C₁₁H₂₀O₁	168.1516	168.1514	0.2	1.2	85.0263 (100); 70.0414 (25); 57.0344 (10); 121.1025 (7)
14	7.332	C₉H₁₈O₃	No molecular ion observable				74.0343 (100); 87.0439 (45); 96.0581 (15); 124.0891 (15)
15	7.410	C₁₀H₁₈O₃	186.1284	186.1256	2.8	15.0	129.0916 (100); 97.0664 (95); 69.0696 (52); 87.0452 (35)
16	7.500	C₁₀H₁₈O₃	No molecular ion observable				74.0322 (100); 87.0419 (65); 111.0801 (45); 143.1059 (30)
17	7.708	C₉H₁₆O₄	No molecular ion observable				74.0323 (100); 138.0652 (80); 69.0680 (50); 97.0640 (45)
18	8.135	C₁₀H₁₈O₄	No molecular ion observable				74.0317 (100); 152.0795 (80); 111.0801 (30); 171.1013 (30)
19	8.197	C₁₁H₁₆O₂	180.1166	180.1150	1.6	8.9	70.0412 (100); 138.1036 (80); 98.0720 (75); 94.0783 (40)
20	8.608	C₁₁H₁₆O₂	180.1155	180.1150	0.5	2.8	98.0725 (100); 70.0417 (70); 152.1201 (25); 83.0494 (20)
21	8.628	C₁₀H₁₆O₄	No molecular ion observable				85.0276 (100); 150.0698 (12); 123.0821 (10);

A lot of fragments are found in the medium polar fraction of aged oleic acid methyl ester. These fragments are aldehydes, saturated acids or methyl esters, with a chain length of 8 to 10 carbon atoms and also a lacton derivative was identified. The lacton results via intermolecular esterification.
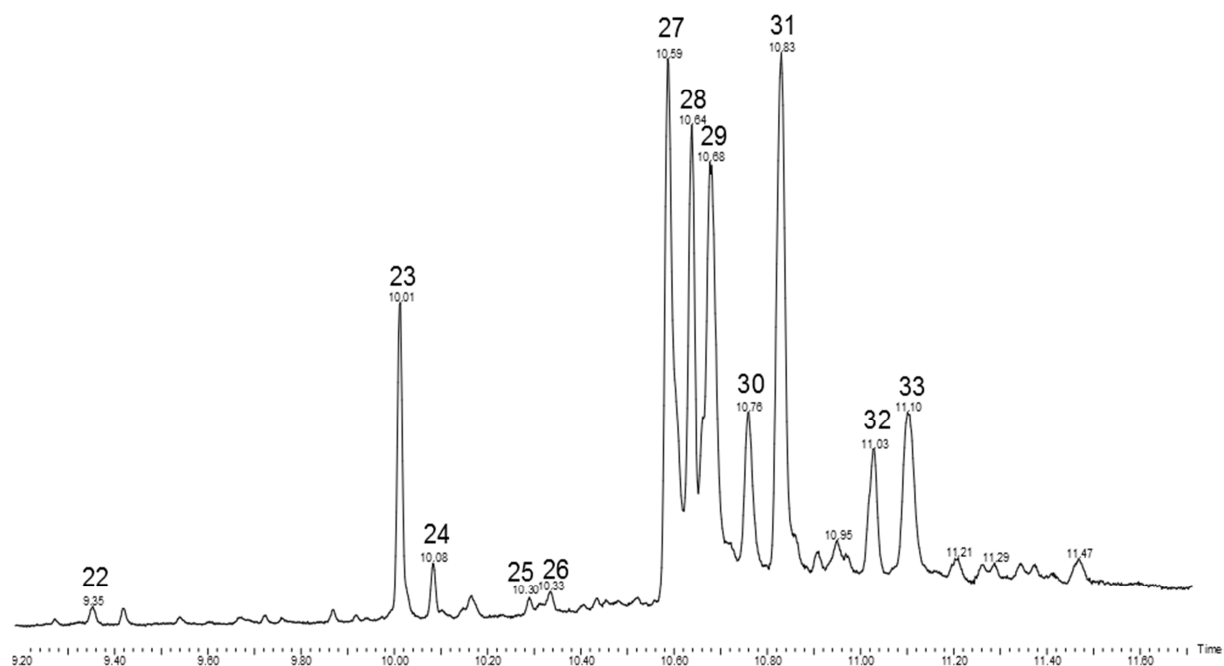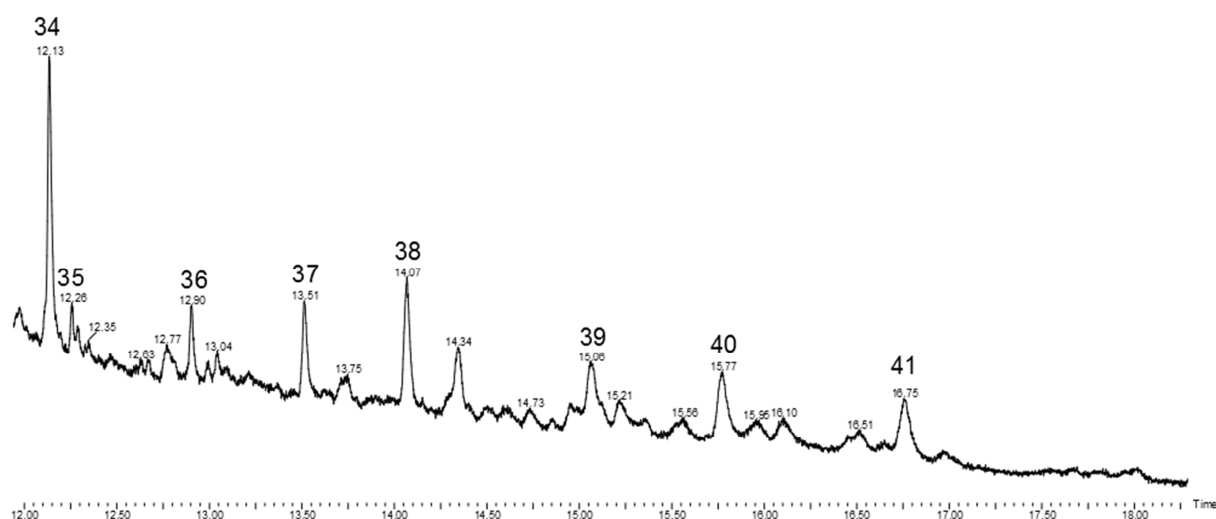

Figure 53: Gas chromatogram of the medium polar fraction of oleic acid methyl ester aged for 21 hours (9-11 min)

The peaks with a retention time of 9-11 minutes of the medium polar fraction of oleic acid methyl ester aged for 21 hours are shown in Figure 53.

Table 35: Identified peaks of the chromatogram in Figure 53
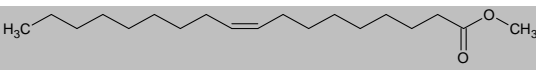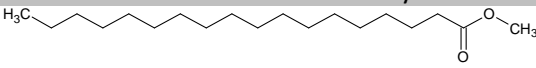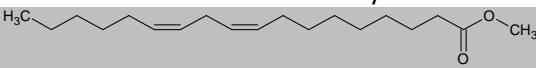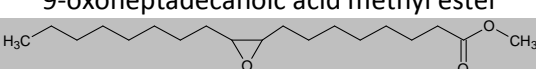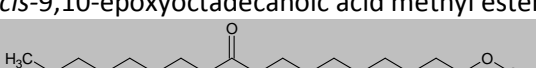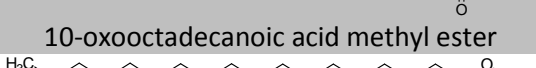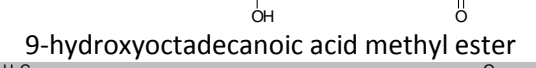
No.	Retention time [min]	Estimated Structure	Chemical Formula	Mass
22	9.354	Not identified	$C_{11}H_{14}O_3$	194
23	10.013	cis-9-octadecenoic acid methyl ester	$C_{19}H_{36}O_2$	296
24	10.083	octadecanoic acid methyl ester	$C_{19}H_{38}O_2$	298
25	10.290	9,12-octadecadienoic acid methyl ester	$C_{19}H_{34}O_2$	294
26	10.335	9-oxoheptadecanoic acid methyl ester	$C_{18}H_{34}O_3$	298
27	10.587	trans-9,10-epoxyoctadecanoic acid methyl ester	$C_{19}H_{36}O_3$	312
28	10.638	cis-9,10-epoxyoctadecanoic acid methyl ester	$C_{19}H_{36}O_3$	312
29	10.677	10-oxooctadecanoic acid methyl ester	$C_{19}H_{36}O_3$	312
30	10.759	9-hydroxyoctadecanoic acid methyl ester	$C_{19}H_{38}O_3$	314
31	10.830	9,10-epoxy-12-octadecenoic acid methyl ester	$C_{19}H_{34}O_3$	310
32	11.029	Not identified	$C_{19}H_{34}O_4$	326
33	11.101	Not identified	$C_{19}H_{34}O_4$	326

Table 36: Difference of the analyzed molecular ions to the calculated molecular masses of the peaks found in the chromatogram in Figure 53 and the characteristic mass fragments of the peak with rel. abundance

No.	Retention time [min]	Chemical Formula	Molecular Mass		Difference		Characteristic Mass in Spectra
			Found	Calculated	Abs [mDa]	ppm	
22	9.354	$C_{11}H_{14}O_3$	194.0932	194.0943	-1.1	-5.7	75.0440 (100); 71.0494 (25); 166.1012 (25); 195.1042 (20)
23	10.013	$C_{19}H_{36}O_2$	296.2720	296.2715	0.5	1.7	69.0667 (100); 74.0326 (85); 83.0831 (62); 264.2434 (50)
24	10.083	$C_{19}H_{38}O_2$	298.2883	298.2872	1.1	3.7	74.0348 (100); 87.0436 (65); 143.1074 (20)
25	10.290	$C_{19}H_{34}O_2$	294.2576	294.2559	1.7	5.8	294.2577 (100); 110.1104 (70); 95.0863 (60); 67.0547 (60)
26	10.335	$C_{18}H_{34}O_3$	298.2576	298.2508	6.8	22.8	156.1515 (100); 200.1416 (65); 168.1167 (50); 140.1218 (40)
27	10.587	$C_{19}H_{36}O_3$	312.2681	312.2664	1.7	5.4	74.0325 (100); 155.1050 (80); 69.0669 (65); 67.0533 (50)
28	10.638	$C_{19}H_{36}O_3$	312.2662	312.2664	-0.2	-0.6	74.0305 (100); 155.1022 (95); 69.0658 (45); 87.0415 (40)
29	10.677	$C_{19}H_{36}O_3$	312.2730	312.2664	6.6	21.1	125.0960 (100); 156.1485 (70); 71.0847 (65); 170.1662 (60)
30	10.759	$C_{19}H_{38}O_3$	No molecular ion observable				87.0418 (100); 155.1051 (80); 169.1208 (70); 69.0683 (55)
31	10.830	$C_{19}H_{34}O_3$	310.2523	310.2508	1.5	4.8	153.1163 (100); 167.1331 (95); 97.0575 (90); 137.0888 (80)
32	11.029	$C_{19}H_{34}O_4$	326.2473	326.2457	1.5	4.6	57.0695 (100); 83.0847 (65); 125.0968 (50); 69.0684 (50)
33	11.101	$C_{19}H_{34}O_4$	326.2505	326.2457	4.8	14.7	141.0903 (100); 155.11056 (95); 87.0430 (70); 95.0850 (60)

The peaks with a retention time of 10-11 minutes (Figure 53) correspond to methyl esters of a fatty acid with 17 or mostly 18 carbon atoms. A high amount of the epoxides of oleic acid methyl ester are in the sample and can be found in the big peaks in this chromatogram. Also 9-oxo- and 9-hydroxy-stearic acid methyl ester were identified in this chromatogram.

The identification of the cis/trans isomer of 9,10-epoxy stearic acid methyl ester (molecule no. 27 and no. 28) was done by comparison with literature data, where the trans-isomer elutes first with the use of a polar capillary column [82], [83]. A comparison of the peak areas of the synthesized epoxides (3.6) with a polar and a nonpolar capillary columns show the same results for both isomer peaks. Here the trans-isomer has a much smaller peak because of the epoxidation of the cis-double bond of oleic acid methyl ester. The smaller epoxide peak (trans–isomer) elutes first in the measurements with both of the different columns. The trans-isomer of the stearic acid methyl ester epoxide could be identified because it elutes first.

Figure 54 shows the chromatogram with the retention time of 12-17 minutes of the medium polar fraction of aged oleic acid methyl ester. In this region the dimerized aging products of oleic acid methyl ester with a fragment should occur.

Figure 54: Gas chromatogram of the medium polar fraction of oleic acid methyl ester aged for 21 hours (12-17 min)

Table 37: Difference of the analyzed molecular ions to the calculated molecular masses of the peaks found in the chromatogram in Figure 54 and the characteristic mass fragments of the peak with rel. abundance

No.	Retention time [min]	Chemical Formula	Molecular Mass		Difference		Characteristic Mass in Spectra
			Found	Calculated	Abs [mDa]	ppm	
34	12.134	$C_{19}H_{34}O_4$	326.2442	326.2457	-1.5	-4.6	239.2371 (100); 325.2361 (70); 137.1298 (60); 221.2272 (50)
35	12.258	$C_{27}H_{48}O_3$	420.3654	420.3603	5.1	12.1	209.1169 (100); 187.1318 (70); 152.1201 (40); 137.1310 (35)
36	12.903	$C_{25}H_{38}O_2$	370.2753	370.2872	-11.9	-32.1	353.2336 (100); 284.2740 (30); 239.2416 (15); 155.1467 (10)
37	13.514	$C_{28}H_{52}O_3$	436.3811	436.3916	-10.5	-24.1	187.1305 (100); 155.1052 (75); 127.1098 (45); 145.1220 (35)
38	14.068	$C_{27}H_{40}O_2$	396.2969	396.3028	-5.9	-14.9	187.1298 (100); 155.1049 (70); 159.1377 (20); 141.1250 (20)
39	15.062		No molecular ion observable				157.1204 (100); 245.1259 (70); 311.2609 (50); 343.2485(20)
40	15.773		No molecular ion observable				189.1132 (100); 144.1151 (90); 367.2874 (30); 285.2092 (25)
41	16.754	$C_{29}H_{52}O_6$	496.3856	496.3764	9.2	18.5	185.1167 (100); 155.1079 (35); 187.1332 (30); 203.1292 (25)

A substance with a higher molecular mass than 300 g/mol and some with more than 400 g/mol can be found from Figure 54. The structures of these molecules are unknown but the linkage between an oleic acid methyl ester and different fragments could be possible.

4.7.1.3   Strong polar Fraction of Oleic acid methyl ester aged for 21 hours
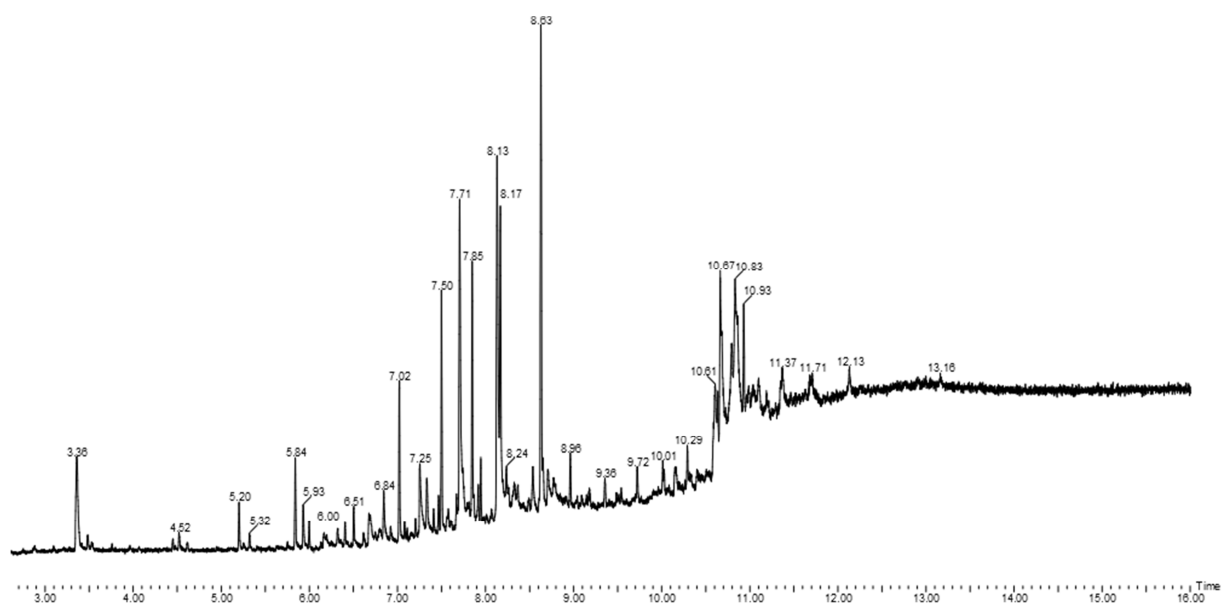
Figure 55: Gas chromatogram of the strong polar fraction of oleic acid methyl ester aged for 21 hours (3-17 min)

Figure 55 shows the whole gas chromatogram of the strong polar fraction of oleic acid methyl ester which was aged for 21 hours in the Rancimat device and Figure 56 the chromatogram within the retention time of 5-9 minutes.
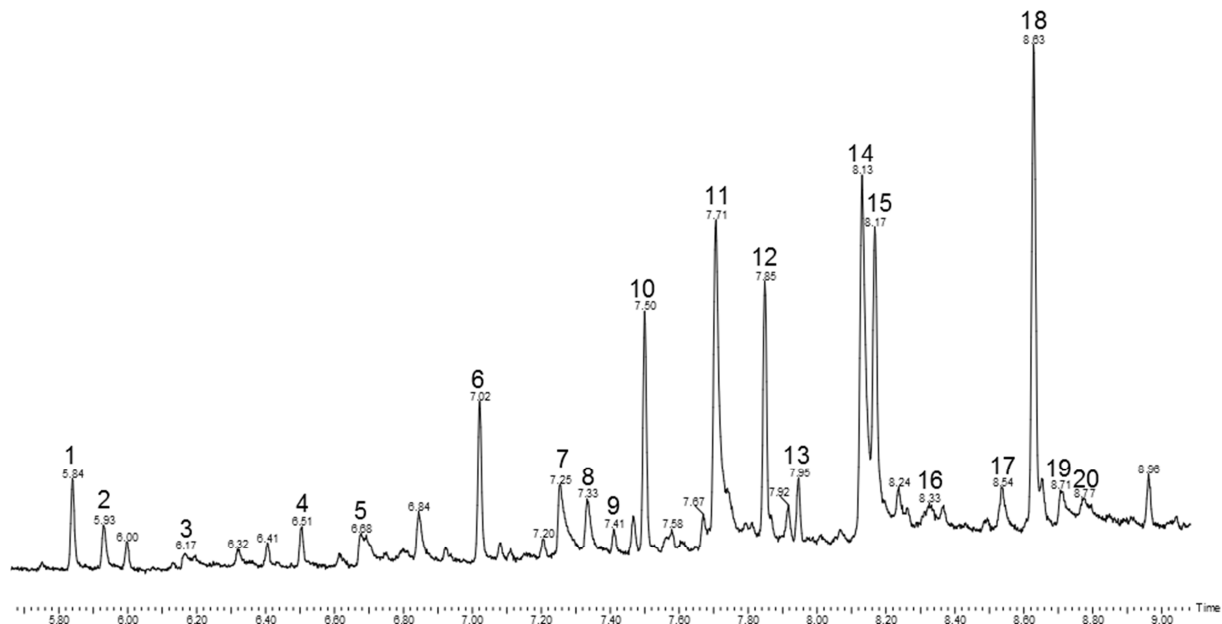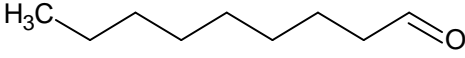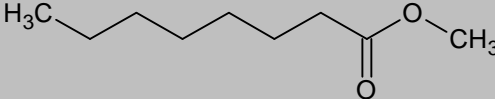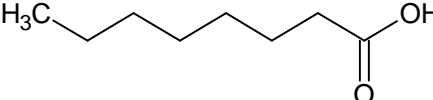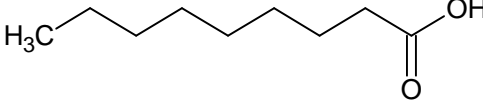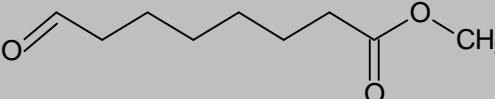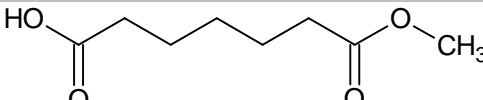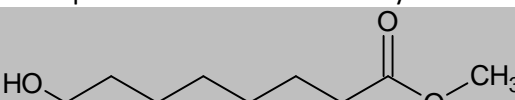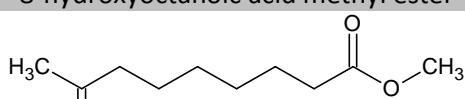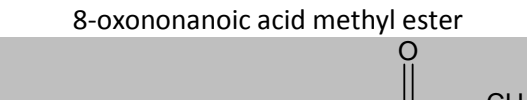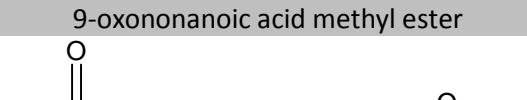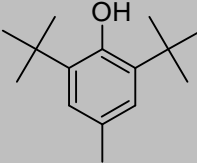
Figure 56: Gas chromatogram of the strong polar fraction of oleic acid methyl ester aged for 21 hours (5-9 min)

Table 38: Identified peaks of the chromatogram in Figure 56

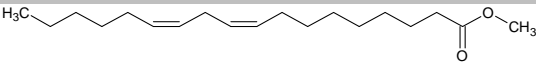| No.	Retention time [min]	Estimated Structure	Chemical Formula	Mass
1	5.839	nonanal	$C_9H_{18}O$	142
2	5.929	octanoic acid methyl ester	$C_9H_{18}O_2$	158
3	6.166	octanoic acid	$C_8H_{16}O_2$	144
4	6.505	Not identified	$C_8H_{12}O_2$	140
5	6.677	nonanoic acid	$C_9H_{18}O_2$	158
6	7.021	8-oxooctanoic acid	$C_9H_{16}O_3$	172
7	7.255	heptanedioic acid monomethyl ester	$C_8H_{14}O_4$	174
8	7.333	8-hydroxyoctanoic acid methyl ester	$C_9H_{18}O_3$	174
9	7.410	8-oxononanoic acid methyl ester	$C_{10}H_{18}O_3$	186
10	7.500	9-oxononanoic acid methyl ester	$C_{10}H_{18}O_3$	186
11	7.707	octanedioic acid monomethyl ester	$C_9H_{16}O_4$	188
12	7.848	2,6-bis(1,1-dimethylethyl)-4-methylphenol (BHT)	$C_{15}H_{24}O$	220
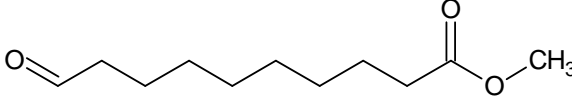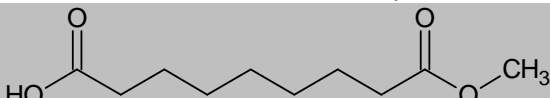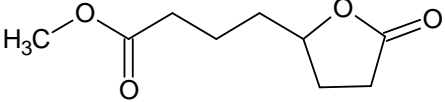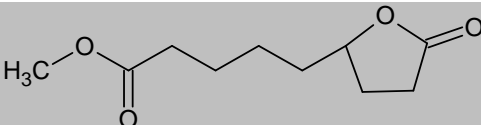
13	7.947		$C_{11}H_{20}O_3$	200
		10-oxodecanoic acid methyl ester		
14	8.131		$C_{10}H_{18}O_4$	202
		nonanedioic acid monomethyl ester		
15	8.167		$C_9H_{14}O_4$	186
		5-(5-oxotetrahydrofuran-2-yl)butanoic acid methyl ester		
16	8.326	Not identified		
17	8.538	Not identified		
18	8.628		$C_{10}H_{16}O_4$	200
		5-(5-oxotetrahydrofuran-2-yl)pentanoic acid methyl ester		
19	8.706	Not identified		
20	8.773	Not identified		

Table 39: Difference of the analyzed molecular ions to the calculated molecular masses of the peaks found in the chromatogram in Figure 56 and the characteristic mass fragments of the peak with rel. abundance

No.	Retention time [min]	Chemical Formula	Mass		Difference		Characteristic Mass in Spectra
			found	calculated	Abs [mDa]	ppm	
1	5.839	$C_9H_{18}O$	142.1320	142.1358	-3.8	-26.7	98.1093 (100); 70.0783 (95); 56.0629 (80); 82.0779 (80)
2	5.930	$C_9H_{18}O_2$	158.1304	158.1307	-0.3	-1.9	74.0340 (100); 87.0435 (50); 71.0488 (30); 127.1123 (20)
3	6.166	$C_8H_{16}O_2$	144.1131	144.1150	-1.9	-13.2	60.0213 (100); 73.0294 (60); 101.0606 (30); 85.1017 (30)
4	6.505	$C_8H_{12}O_2$	140.0833	140.0837	-0.4	-2.9	87.0445 (100); 115.0757 (90); 74.0364 (80; 127.0766 (40)
5	6.677	$C_9 H_{18} O_2$	158.1329	158.1307	2.2	13.9	73.0290 (100); 60.0209 (80); 115.0760 (30); 129.0921 (25)
6	7.021	$C_9H_{16}O_3$	172.1037	173.1099	-6.2	-36.0	87.0434 (100); 74.0352 (95); 129.0910 (55); 97.0653 (50)

7	7.255	$C_8H_{14}O_4$	No molecular ion observable				74.0361 (100); 115.0759 (45); 69.0696 (40); 128.0841 (30)
8	7.333	$C_9H_{18}O_3$	No molecular ion observable				74.0360 (100); 87.0445 (50); 124.0885 (20); 144.1150 (20)
9	7.410	$C_{10}H_{18}O_3$	No molecular ion observable				129.0910 (100); 97.0667 (90); 87.0446 (40); 155.1101 (22)
10	7.500	$C_{10}H_{18}O_3$	No molecular ion observable				74.0345 (100); 87.0430 (70); 111.0807 (40); 143.1063 (35)
11	7.707	$C_9H_{16}O_4$	No molecular ion observable				74.0336 (100); 138.0663 (70); 97.0643 (40); 157.0864 (20)
12	7.848	$C_{15}H_{24}O$	220.1830	220.1827	0.3	1.4	205.1508 (100); 220.1812 (30); 145.1016 (10); 177.1293 (10)
13	7.947	$C_{11}H_{20}O_3$	No molecular ion observable				74.0362 (100); 87.0448 (60); 125.0979 (50); 157.1234 (30)
14	8.131	$C_{10}H_{18}O_4$	No molecular ion observable				74.0338 (100); 152.0822 (60); 83.0854 (30); 171.1022 (20)
15	8.167	$C_9H_{14}O_4$	186.0892	186.0892	-3.8	-20.4	85.0227 (100); 126.0676 (20); 74.0350 (20); 155.0703 (15)
16	8.326		No molecular ion observable				74.0365 (100); 101.0250 (100); 122.0745 (60); 150.0692 (50)
17	8.538		No molecular ion observable				83.0138 (100); 84.0212 (100); 166.0679 (65); 167.0736 (65)
18	8.628	$C_{10}H_{16}O_4$	No molecular ion observable				85.0196 (100); 150.0676 (15); 123.0805 (15); 74.0353 (15)
19	8.706		No molecular ion observable				136.0894 (100); 94.0787 (70); 74.0366 (70); 99.0442 (60)

20	8.773	No molecular ion observable	167.0724 (100); 136.0872 (40); 114.0350 (15); 111.0449 (10)

The strong polar fraction contains also a lot of formed fragments like the medium polar fraction. These fragments have a retention time from 5-9 minutes. Identified molecules were aldehydes, acids or methyl esters. Also lactone derivatives with a different carbon chain length could be identified. Some of them are the same molecules found also in the medium polar fraction. The column chromatography does not separate the aging products completely in one of the polar fractions. This could also be shown in the HPLC analysis (4.4)

The identified BHT (no. 12) is an antioxidant and is used in some solvents for stabilization. Therefore, it is probable that this substance is an impurity.
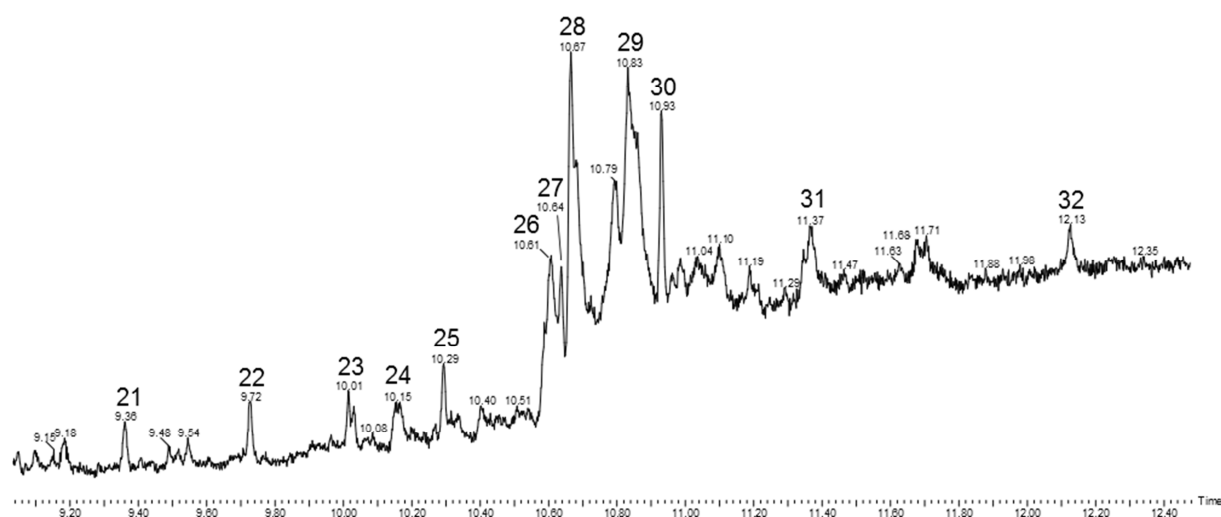
Figure 57: Gas chromatogram of the strong polar fraction of oleic acid methyl ester aged for 21 hours (10-12 min)

Figure 57 shows the chromatogram of the strong polar fraction of the aged oleic acid methyl ester with the retention time of 10-12 minutes.

Table 40: Identified peaks of the chromatogram in Figure 57
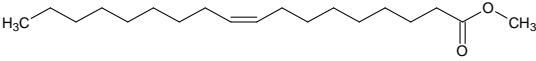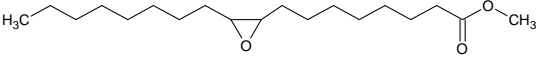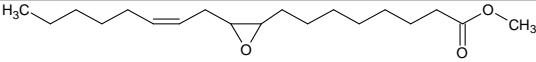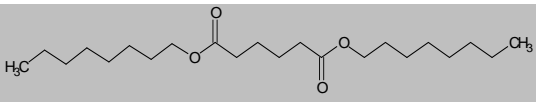
No.	Retention time [min]	Estimated Structure	Chemical Formula	Mass
21	9.355	Not identified		
22	9.724	Not identified		
23	10.011	*cis*-9-octadecenoic acid methyl ester	$C_{19}H_{36}O_2$	296
24	10.153	Not identified	$C_{19}H_{34}O_2$	294
25	10.291	9,12-octadecadienoic acid methyl ester	$C_{19}H_{34}O_2$	294
26	10.607	Not identified	$C_{19}H_{34}O_3$	310
27	10.637	9,10-epoxy octadecanoic acid methyl ester	$C_{19}H_{36}O_3$	312
28	10.665	Not identified	$C_{19}H_{36}O_3$	312
29	10.832	9,10-epoxy-12-octadecenoic acid methyl ester	$C_{19}H_{34}O_3$	310
30	10.931	hexanedioic acid dioctyl ester	$C_{22}H_{42}O_4$	370
31	11.364	Not identified		
32	12.138	Not identified		

Table 41: Difference of the analyzed molecular ions to the calculated molecular masses of the peaks found in the chromatogram in Figure 57 and the characteristic mass fragments of the peak with rel. abundance

No.	Retention time [min]	Chemical Formula	Mass		Difference		Characteristic Mass in Spectra
			Found	Calculated	Abs [mDa]	ppm	
21	9.355		No molecular ion observable				166.1015 (100); 83.0142 (55); 195.1033 (50)
22	9.724		No molecular ion observable				208.1114 (100); 209.1189 (80); 83.018 (65); 167.1073 (35)
23	10.011	$C_{19}H_{36}O_2$	296.2801	296.2715	8.6	29.0	69.0700 (100); 74.0366 (90); 83.0831 (62); 264.2743 (50)
24	10.153	$C_{19}H_{34}O_2$	294.2590	294.2559	3.1	10.5	165.1284 (100); 179.1451 (95); 294.2594 (70); 308.2372 (50)
25	10.291	$C_{19}H_{34}O_2$	294.2569	294.2559	1.0	3.4	294.2568 (100); 150.1039 (54); 124.1258 (50); 135.1164 (45)
26	10.607	$C_{19}H_{34}O_3$	310.2516	310.2508	0.8	2.6	127.1124 (100); 171.1031 (95); 57.0705 (90); 185.1186 (80)
27	10.637		No molecular ion observable				74.0367 (100); 155.1086 (65); 87.0442 (50); 67.0549 (50)
28	10.665	$C_{19}H_{36}O_3$	312.2686	312.2664	2.2	7.0	155.1064 (100); 187.1342 (20); 109.1027 (20); 125.0984 (10)
29	10.832	$C_{19}H_{34}O_3$	310.2528	310.2508	2.0	6.4	75.0263 (100); 153.1281 (70); 167.1449 (50); 244.1490 (50)
30	10.931	$C_{22}H_{42}O_4$	370.3145	370.3083	6.2	16.7	129.0529 (100); 112.1249 (30); 70.0780 (30); 259.1927 (10)
31	11.364		No molecular ion observable				155.0718 (100); 292.2387 (20); 130.1026(10); 250.2425 (10)
32	12.138		No molecular ion observable				239.2418 (100); 221.2290 (80); 325.2396 (80); 166.0665 (65)

Identified compounds in the strong polar fraction were oleic acid methyl ester and its oxidized derivatives such as epoxides.

The identified molecule hexanedioic acid dioctyl ester (no. 30) is a known plasticizer in the polymeric industry. Although its structure has two ester groups, this compound is an impurity from the sample preparation or treatment.

4.7.2 MALDI-TOF-MS

To analyze the progress of aging of oleic acid methyl ester a MALDI-TOF-MS was used. Dithranol and the sodium salt of trifluoracetate were used as matrix. The measurements were done by Prof. Saf from the Graz University of Technology, Institute for Chemistry and Technology of Materials (ICTM).

The investigated samples were an un-aged (0 hours) and two differently aged samples of oleic acid methyl ester. The two samples were aged for 21 and 42 hours in the Rancimat device. These three samples were each fractionated by column chromatography (3.7.1) in a nonpolar, a medium polar and a strong polar fraction.

The analysis by MALDI-TOF-MS should give the content of the sample with a higher molecular mass compared to the GC-TOF-MS. In the GC, these high mass molecules cannot be analyzed because of their high boiling points leading to decomposition.

The chosen MALDI-TOF-MS method was the same for all the analyzed samples, so the comparability of the results among different analyses is better. But because of the use of the same method for all measurements and not the optimal setting for each sample the analyses are not optimized for every single sample and therefore the mass accurateness decreases.

The result of the fractionation with column chromatography of the investigated oleic acid methyl esters is summarized in Table 42.

Table 42: Amount of the fractions of un-aged and aged oleic acid methyl ester

Oleic acid methyl ester	nonpolar [%]	medium polar [%]	strong polar [%]
un-aged 0h	96	2	0.5
21 hours	33	60	7
42 hours	21	73	6

Table 42 gives the result of the fractionation of the oleic acid methyl esters. The measured IP with the Rancimat device for oleic acid methyl ester was 1.5 hours. With an aging time of 21 or 42 hours the samples are aged for beyond their IP. Column chromatography of oleic acid methyl ester gives similar results to the time resolved fractionation of B100 biodiesel. Because of the absence of natural antioxidants, the IP is lower in oleic acid methyl ester compared to the mixture in the rape seed oil Biodiesel B100. The un-aged oleic acid methyl ester (0 hours) consists almost exclusively of the nonpolar fraction. Just impurities from the synthesis of the methyl ester could be found in the polar fractions. The synthesis of the methyl ester was not performed under inert conditions (3.4). It is possible that in the methylation step also fragments, dimers or oligomers were formed. With longer aging time the samples get more and more polar like the biodiesel B100 sample. The oleic acid methyl ester reacts with oxygen and forms epoxides, ketones, aldehydes and also dimeric and oligomeric molecules.
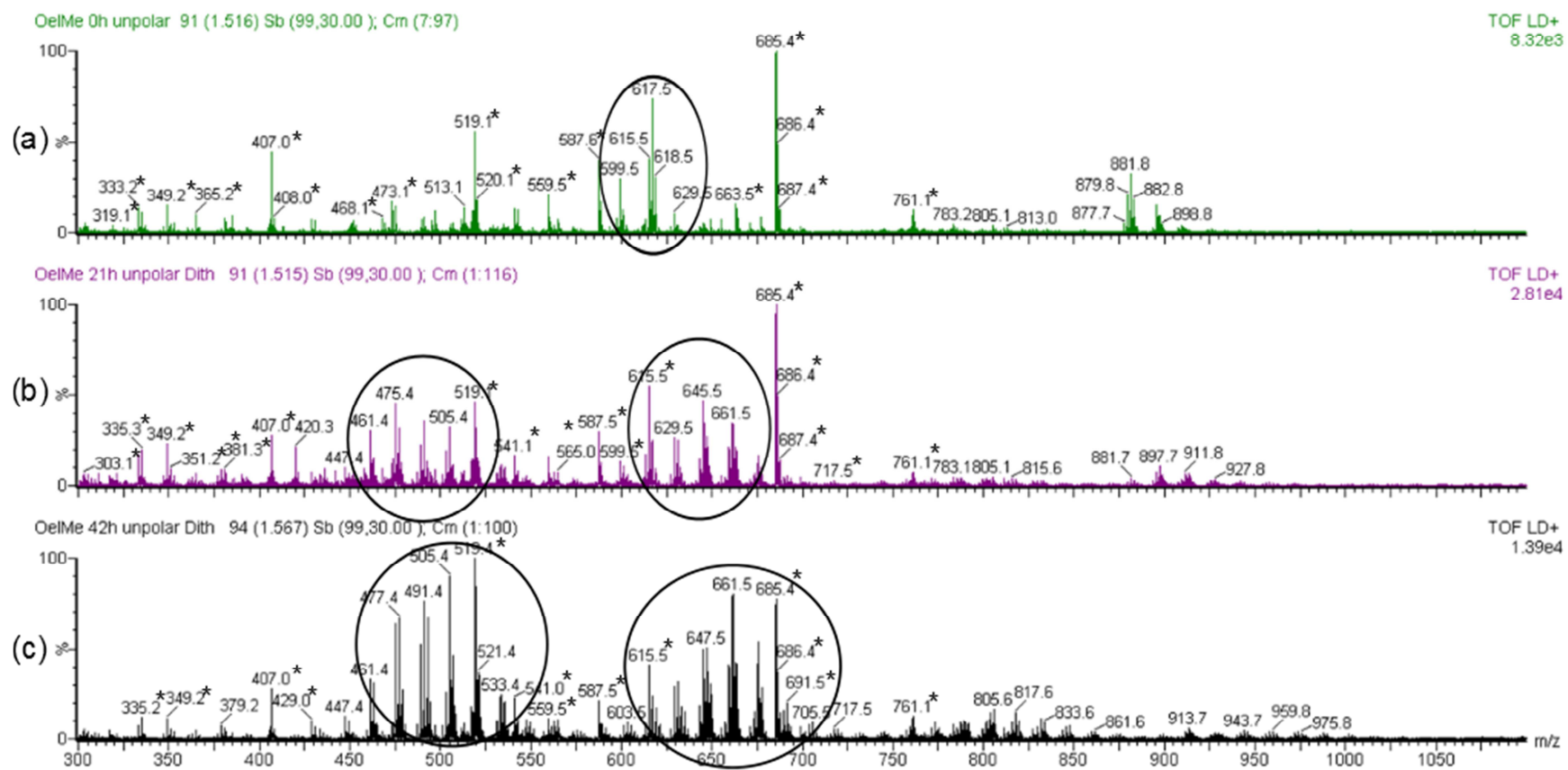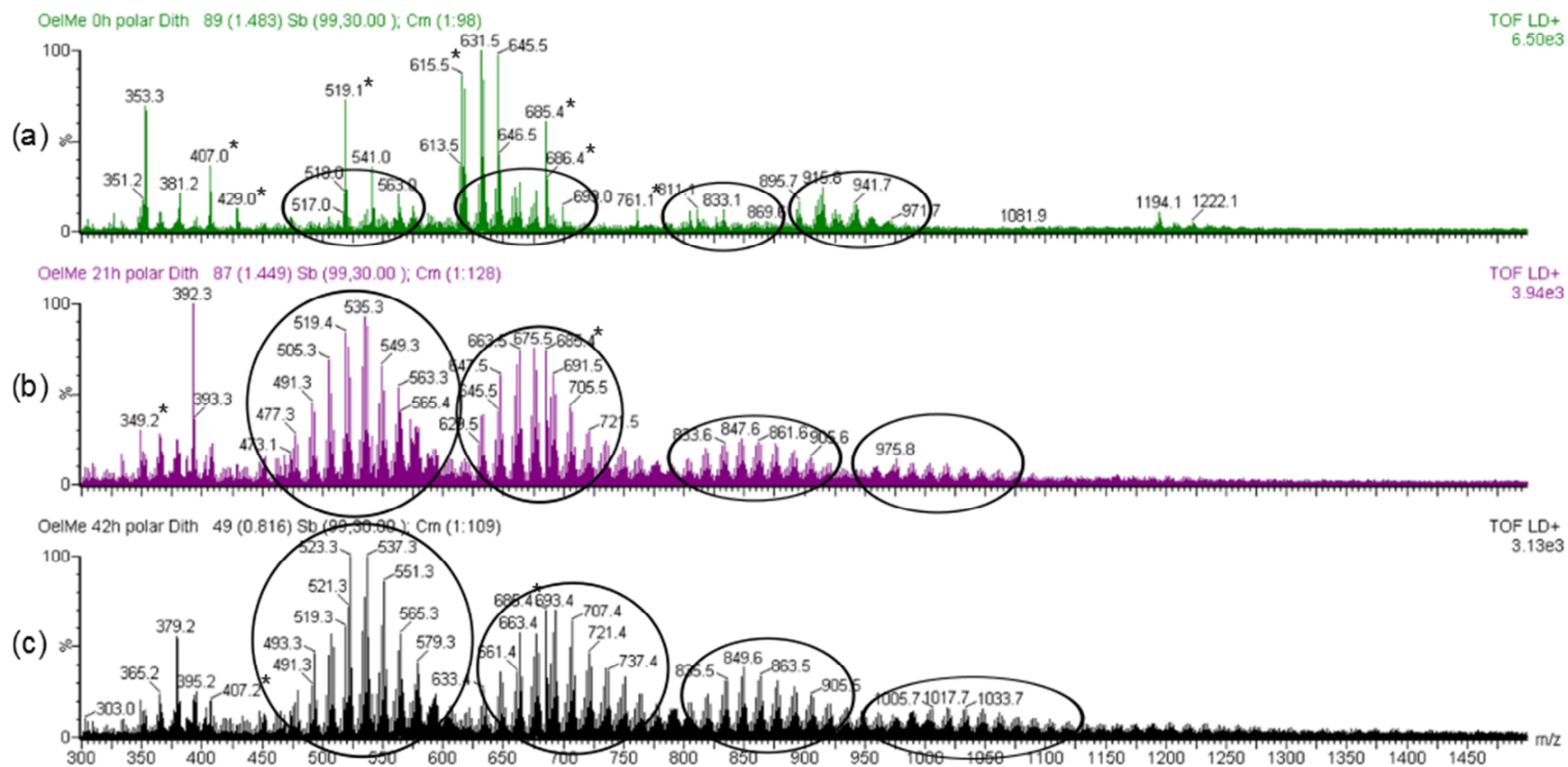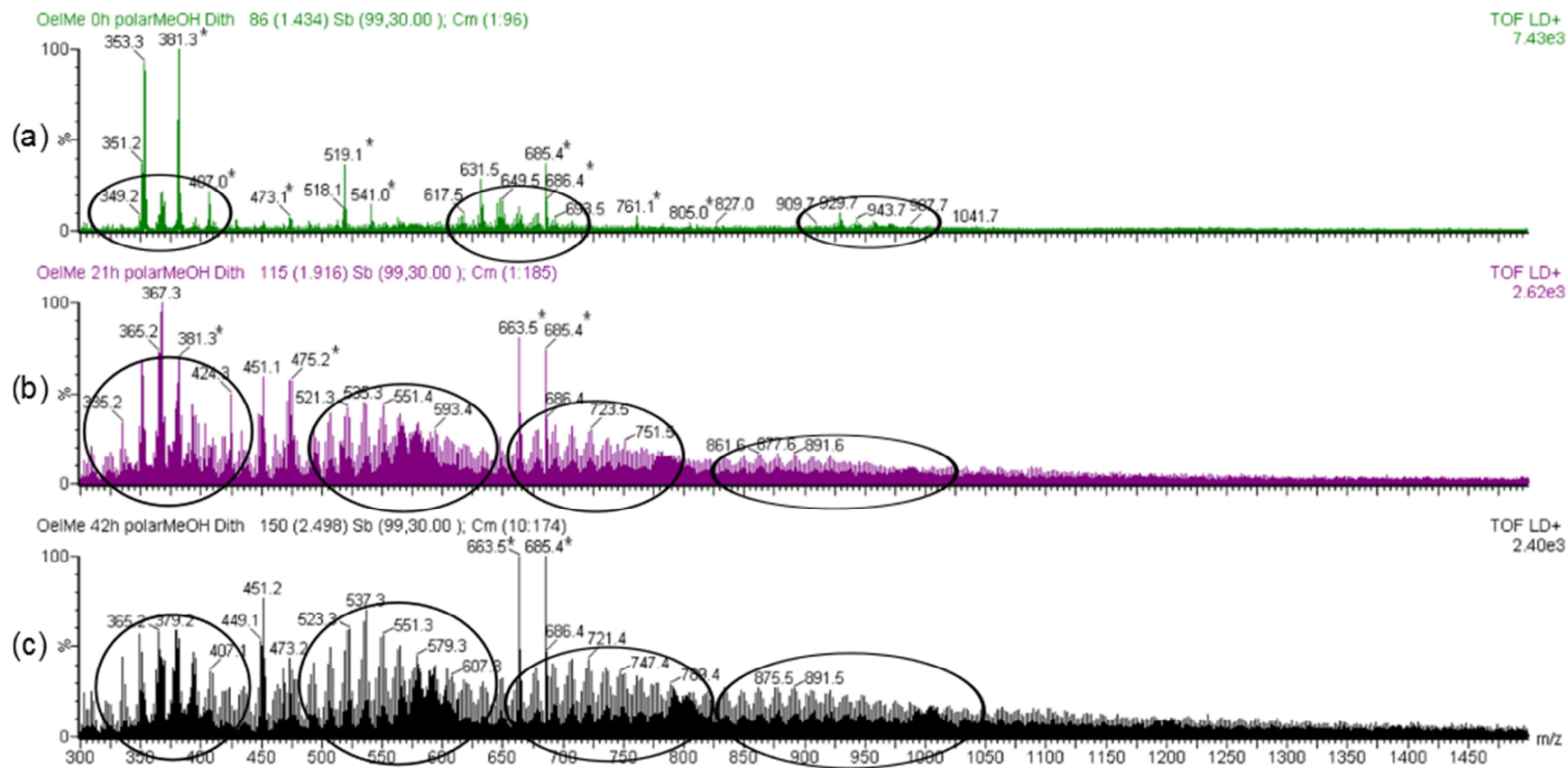
Figure 58: MALDI-TOF mass spectra of the nonpolar fraction of oleic acid methyl ester ((a) unaged; (b) 21 hours and (c) 42 hours); M: 300-1100; marked masses are from the matrix
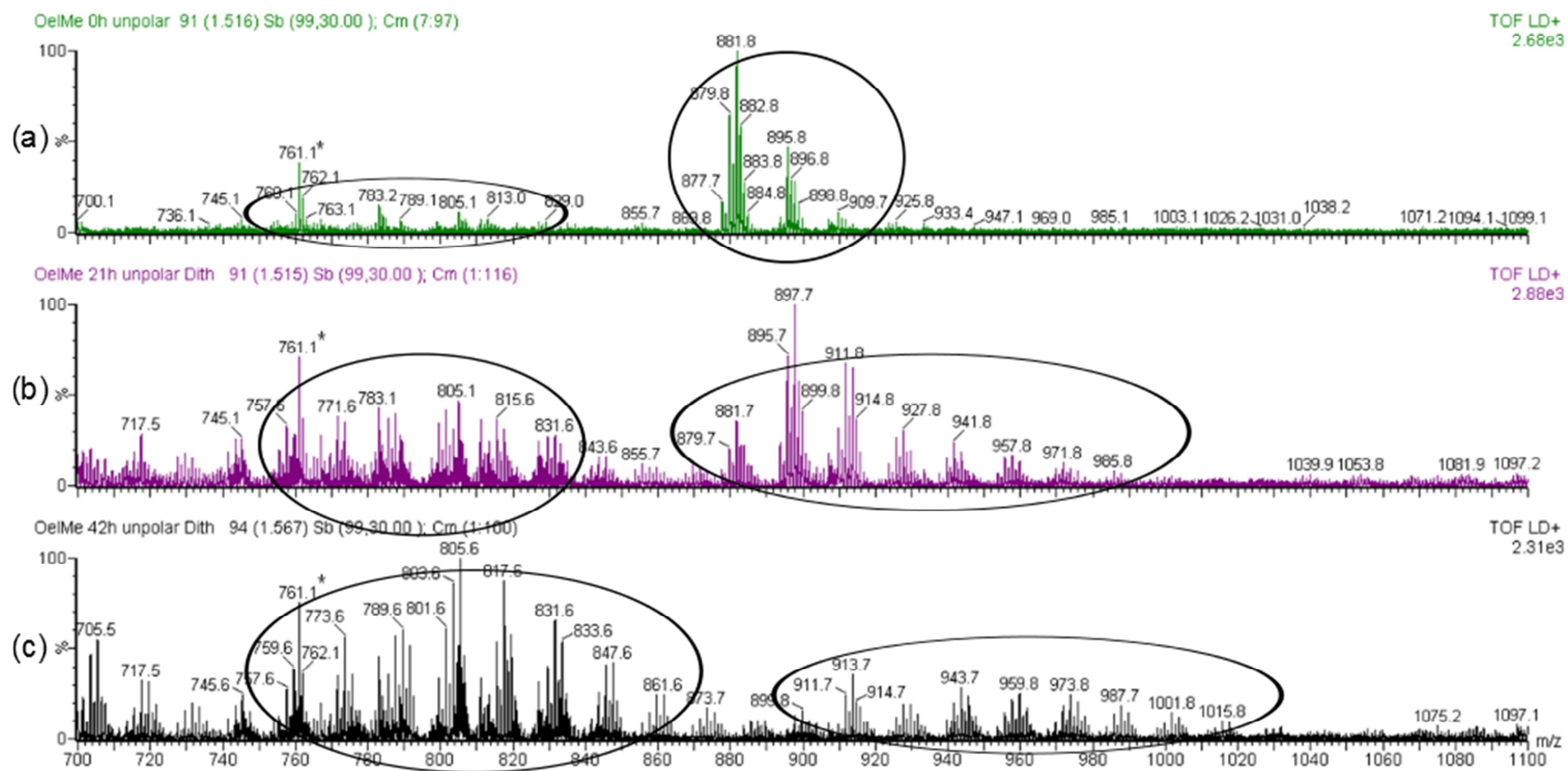
Figure 59: MALDI-TOF mass spectra of the nonpolar fraction of oleic acid methyl ester ((a) unaged; (b) 21 hours and (c) 42 hours); M: 700-1100; marked masses are from the matrix

The MALDI-TOF mass spectra of the nonpolar fraction of oleic acid methyl ester show the process of the accelerated aging with the Rancimat device. With the higher aging time of oleic acid methyl ester the groups of peaks marked with the circles in Figure 58 and Figure 59 shift to the right to higher molecular masses. The nonpolar un-aged sample (Figure 59 a) just shows some peaks at a molecular mass between 877 and 909 g/mol. The sample aged for 21 hours (Figure 59 b) has a mass peak region from 879 to 985 g/mol and the sample aged for 42 hours (Figure 59 c) a found mass range from 899 to 1015 g/mol. This shift to higher molecular masses with longer aging times can be observed in all four groups found. The shift to the higher molecular masses comes from the further oxidation of the formed oligomers. Oxygen can react with an oligomer and increases the molecular mass. Longer aging and therefore a longer reaction time leads to higher molecular masses.

Compared to the matrix peak at 685.4 g/mol, Figure 58 shows that the intensities of the mass peaks in the long aged sample (c) are higher than in the un-aged (a) and also higher than the peaks of the sample aged for 21 hours (b). Higher intensities can be interpreted as higher concentration of these molecules in the sample.

The highest peak of a group to the next highest group is usually 14 ($-CH_2-$) or sometimes 16 (+ oxygen) mass units higher. As an example Table 43 gives this result for the last mass region of the nonpolar fraction of the oleic acid methyl ester aged for 42 hours (Figure 59 c mass range from 894 to 1016 g/mol)

Table 43: Difference between the highest peak of a molecular group to the next highest peak in the group in the last mass region of the nonpolar fraction of the 42 hours aged oleic acid methyl ester (Figure 59 c).

Highest peak in group	Difference to peak before
899.8	---
913.7	14
929.7	16
943.7	14
959.8	16
973.8	14
987.8	14
1001.7	14
1015.8	14

A comparison of the nonpolar samples of oleic acid methyl ester with an aging time of 21 hours (b) and 42 hours (c) shows that the most intense peaks of a group in the sample aged for 21 hours can be found in the sample aged for 42 hours with a 16 g/mol higher molecular mass. During the longer aging time an addition of oxygen to the molecule can occur. For example the highest peak of Figure 59 b (21 hours) is 898 g/mol while in Figure 59 c (42 hours) the highest is 914 g/mol in this group.

The marked peaks within the circles are mass regions found in the nonpolar fractions during the aging of oleic acid methyl ester. Table 44 gives the marked mass ranges found in the nonpolar fraction for aging oleic acid methyl ester and the assumed structure within this molecular mass range.

Table 44: Mass regions in the nonpolar fraction during the aging of oleic acid methyl ester (Figure 58 a-c and Figure 59 a-c)

Mass region [g/mol]	Assumed molecular structure with the Na^+-ion
460-530	Oleic acid methyl ester and fragment (C8-C11)
600-700	2x Oleic acid methyl ester
760-850	2x Oleic acid methyl ester and fragment
880-1020	3x Oleic acid methyl ester

The assumed structures in Table 44 should give a hint of the molecular size of the mass regions. The mass of the fragment reach from 159 g/mol for a C8 to 197 g/mol for a C11 fragment. These fragments occur because of the isomerization of the double bond during the autoxidation reaction. Two oleic acid methyl esters, which are linked with a C-C bond, have a mass of 615 g/mol. An oleic acid methyl ester trimer has a mass of 911 g/mol, when linked with a simple C-C bond. Higher masses than these di and trimers could be found. The higher masses could result from oxo- or dioxo- linkage to form oligomers or an addition of oxygen to the carbon chain like the forming of epoxides, hydroxides, ketones or hydroperoxides.

Figure 60: MALDI-TOF mass spectra of the medium polar fraction of oleic acid methyl ester ((a) unaged; (b) 21 hours and (c) 42 hours); M: 300-1500; marked masses are from the matrix

Figure 61: MALDI-TOF mass spectra of the strong polar fraction of oleic acid methyl ester ((a) unaged; (b) 21 hours and (c) 42 hours); M: 300-1500; marked masses are from the matrix

The high resolution MALDI-TOF mass spectra of both of the polar fractions of oleic acid methyl ester (Figure 60 and Figure 61) show quite similar results to the mass spectra of the nonpolar fractions (Figure 58) before. The marked groups shift with longer aging times (from (a) to (c) in both figures) to higher molecular masses. This shift occurs because of the further oxidation and addition of oxygen during the aging process. The intensities of the peaks are getting higher with the longer aging time compared to the matrix mass of 685.4 g/mol marked with a star in all spectra, especially from the un-aged (a) to the aged fractions (b and c). Also the amounts of both polar phases increase with longer aging times compared to the un-aged sample (Table 42).

The peaks marked with the circles are mass regions found in the polar fractions during the aging of oleic acid methyl ester. Table 45 gives the marked mass ranges found in the polar fractions for aged oleic acid methyl ester and the estimated structure within this molecular mass range.

Table 45: Found mass regions in the medium and strong polar fraction during the aging of oleic acid methyl ester (Figure 60 a-c and Figure 61 a-c)

Polarity	Mass region [g/mol]	Estimated molecular structure with the Na^+-ion
Medium polar	470-600	Oleic acid methyl ester and fragment (C8-C11)
	650-750	2x Oleic acid methyl ester
	800-925	3x Oleic acid methyl ester
	950-1100	3x Oleic acid methyl ester and fragment
Strong polar	320-400	Oxidized oleic acid methyl ester
	470-600	Oleic acid methyl ester and fragment (C8-C11)
	650-800	2x Oleic acid methyl ester and 2x Oleic acid methyl ester with fragment
	850-1050	3x Oleic acid methyl ester and 3x Oleic acid methyl ester with fragment

Table 45 lists the estimated molecular structures of the found mass regions of the polar fractions. Like in the nonpolar fraction, the found molecules are combined to mass regions where peaks in the mass spectra occur. Fragments have a mass from 159 g/mol for a C8 to 197 g/mol for a C11-fragment. Two oleic acid methyl esters, which are linked with a C-C bond, have a mass of 615 g/mol. An oleic acid methyl ester trimer has a mass of 911 g/mol, when linked with simple a C-C bond. The wider mass regions result from all the diverse aging products formed from oleic acid methyl ester. A high variety of oxidation products have a higher molecular mass than the monomeric oleic acid methyl ester. This variety comes from different carbon chain lengths and different oxidation reactions with oxygen to form epoxides, hydroxides, hydroperoxides, ketones or ether compounds.

4.7.3   Comparison of the Size-Exclusion-Chromatography (SEC) and MALDI-TOF-MS

Two different analytical systems were used for the determination of the content of oligomers in aged oleic acid methyl ester samples. While the SEC separates the molecules by their size and shape, the MALDI-TOF-MS separates by their molecular mass, specifically their flying time to the detector. Furthermore, the soft ionization of the MALDI guarantees that no fragmentation of the molecules occurs.

For comparison the same samples were used for both types of analytical techniques. The samples were the three fractions of the differently aged oleic acid methyl ester.

Standard molecules were used for a better comparison of the analytical systems. With these molecules the retention times in the SEC are connected to their molecular mass. The standard molecules are listed in Table 46 with their measured retention times of the SEC and their molecular mass. The standard molecule monoolein is the 1-monogylcerid, diolein the 1,3-diglycerid and triolein the triglyceride of oleic acid.

Table 46: Retention time of the used standards

	Retention time RT [min] (SEC)	M [g/mol]	$[M + Na]^+$ [g/mol] (MALDI-TOF-MS)
Oleic acid methyl ester	21.8	296.5	319.5
Stearic acid	21.2	284.5	307.5
Monoolein	20.6	356.5	379.5
Diolein	19.2	621.0	644.0
Triolein	18.5	885.4	908.4
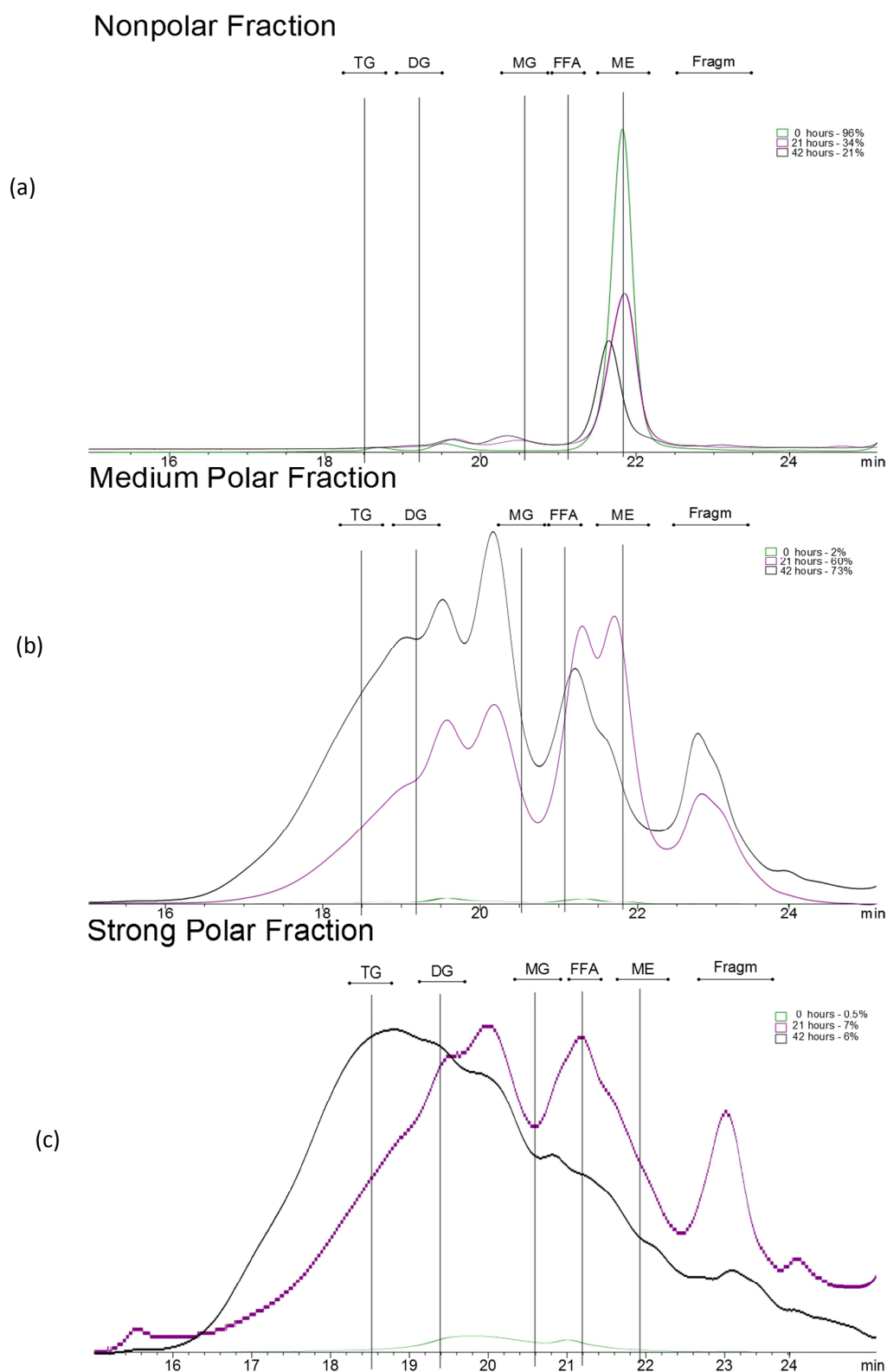
Figure 62: SEC-analysis of the aged oleic acid methyl ester samples. The marks TG (triglycerid), DG (diglycerid), MG (monoglycerid), FFA (free fatty acid), ME (methyl ester) and Fragm (fragment) are for the retention times of the used standards. The areas of the shown graphs correlated to their concentration in the fractions.

The SEC-analysis was done with all the three fractions of the un-aged, and the oleic acid methyl esters aged for 21 and 42 hours. The marks show the retention times of the used standards, which were used for these experiments. These standards should show the molecular masses in the SEC analysis with a specific retention time. The standards are different to the formed oligomers as aging products in size and shape. The glycerides are fatty acids, which are linked at the end of the carbon chain via an ester bond to glycerine. On the other hand, the fatty acid methyl esters of the oligomers as aging products are linked in the middle of their carbon chain with oxygen. This causes different shapes of the molecules which influence the separation by size exclusion chromatography although they have nearly the same masses. The masses of the molecules could not be determined exactly, but the standards should give an approximate molecular weight.

The shown area proportions of each fraction give the amount in the original sample before the separation of the polar content (Table 42). With a lower amount of a fraction in the sample, the area of the chromatogram is also smaller. So the area of the polar fractions of the un-aged sample (Figure 62 b and c green line) is small compared to the two aged samples.

Figure 62 (a) shows the nonpolar fractions of the oleic acid methyl ester samples. A high amount of the analytes is in the mass range of the methyl ester as expected. The peak of the sample aged for 42 hours (black line) has a smaller retention time than the others and therefore a higher molecular mass. This higher molecular mass comes from the oxidation of the methyl ester. The aged samples also show peaks with a smaller retention time and these molecules have therefore a higher molecular weight. The molar mass of those peaks are between the mono- and diglyceride standards. These peaks could be the linkage of an oleic acid methyl ester with a fragment with 8-11 carbon atoms or a second oleic acid methyl ester.

The medium polar fraction of the differently long aged oleic acid methyl ester is shown in Figure 62 (b). The amount of the un-aged medium polar fraction is just 2% of the total un-aged sample. So the area under the green line (0 hours aged) is much smaller than the area under the two polar fraction graphs, which have an amount of 60% or 73% in the sample. The longer aged sample (42 hours, black line) has a higher peak area with smaller retention times than the graph of the sample aged for 21 hours and so a higher molecular mass. Also peaks with a higher retention time than the methyl ester were found. These peaks come from molecules with a lower molecular mass and are fragments of the oxidation. The maximum of the sample aged for 21 hours (violet) is in the range from 21 to 22 minutes and comes from methyl ester or its oxidized derivatives. With the longer aging time this peak gets smaller so the molecules get oligomerized (smaller retention times) or fragmented (bigger retention times).

The strong polar fraction (Figure 62 (c)) shows similar results to the medium polar fraction. The retention times of the peaks found are lower, and therefore the molecular masses higher, than in the medium (b) or nonpolar fraction (a). The shape of the sample aged for 21 hours (violet) is a result of a too low concentration for the refraction index detector. To get the correct scale for the area correlation in this figure, this graph has to be magnified extremely. Therefore small differences or a drift in the baseline have a big influence to the results. The chromatogram is not that exact and just should give a hint for the molecular masses in its sample. However, Figure 62 (c) as Figure 62 (b) shows that with a longer aging time a shift to higher molecular masses happens.
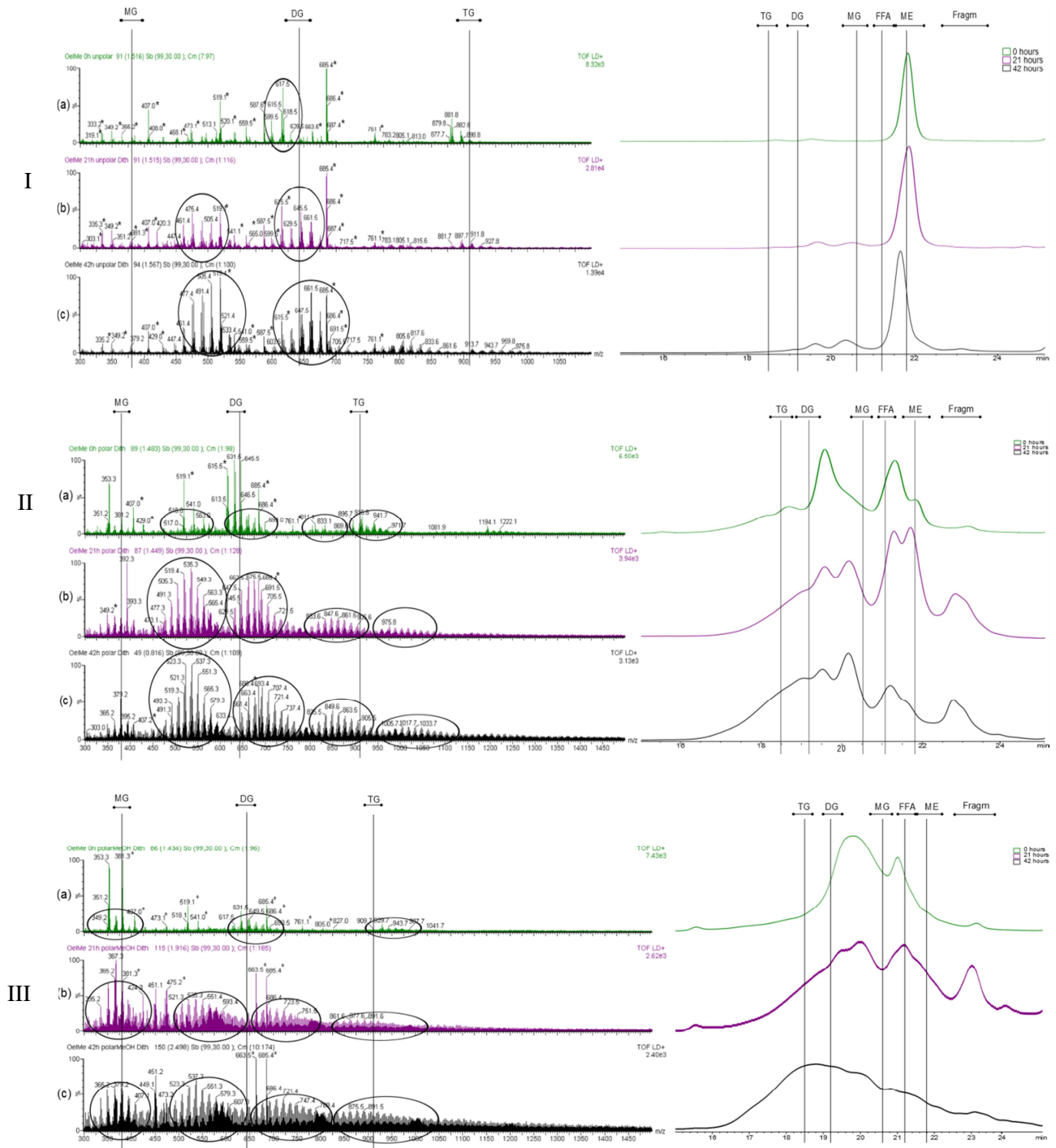
Figure 63: MALDI-TOF-MS (left) in comparison to SEC (right). The plotted marks correlate to the mass or the retention time of the standards used. TG (Triglycerid), DG (Diglycerid), MG (Monoglycerid), FFA (free fatty acid), ME (Methyl ester) and Fragm (Fragment)

The vertical lines in the MALDI-TOF-MS (Figure 63, left side) represent the masses of the triolein (TG), diolein (DG), and monoolein (MG) standards with an attached Na$^+$-ion (M: 23 g/mol) which is needed for the measurement. All peaks in this figure have this Na$^+$-ion because of the ionization. The standards should give an approximate estimation of the molecular masses (left side) to the retention times of the SEC (right side). In the MALDI-TOF-MS measurements the molecular masses increase from left to right while in the SEC-analysis the mass is decreasing with a higher retention time.

In Figure 63, the SEC-results (right side) are not shown in their ratio to their content in the sample (Table 42), but they are normalized to the highest peak of the chromatogram. This correlates better to the MALDI-TOF-MS results.

The nonpolar fraction of the oleic acid methyl ester samples is shown in Figure 63 (I). The oleic acid methyl ester is not detected in the MALDI-TOF-MS measurement. But all the other the peaks could be found with both analytical procedures. The peaks do not match exactly because of their different kind of linkage. While the used standards are linked via an ester group at the end of the fatty acid with glycerin, the formed oligomers are connected in the middle of each carbon chain with an undefined amount of oxygen. This gives a different shape and also size of the molecule and leads to this little shift.

In the SEC-analysis the stronger aged nonpolar sample (42 hours, Figure 63 (I), black) shows an increase of the baseline before the TG marker and also the MALDI-TOF-MS measurement shows peaks after the TG marker. Single molecule peaks found in the MALDI-TOF-MS are summarized to peak groups and both analytical methods show the same peak area ratios. The aged samples have two groups between the MG and almost to the DG marker in both procedures and further a small amount of a much higher masses than the TG standard.

Figure 63 (II) and (III) show the medium and strong polar fraction of the oleic acid methyl ester samples. In both analytical procedures, especially in the aged samples, molecules with a higher molecular mass than the TG are present. The retention times of the polar peaks in the SEC analysis are getting slightly lower with higher polarity and aging time. And also the MALDI-TOF-MS measurements show this trend.

The SEC result of the strong polar fraction (Figure 63 (III)) has no clear peaks because of the overlapping peak width of different peaks. The broad peak width comes from the big variety of molecules in these samples. And also the peaks found by MALDI-TOF-MS has wide regions with slightly higher masses (marked in circles) followed by or overlapped with the next regions.

4.8 Further Reactions of the Epoxides as Aging Products

Because of the fact that epoxides are one of the major oxidation products, a reaction was performed to show that these epoxides are also quite reactive at even 70°C (reflux hexane) and can also give further aging products. The Racimat conditions are even harsher with 110°C and a permanent oxygen flow.

Formic and acetic acid were added to the reaction mixture, because these acids also occur during the aging of biodiesel. In the Rancimat accelerated aging, these acids are formed in B100 biodiesel to an amount of $0.56\%_{m/m}$ for formic and $0.14\%_{m/m}$ for acetic acid after an aging time of 12 hours. About 98% of formic and 65% of the acetic acid are stripped out of the biodiesel system and are collected in the water vessel [84], but in a closed system like the PetroOxy, these acids remain in the biodiesel system and can further react with aging products or catalyzes aging reactions.
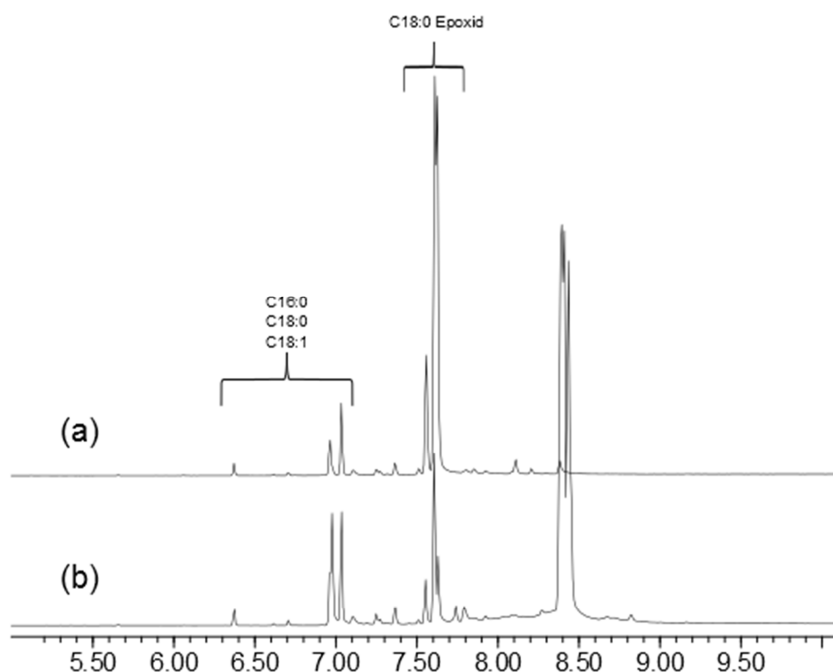
Figure 64: GC-MS from (a) a prepared epoxide out of oleic acid and (b) this epoxide after the reaction with formic and acetic acid.

The chromatograms (Figure 64) show that a new peak at 8.4 min appears after the treatment of the epoxide with formic and acetic acid. The comparison of the database gives a molecule with two hydroxyl-groups at the carbons 9 and 10. So the oxidized aging product out of oleic acid methyl ester can also react further and give also a still reactive molecule with functional hydroxyl-groups.
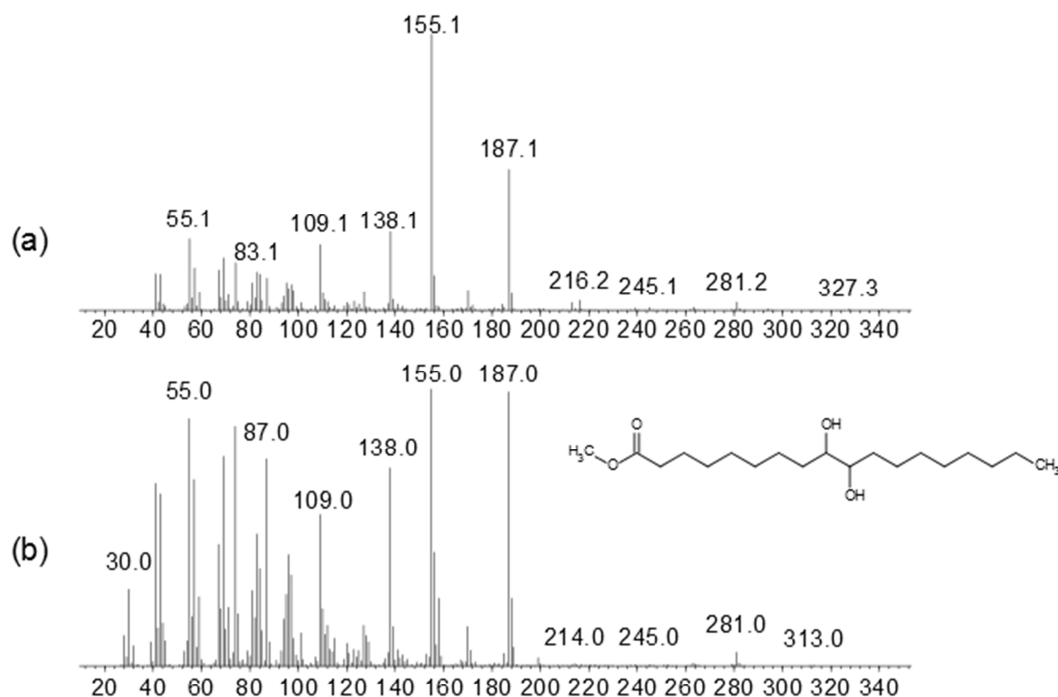
Figure 65: Mass spectra of (a) GC-MS Peak at retention time 8.4 min (b) reference spectra of the database

The formed molecule is identified as 9,10-dihydroxy stearic acid methyl ester. The reaction was performed in an excess of formic and acetic acids. These acids have a purity of 98% or 96% and introduce a certain amount of water. The found diol is formed by the nucleophilic addition of water to the epoxide. The added acids catalyze the ring opening reaction with the nucleophile [85].

Due to the diol structure, further reaction steps are possible like the esterification with an acid, dimerization [86], fragmentation at the carbons 9 and 10 or the building of a lactone (Table 38 no. 15 and no. 18).

4.9   Esterification of aged Oleic acid methyl ester

4.9.1   GC-TOF-MS

The three fractions of oleic acid methyl ester aged for 21 hours were analyzed with a GC-TOF-MS after the saponification, esterification and sample clean up steps.

Molecules with a high molecular mass like the oligomers cannot be detected by gas chromatography because of their high boiling points. The reaction should break the oligomers in smaller molecules for the detection for the GC. All ester linkages of oligomers to fragments or other methyl esters are broken in the saponification step. For the injection in the GC-TOF-MS, the second reaction step produces the methyl esters out of the fatty acid salts. It can be assumed, that these reaction steps should give new peaks in the chromatogram and these new methyl ester peaks should be fragments or monomers previously attached to an oligomer.
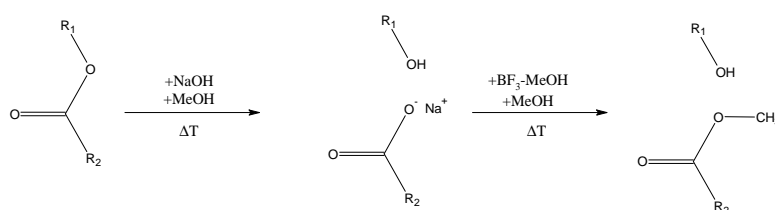
Figure 66: Reaction scheme of the saponification and re-esterification step. R_1 is the oligomer and R_2 is the carbon chain of the newly formed methyl ester

The reaction scheme (Figure 66) shows, how it is possible that new peaks appear in the gas chromatogram. While a fragment is bound to an oligomer, it cannot get detected. After the reaction steps it is possible to detect the newly formed methyl esters.

The previous GC-TOF-MS analysis (4.7.1) identified some aging products with a free carboxylic acid as functional group. These existing carboxylic acids also get methylated in the esterification step. They have a lower retention time because of the lower polarity and higher volatility. Therefore not all of the new peaks are molecules originating from an oligomer.

97
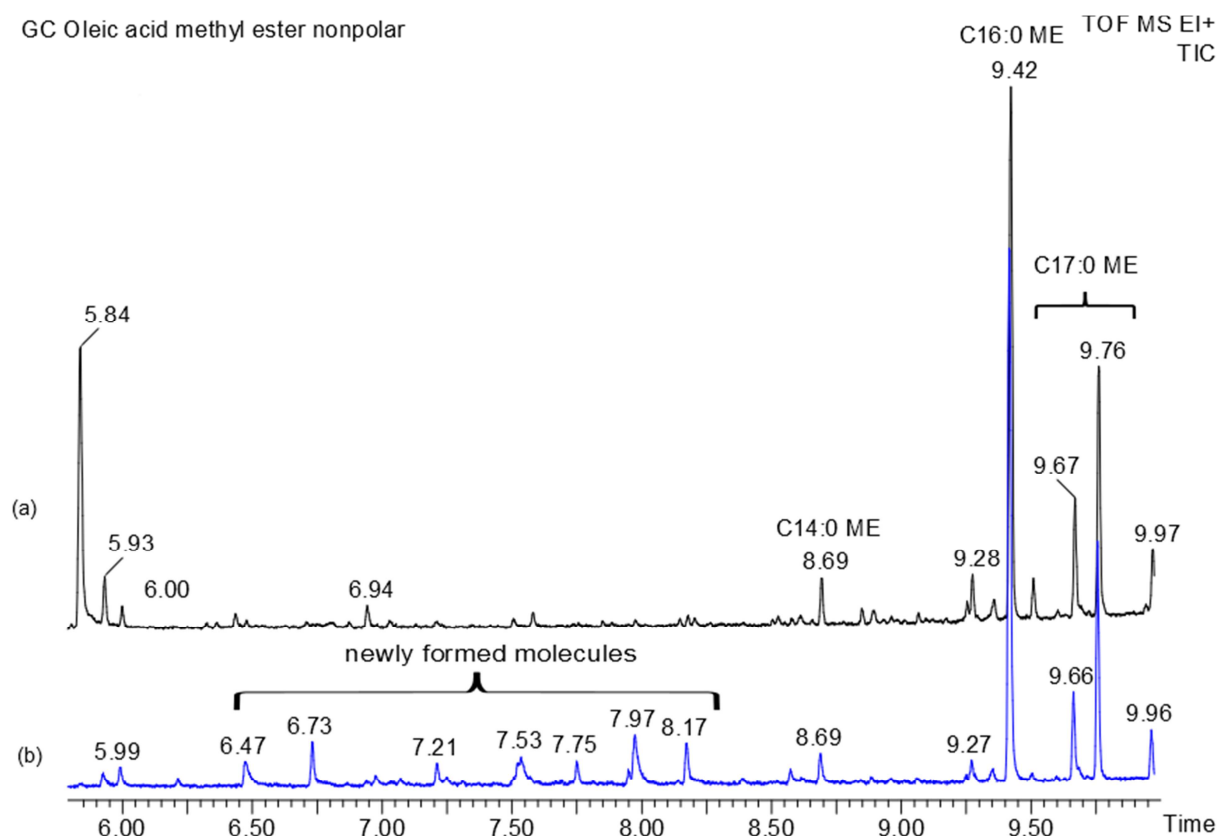
Figure 67: GC-TOF-MS –analysis of the nonpolar fraction of the oleic acid methyl ester aged for 21 hours before (a, black) and after the saponification and re-esterification steps (b, blue); retention time: 6-10 Minutes.
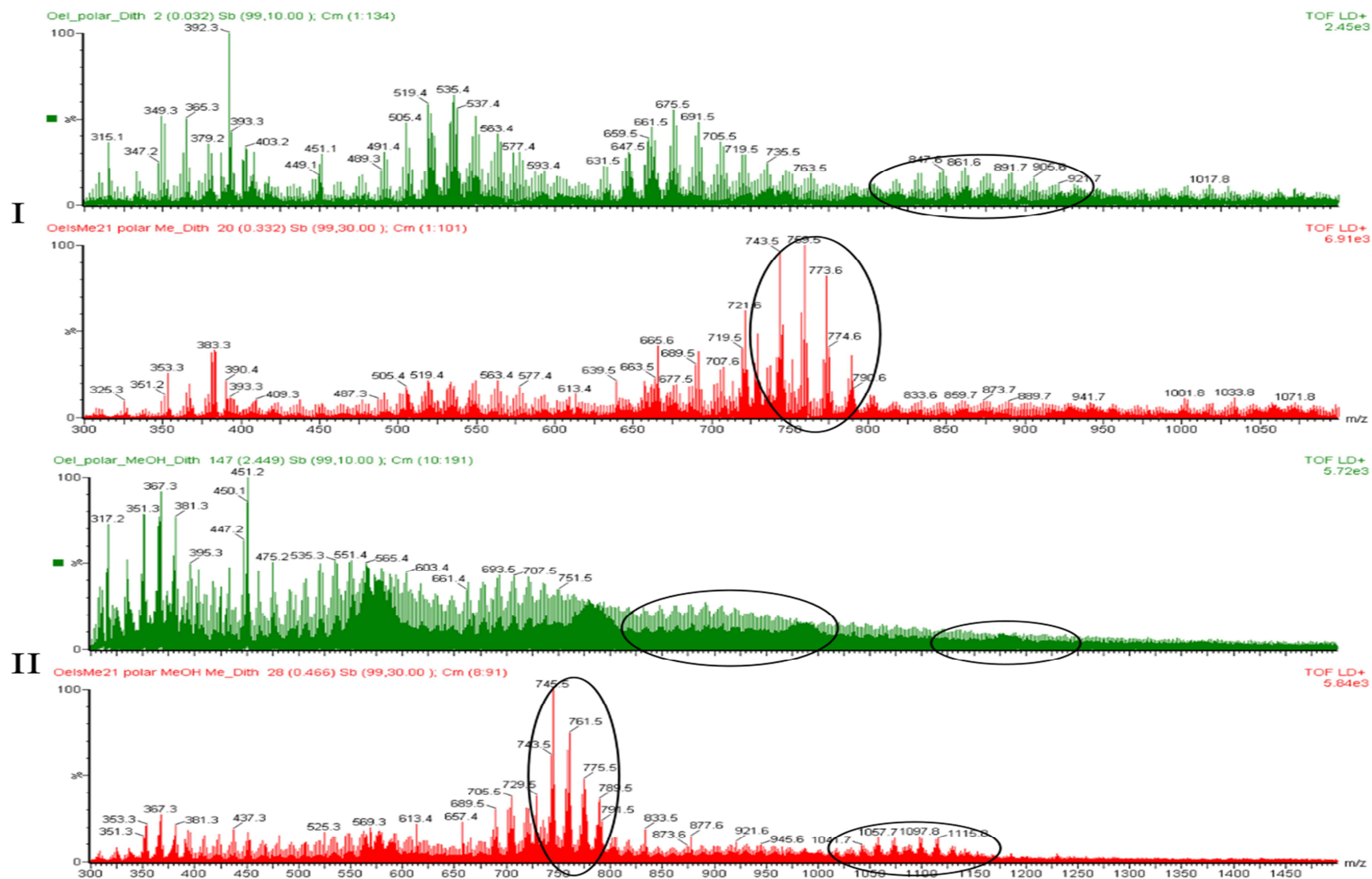
After the saponification and esterification step some new peaks occur in the GC chromatogram. These newly formed molecules are dimethoxy acetals and dicarboxylic acid methyl esters. The dimethoxy acetals have a carbon chain length from 8-10 and are formed during the esterification step out of the respective aldehydes [87]. Also dicarboxylic acid methyl esters with 8-10 carbon atoms in their chain could be found. It is possible, that the dicarboxylic acids originate from the oligomers, which are linked with a fragment via an ester. During the saponification step the sodium salts were created and while the esterification, dicarboxylic acid methyl esters were produced. Before the reaction steps, the respective acids of these newly formed methyl esters cannot be detected, or are in a too low concentration in the sample. Therefore, these methyl esters are probably from an oligomer.

Table 47: Identified molecules after the saponification and re-esterification steps

Retention time [min]	Molecule
6.47	C9:0 ME
6.73	1,1 Dimethoxy octane
7.21	1,1 Dimethoxy nonane
7.53	Octane dioic acid dimethyl ester
7.75	6,6 Dimethoxy octanoic acid methyl ester
7.97	Nonanedioic acid dimethyl ester
8.17	1,1 Dimethoxy decane
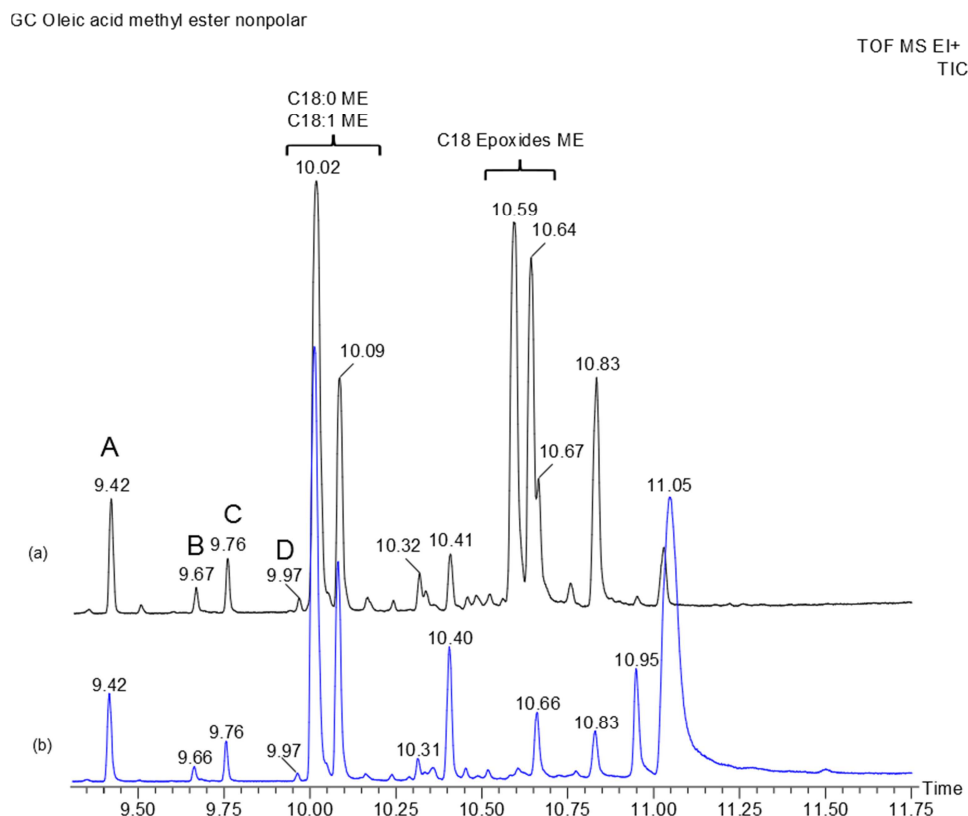
Figure 68: GC-TOF-MS –analysis of the nonpolar fraction of the 21 hours aged oleic acid methyl ester before (a, black) and after the saponification and re-esterification steps (b, blue). 9-12 Minutes

Most of the peaks in the chromatogram (Figure 68) do not change after the reaction steps (like the oleic or stearic acid methyl esters). The biggest differences are that the stearic acid methyl ester epoxides (retention time 10.59 and 10.64 minutes) react during the saponification step and are not found in the chromatogram after the reaction steps. The reactivity of epoxides is shown in section 4.8. Furthermore a new peak with a retention time of 10.95 minutes is found and a big new peak occurs with a retention time of 11.05 minutes.

The peak with the retention time of 11.05 minutes is an hydroxy methoxy stearic acid methyl ester isomer. This is probably the reaction product of the reaction of the epoxides and the saponification and re-esterification step [88], [89]. The further reactivity of the formed epoxides as aging products is shown in section 4.8.

The peak area ratios of the C18:0 and C18:1 methyl esters are bigger compared to the peaks A-D after the reaction steps. So it is possible, that also some of the C18:0 and C18:1 methyl ester molecules in the blue graph (b) are from an oligomer before the saponification step (a). The peak area ratio of C18:0 to C18:1 methyl ester remains constant before and after the reaction steps. During the reaction the amount of C18:0 and C18:1 methyl ester increases compared to the other molecules.
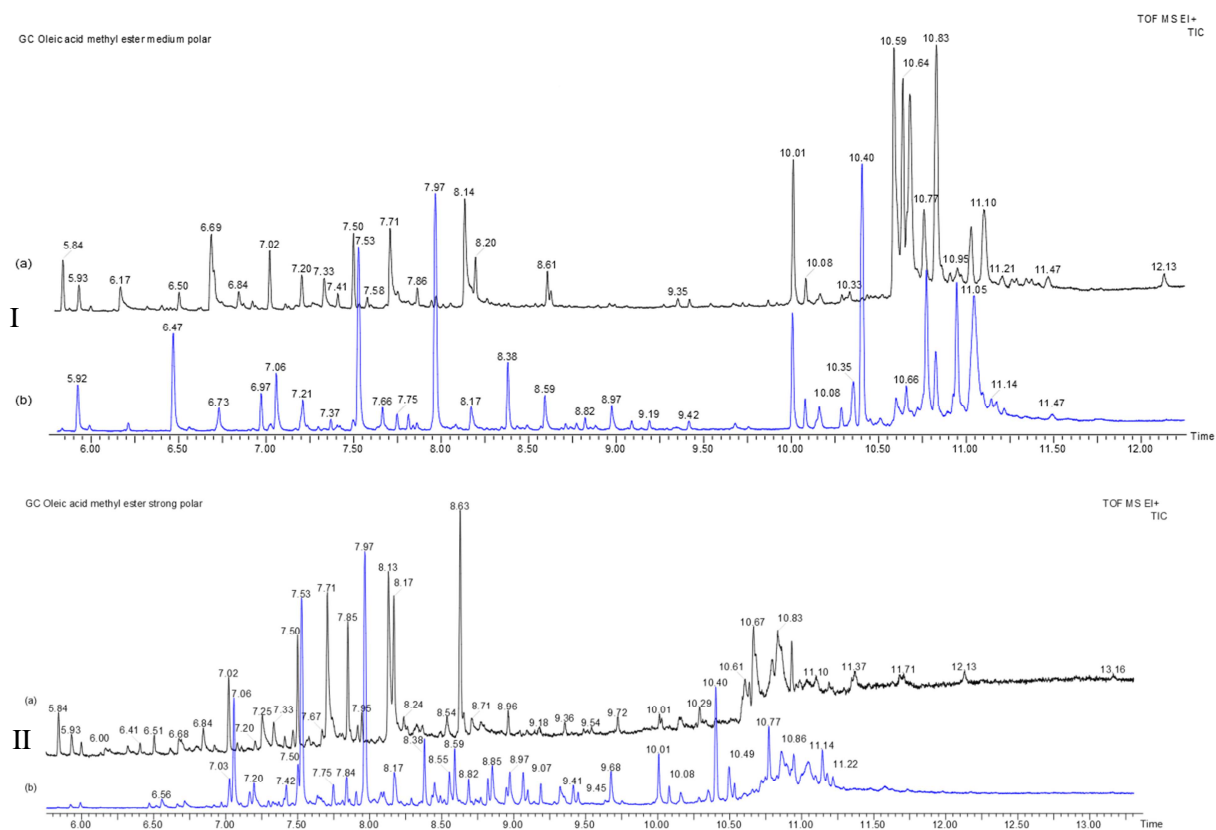
Figure 69: GC-TOF-MS–analysis of the medium (I) and strong polar (II) fraction of the oleic acid methyl ester aged for 21 hours before (a, black) and after the saponification and re-esterification steps (b, blue).

In both polar fractions (Figure 69) a lot of newly formed molecules occur in high amounts. Table 48 lists some of the molecules with the highest peak areas of these newly formed peaks and also their appearance in the nonpolar fraction.

Table 48: Some newly formed molecules after the saponification and re-esterification steps, n.i.: not identified

Retention time [min]	Molecule	nonpolar fraction	medium polar fraction	strong polar fraction
6.47	C9:0 ME	X	X	
7.06	Heptanedioic acid dimethyl ester		X	X
7.53	Octanedioic acid dimethyl ester	X	X	X
7.97	Nonanedioic acid dimethyl ester	X	X	X
8.38	Decanedioic acid dimethyl ester		X	X
10.40	n.i. seems that 2 peaks are overlapping	X	X	X
10.77	n.i.		X	X

The C9:0 methyl ester is just found in the medium polar fraction in relatively high amounts after the reaction steps, while in the strong polar fraction a really small peak of this methyl ester appears. But the respective C9:0 acid was also identified in the medium polar fraction before the reaction. Therefore, this methyl ester is probably just the methylated acid from the original sample. The C9:0 acid was in a lower amount in the strong polar fraction than in the medium polar. And also the newly formed C9:0 methyl ester occurs in a very small amount after the reaction.

Most of the new peaks in both polar fractions are dimethyl esters of dicarboxylic acids with a carbon chain length of 7-10. Their appearance in the chromatograms shows that the fragments of oleic acid methyl esters react to an unidentified dimer or oligomer. But it is also possible that these methyl esters are resulting from the identified acids before the reaction. These acid peaks disappear in the second (blue) chromatogram, so they react to the methyl ester in the methylation step. The detector response factors of the GC-TOF-MS of all the free acids to the respective methyl esters are unknown. If all of the found molecules are from these acids, or if there are more additional methyl esters from an oligomer is impossible to say without the correlating response factors for this method.

The peak at a retention time of 10.40 minutes seems to be a co-elution of two different molecules because the left and right shoulder of this peak shows different ionization fragments.

4.9.2 MALDI-TOF-MS

All the three fractions of oleic acid methyl ester aged for 21 hours were also analyzed after the saponification and esterification step by MALDI-TOF-MS. With the comparison of the mass spectra before these reaction steps it should be possible to identify if there are differences in the oligomeric regions and if there is a mass decrease because of the loss of the fragments linked by ester bonds or methyl esters to an oligomer during the reaction step.

Also here, as in the comparison of the aging process with longer aged methyl ester (4.7.2), the same MALDI-TOF-MS method was used with the best results for all of the different fractions and not the best for each of the fractions. With the same method the results are better to compare with each other, but also the mass accurateness decreases.

The comparison of the nonpolar fractions of oleic acid methyl ester aged for 21 hours before and after the saponification and esterification step is shown in Figure 70. The biggest differences are highlighted in the marked areas.

The oligomeric molecule groups in the mass range of 890-950 g/mol cannot be identified after the reaction step and also the molecule groups in the mass range 780-840 g/mol are significantly reduced. Furthermore, a new oligomeric molecule group appears in a high amount next to the other existing

groups in the mass range of 700-800 g/mol after the reaction steps. A loss of a fragment or a whole oleic acid methyl ester derivative seems to be possible and explains this mass shift of the oligomers.

Further new molecule groups are found in the mass range of 350-400 g/mol. Oxidized species of oleic acid methyl esters or two fragments linked together can reach this mass range. But also a loss of a fragment of the dimers in a mass range of 500-530 or a monomer of the dimers at 610-700 could be possible to produce these molecule groups.

The other two still existing molecule groups with the mass range of 460-530 and 600-700 g/mol do not change their position in the mass range a lot but the discrete mass group peaks seem to be wider. Because of the soft ionization method of the MALDI each molecule creates its own mass peak and no fragmentation occur during the ionization. A wide mass group peak indicates therefore that far more molecules are produced in these mass areas.
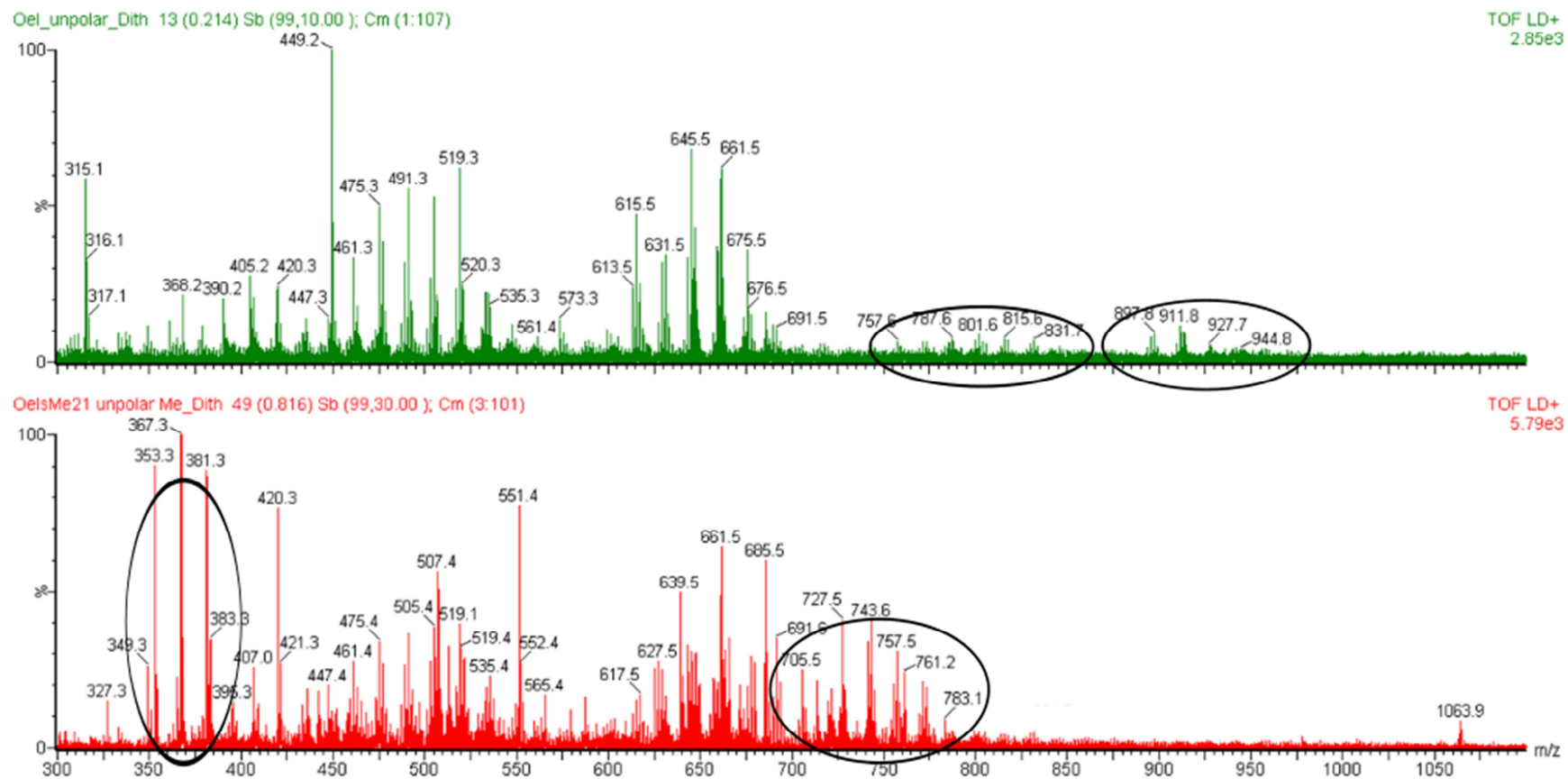
Figure 70: MALDI-TOF Mass spectra of the nonpolar fraction of oleic acid methyl ester aged for 21 hours (before (green) and after (red) the saponification and esterification step)

Figure 71: MALDI-TOF Mass spectra of the medium (I) and strong (II) polar fraction of oleic acid methyl ester aged for 21 hours (before (green) and after (red) the saponification and esterification step)

The MALDI-TOF-MS results of both polar fractions, the medium (I) and the strong (II) polar fractions after the reactions steps are shown in Figure 71. And also here the biggest differences in the mass spectra are highlighted in the marked areas.

The outstanding difference of the comparison with the received mass spectra before and after the reaction steps in the medium polar fraction (I in Figure 71) is the occurrence of a new peak group in the mass range of 720-800 g/mol in a high amount. Furthermore, a decrease of the peaks in the mass range of 850-920 g/mol after the reaction occurs.

The reduction of the peak group in the mass range of 850-950 g/mol and the occurrence of a new peak group in the range of 720-800 g/mol is also found in the strong polar fraction (II) after the reaction step. Additionally the peak group with a mass of 1150-1220 g/mol is reduced and cannot be identified as an individual group, but a new group occurs at 1020-1120 g/mol during the reaction.

These shifts may result from the loss of a fragment group from the original oligomer. Because of the reaction, these losses result from the breaking of ester linkages.

5   Summary and Outlook

As mentioned in the introduction, the aim of this work was the investigation of aging products formed during the accelerated aging in biodiesel and biodiesel/petrodiesel blends. It was focused on the higher molecular mass range with the formation of dimers and oligomers.

This could be achieved by the aging with a Rancimat device followed by column chromatography to separate polar compounds from the nonpolar biodiesel. It can be shown, that the polar content start to increase after reaching the IP of the B100 biodiesel and the B50 and B7 blends. A correlation of the aging time and formed polar compounds could be found. Surprisingly, a B50 blend forms almost the same amount of polar compounds as B100 biodiesel (65% and 58% respectively) and also the B7 blend forms 22% polar compounds after a prolonged aging time.

All the fractions were analyzed by SEC to quantify the dimeric content and the component distribution. In all the polar fractions of aged B100 biodiesel and B50 and B7 blends dimers could be found. The total dimeric content of B100 after an aging time of 42 hours was 55% of the initial sample. B50 has an amount of 38% and B7 an amount of 9% of dimers after a prolonged aging time.

The identification of aging products by high resolution mass spectroscopy was performed with aged oleic acid methyl ester. Various aging products could be identified by GC-TOF-MS, especially in the mass range of the formed fragments and oxidized monomers. An identification of dimers could not be achieved because of the unfavorable molecular structure, vaporization or ionization technique. Analyses by MALDI-TOF-MS show the formation of a high variety of dimers and also the presence of molecules with a much higher molecular mass (dimers linked with fragments and trimers). As a result of the high variety of these molecules wider peak groups than the few initially assumed dimers can be found. The molecules vary in different carbon lengths, linkage or oxidation stage. No preferred dimer as reference molecule for the aging of biodiesel could be identified. A correlation of the aging time and molecular weight could be found. A prolonged aging leads to molecules with a higher mass. Fatty acid dimers and also trimers could be identified as aging products.

A performed saponification and methylation reaction of the oligomers shows the type of the linkage of the monomers. This reaction breaks ester groups and the newly formed methyl esters can be identified by GC and MALDI-TOF-MS. The decrease of peaks after the reaction step and the formation of new peaks indicates the presence of ester-linked oligomers.

The formation of di- and oligomers as aging products in biodiesel is shown in this work. The biodiesel samples were B100 biodiesel, B50 and B7 biodiesel blend. Evidence was found that also the petrodiesel component forms oligomers. Further experiments with the petrodiesel B0 could support a deeper understanding of the formation of di- and oligomers in the blends. Furthermore an analysis by HPLC/LCMS where the samples do not have to be vaporized like in the GCMS could give additional information about the aging process of biodiesel.

6 List of Tables

7   List of Figures

8 Bibliography

[1] G. Knothe, J. Van Gerpen and J. Krahl, The Biodiesel Handbook, Champain, IL, USA: AOCS Press, 2005.

[2] E. Santacesaria, G. Martinez Vicente, M. Di Serio and R. Tesser, "Main Technologies in Biodiesel Production: State of the Art and Future Challenges," *Catalysis Today,* vol. 195, pp. 2-13, 2012.

[3] F. Ataya, M. A. Dubé and M. Ternan, "Acid-Catalyzed Transesterification of Canola Oil to Biodiesel under Single- and Two-Phase Reaction Conditions," *Energy and Fuels,* vol. 21, pp. 2450-2459, 2007.

[4] J. Van Gerpen, "Biodiesel Processing and Production," *Fuel Processing Technology,* vol. 86, pp. 1097-1107, 2005.

[5] W. Du, Y. Xu, D. Liu and J. Zeng, "Comparative Study on Lipase-Catalyzed Transformation of Soybean Oil for Biodiesel Production with different Acyl Accepors," *Journal of Molecular Catalysis B: Enzymatic,* vol. 30, pp. 125-129, 2004.

[6] M. Szczesna-Antczak, A. Kubiak, T. Antczak und S. Bielecki, „Enzymatic Biodiesel Synthensis - Key Factors affecting Efficiency of the Process," *Renewable Energy,* Bd. 34, pp. 1185-1194, 2009.

[7] U. Schuchardt, R. Sercheli and R. M. Vargas, "Transesterification of Vegetable Oils: a Review," *Journal of the Brazilian Chemical Society,* vol. 9, no. 1, pp. 199-210, 1998.

[8] A. Demirbas, "Biodiesel Production via Non-Catalytic SCF Method and Biodiesel Fuel Characteristics," *Energy Conversion and Management,* vol. 47, pp. 2271-2282, 2006.

[9] K. Bunyakiat, S. Makmee, R. Sawangkeaw und S. Ngamprasertsith, „Continous Production of Biodiesel via Transesterification from Vegetable Oils in Supercritical Methanol," *Energy and Fuels,* Bd. 20, pp. 812-817, 2006.

[10] R. A. Sheldon, "Green and sustainable Manufacture of Chemicals from Biomass: State of the Art," *Green Chemistry,* vol. 16, pp. 950-963, 2014.

[11] K. Schroeder und F. Shahidi, „Glycerin," in *Bailey´s Industrial Oil and Fat Products*, Hoboken, NJ, USA, John Wiley & Sons, Inc, 2005, pp. 6:191-6:223.

[12] Codex Standard for Named Vegetable Oils, *Codex Stan 210-1999,* 1999.

[13] S. Gärtner, G. Reinhardt and J. Braschkat, "ifeu- Institute for Energy and Environmental Research Heidelberg GmbH - Life Cycle Assessment of Biodiesel: Update and New Aspects," Heidelberg, Germany 2003. [Online]. Available: http://www.ifeu.de/landwirtschaft/pdf/rme-2003-study-ifeu.pdf. [Accessed 18 03 2014].

[14] G. Jungmeier, I. Kaltenegger, L. Canella and J. Spitzer, "Umweltbewertung der

Biodieselproduktion in der Steiermark im Vergleich zu mineralischem Diesel," Joanneum Research, Institut für Energieforschung, 2008.

[15] M. Quirin, S. Gärtner, M. Pehnt and G. Reinhardt, "ifeu- Institute for Energy and Environmental Research Heidelberg GmbH - CO2 Mitigation through Biofuel in the Transport Sector: Status and Perspectives," Heidelberg, Germany 2004. [Online]. Available: http://www.ifeu.de/landwirtschaft/pdf/co2mitigation.pdf. [Accessed 19 03 2014].

[16] E. A. Nanaki and C. J. Koroneos, "Comparative LCA of the use of biodiesel, diesel and gasoline for transportation," *Journal of Cleaner Production,* vol. 20, pp. 14-19, 2012.

[17] S. C. Davis, K. J. Anderson-Teixeira and E. H. DeLucia, "Life-cycle analysis and the ecology of biofuels," *Trends in Plant Science,* vol. 14, no. 3, pp. 140-146, 2009.

[18] European Parliament and Council, "Directive 2009/28/EC of the European Parliament and of the Council of 23 April 2009 on the promotion of the use of energy from renewable sources and amending and subsequently repealing Directives 2001/77/EC and 2003/30/EC, Article 3 (1)-(4)," Official Journal of the European Union, Brussels, Belgium, 2009.

[19] Fachagentur Nachwachsende Rohstoffe e.V. (FNR), "Basisdaten Bioenergie Deutschland," Gülzow, Germany Aug 2013. [Online]. Available: http://mediathek.fnr.de/media/downloadable/files/samples/b/a/basisdaten_9x16_2013 _web_neu2.pdf. [Accessed 03 03 2014].

[20] European Biodiesel Board, "Statistic of the EU biodiesel industry," Brussels, Belgium, 2013. [Online]. Available: http://www.ebb-eu.org/stats.php. [Accessed 03 03 2014].

[21] Observatoire des énergies renouvelables, "The State of Renewable Energies in Europe Edition 2013 13th EurObserv'ER Report," Paris, France 2013. [Online]. Available: http://www.energies-renouvelables.org/observ-er/stat_baro/barobilan/barobilan13-gb.pdf. [Accessed 03 03 2014].

[22] Verband der Deutschen Biokraftstoffindustrie e.V., "Factsheet Biodiesel," Berlin, Germany Nov. 2012. [Online]. Available: http://www.biokraftstoffverband.de/index.php/daten-und-fakten.html?file=tl_files/download/Daten_und_Fakten/factsheet_biodiesel.pdf. [Accessed 03 03 2014].

[23] European Committee for Standardization (CEN), *EN 590:2010 - Automotive fuels. Diesel. Requirements and test methods,* Brussels, Belgium, 2010.

[24] European Committee for Standardization (CEN), *EN 14214:2012+A1:2014, Liquid petroleum products - Fatty acid methyl esters (FAME) for use in diesel engines and heating applications - Requirements and test methods,* Brussels, Belgium, 2014.

[25] Volkswagen AG, VW-Selbststudienprogram 403- Der 2,0l-TDI-Motor mit Common-Rail-Einspritzsystem- Konstruktion und Funktion, Wolfsburg, Germany: http://www.motor-talk.de/forum/aktion/Attachment.html?attachmentId=714834& [Accessed 03 03 2014].

[26] J. Barker, P. Richards, C. Snape and W. Meredith, "Diesel Injector Deposits - An Issue that has evolved with Engine Technology," *Society of Automotive Engineers of Japan,* pp. SAE 2011-01-1923 , 2011.

[27] G. E. Smith, J. P. Grady und L. Grainawi, „Ultra Low Sulfur Diesel Sgtorage and Dispensing Systems - What the Railroad Industry needs to know about Corrosion," in *Arema - Annual Conference*, Minneapolis, MN, USA http://www.arema.org/files/library/2011_Conference_Proceedings/Ultra_Low_ Sulfur_Diesel_Storage_and_Dispensing_Systems-What_Railroad_Industry_Needs_to_Know-Corrosion.pdf [Accessed 21 03 2014], 2011.

[28] R. A. A. Munoz, D. M. Fernandes, D. Q. Santos, T. G. Barbosa, R. M. Sousa and Z. Fang, "Biodiesel: Production, Characterization, Metallic Corrosion and Analytical Methods for Contaminants," in *Biodiesel - Feedstocks, Production and Applications*, InTech - Open Science, 2012, pp. 129-176.

[29] Robert Bosch GmbH, "Diesel Systems- Common Rail System CRS1-16 mit 1600 bar und Magnetvntil-Injektoren," Stuttgard, Germany 2011. [Online]. Available: http://www.bosch-kraftfahrzeugtechnik.de/media/db_application/downloads/pdf/antrieb/de_5/ 04_DS_Sheet_Common_Rail_System_CRS1-16_mit_1600_bar_20110826.pdf. [Accessed 18 03 2014].

[30] E. N. Frankel, Lipid Oxidation, Bridgwater, UK: The Oily Press, 2005.

[31] S. Kubow, "Routes of Formation and toxic Consequences of Lipid Oxidation Products in Foods," *Free Radical Biology & Medicine,* vol. 12, pp. 63-81, 1992.

[32] C. Scrimgeur and F. Shahidi, "Chemistry of Fatty Acids," in *Bailey´s Industrial Oil and Fat Products*, Hoboken, NJ, USA, John Wiley & Sons, Inc, 2005, pp. 1:1-1:45.

[33] F. D. Gunstone and T. P. Hilditch, "The Union of Gaseous Oxygen with Methyl Oleate, Linoleate, and Linolenate," *Journal of the Chemical Society,* pp. 836-841, 1945.

[34] R. T. Holman and O. C. Elmer, "Rates of Oxidation of Unsaturated Fatty Acids and Esters," *Journal of the American Oil Chemists´Society,* vol. April, pp. 127-129, 1947.

[35] H. D. Belitz, W. Grosch and P. Schieberle, Lehrbuch der Lebensmittelchemie, Berlin, Germany: Springer-Verlag, 2001.

[36] H. W. Gardner, "Oxygen Radical Chemistry of Polyunsaturated Fatty Acids," *Free Radical Biology & Medicine,* vol. 7, pp. 65-86, 1989.

[37] M. H. Gordon, J. Pokorny and N. Yanishlieva, "The development of oxidative rancidity in foods," in *Antioxidants in food*, Cambridge, UK, Woodhead Publishing Ltd, 2001, pp. 7-21.

[38] K. M. Schaich und F. Shahidi, „Lipid Oxidation: Theoretical Aspects," in *Bailey´s Industrial Oil and Fat Products*, Hoboken, NJ, USA, John Wiley & Sons, Inc, 2005, pp. 1:269 - 1:3556.

[39] H. P. Kaufmann, H. Gruber and H. Brüning, "Diels-Alder-Reaktionen auf dem Fettgebiet," *Fette-Seifen-Anstrichmittel,* vol. 63, no. 7, pp. 633-636, 1961.

[40] A. Maschka and G. Müller, "Modellversuche zum Standölprozeß," *Monatshefte für Chemie und verwandte Teile anderer Wissenschaften,* vol. 86, no. 3, pp. 397-407, 1955.

[41] M. Arca, B. K. Sharma, N. P. Price, J. M. Perez and K. M. Doll, "Evidence Contrary to the Accepted Diels-Alder Mechanism in the Thermal Modification of Vegetable Oil," *Journal of the American Oil Chemists´Society,* vol. 89, pp. 987-994, 2012.

[42] H.-S. Hwang, K. M. Doll, J. K. Winkler-Moser, K. Vermillion und S. X. Liu, „No Evidence Found for Diels–Alder Reaction Products in Soybean Oil Oxidized at the Frying Temperature by NMR Study," *Journal of the American Oil Chemists' Society,* Bd. 90, pp. 825-834, 2013.

[43] M. V. Ruiz-Méndez, S. Marmesat, A. Liotta and M. C. Dobarganes, "Analysis of used Frying Fats for the Production of Biodiesel," *Grasas y Aceites,* vol. 59, no. 1, pp. 45-50, 2008.

[44] G. G. Pereira, S. Marmesat, D. Barrera-Arellano and M. C. Dobarganes, "Evolution of Oxidation in Soybeanoil and its Biodiesel under the Conditions of the Oxidation Stability Test," *Grasas y Aceites,* vol. 64, no. 5, pp. 482-488, 2013.

[45] K. M. Schaich, "Thinking outside the Classical Chain Reaction Box of Lipid Oxidation," *Lipid Technology,* vol. 24, no. 3, pp. 55-58, 2012.

[46] R. Boensch, W. Kastl, P. Mitschke und H. Saft, „Method for Improving the Long Term Stability of Biodiesel". Germany Patent WO2004053036 (A1), 24 06 2004.

[47] N. A. Santos, A. M. Cordeiro, S. S. Damasceno, R. T. Aguiar, R. Rosenhaim, J. R. Carvalho Filho, I. M. Santos, A. S. Maia and A. Souza, "Commercial Antioxidants and Thermal Stability Evaluation," *Fuel,* vol. 97, pp. 638-643, 2012.

[48] S. Jain and M. P. Sharma, "Effect of Metal Contents on Oxidation Stability of Biodiesel/ Diesel Blends," *Fuel,* vol. 116, pp. 14-18, 2014.

[49] S. Schober and M. Mittelbach, "The Impact of Antioxidants on Biodiesel Oxidation Stability," *European Journal of Lipid Science and Technology,* vol. 106, pp. 382-389, 2004.

[50] M. Mittelbach and S. Schober, "The Influence of Antioxidants on the Oxidation Stability of Biodiesel," *Journal of the American Oil Chemists´ Society,* vol. 80, pp. 817-823, 2003.

[51] European Committee for Standardization (CEN), *EN 15751:2014, Automotive fuels - Fatty acid methyl ester (FAME) fuel and blends with diesel fuel - Determination of oxidation stability by accelerated oxidation method,* Brussels, Belgium, 2014.

[52] S. Flitsch, P. Neu, S. Schober and M. Mittelbach, "Time-resolved Characterization of Aging Products from Biodiesel," in *[Poster] 15. Austrian Chemistry days*, Graz, Austria, 2013.

[53] European Committee for Standardization (CEN), *EN 16091:2011, Liquid petroleum products - Middle distillates and fatty acid methyl ester (FAME) fuels and blends - Determination of oxidation stability by rapid small scale oxidation method,* Brussels, Belgium, 2011.

[54] L. S. Ettre, "Nomenclature for Chromatography (IUPAC Recommendations 1993)," *Pure and Applied Chemistry,* vol. 65, no. 4, pp. 819-872, 1993.

[55] K. Schwetlick, Organikum organisch- chemisches Grundpraktikum 21. Edition, Weinheim, Germany: Wiley-VCH Verlag GmbH, 2001.

[56] S. Kromidas, M. Quaglia, E. Machtejevas, T. Hennessy and K. K. Unger, "Gelfiltration-Größenausschluss-Chromatographie von Biopolymeren-Optimierungsstrategien und Fehlersuche," in *HPLC richtig Optimiert- EinHandbuch für Praktiker*, Weinheim, Germany, WILEY-VCH Verlag GmbH & Co. KGaA, 2006, pp. 397-418.

[57] A. M. Striegel, W. W. Yau, J. J. Kirkland and D. D. Bly, Modern Size-Exclusion Liquid Chromatography- Practice of Gel Permeation and Gel Filtration Chromatography - Second Edition, Hoboken, New Jersy, USA: John Wiley & Sons, Inc, 2009.

[58] Phenomenex, "A User´s Guide to Gel Permeation Chromatography - Technical Notes 3," Torrance, CA, USA 2000. [Online]. Available: http://phx.phenomenex.com/lib/PEG19951_Gel%20Permeation%20guide.pdf. [Accessed 06 03 2014].

[59] J. H. Gross, Mass Spectrometry- ATextbook 2nd Edition, Heidelberg, Germany: Springer Verlag, www.ms-textbook.com [Accessed 13 03 2014], 2011.

[60] E. de Hoffmann und V. Stroobant, Mass Spectrometry- Principles and Applications- Second Edition, Chichester, UK: John Wiley & Sons Ltd, 2002.

[61] H.-. J. Hübschmann, Handbook of GC/MS- Fundamentals and Applications, Weinheim, Germany: Wiley-VCH Verlag GmbH & Co KGaA, 2009.

[62] The American Society for Testing and Materials, Index of Mass Spectral Data, Philadelphia, USA, 1969.

[63] W. W. Christie, "The AOCS Lipid Library- Mass Spectrometry of Fatty Acid Derivates," 02 2014. [Online]. Available: http://lipidlibrary.aocs.org/ms/masspec.html. [Accessed 11 03 2014].

[64] National Institute of Standards and Technology, *NIST Standard Reference Database- Main EI MS library with Search Program,* Gaithersburg, MD, USA: http://www.nist.gov/srd/nist1a.cfm, [Accessed 11 03 2014].

[65] John Wiley & Sons Inc, *Wiley Registry of Mass Spektra Data,* Hoboken, NJ, USA: http://onlinelibrary.wiley.com/book/10.1002/9780470175217, [Accessed 06 03 2014].

[66] K. P. Vollhardt und N. E. Schore, Organic Chemistry- Third Edition, Weinheim, Germany: Wiley-

VCH Verlag GmbH, 2000.

[67] X. Chen, J. A. Carroll und R. C. Beavis, „Near-Ultraviolet-Induced Matrix-Assisted Laser Desorption/Ionization as a Function od Wavelength," *American Society for Mass Spectrometry,* Bd. 9, pp. 885-981, 1998.

[68] Y. Zhen, N. Xu, B. Richardson, R. Becklin, J. R. Savage, K. Blake and J. M. Peltier, "Development of an LC-MALDI Method for the Analysis of Protein Complexes," *American Society for Mass Spectrometry,* vol. 15, pp. 803-822, 2004.

[69] M. C. McMaster, GC/MS- A Practical User´s Guide- Second Edition, Hoboken, NJ, USA: John Wiley & Sons, Inc, 2008.

[70] H. E. Zimmer and C. Döring, "Optimisation of Drying Processes in the Pharmaceutical Industry," in *17th International Drying Symposium*, Magdeburg, Germany, 2010 http://www.in-process.com/uploads/IDS_Magdeburg_2010_IPI_1ca.pdf [Accessed 11 03 2014].

[71] A. W. Bristow and K. S. Webb, "Intercomparison Study on Accurate Mass Measurement of Small Molecules in Mass Spectrometry," *American Society for Mass Spectrometry,* vol. 14, pp. 1086-1098, 2003.

[72] S. Broecker, Dissertation - Aufbau und Anwendung einer Methode zur Identifizierung und Quantifizierung von Giften und deren Metaboliten in Blut und Haaren in der Systematischen Toxikologischen Analyse mittels LC-QTOF-MS, Humboldt-Universität, Berlin, Germany, 2012.

[73] I. Ojanperä, A. Pelander, S. Laks, M. Gergov, E. Vuori and M. Witt, "Application of Accurate Mass Measurement to Urine Drug Screening," *Journal of Analytical Toxicology ,* vol. 29, pp. 34-40, 2005.

[74] D. H. Russell and R. D. Edmondson, "High-resolution Mass Spectrometry and Accurate Mass Measurements with Emphasis on the Characterization of Peptides and Proteins by Matrix-assisted Laser Desorption/Ionization Time-of-Flight Mass Spectrometry," *Journal of Mass Spectrometry,* vol. 32, pp. 263-276, 1997.

[75] M. P. Balogh, "A Mass Spectrometry Primer, Part III," *LCGC North America,* no. Dec 2008 http://www.chromatographyonline.com/lcgc/article/ articleDetail.jsp?id=570536&pageID=1&sk=&date= [Accessed 12 03 2014].

[76] The American Oil Chemists' Society, *AOCS Official Method Cd 20-91, Determination of Polar Compounds in Frying Fats,* Urbana, Illinous, USA, 1991.

[77] Deutsche Gesellschaft für Fettwissenschaft e.V., *DGF-Standard Methods C-III 3c (10), Polymerized Triacylglycerols, Determination in severely heat stressed Fats and Oils (deep-frying fats) by High-Performance Size-Exclusion Chromatography (HPSEC),* Münster, Germany: Wissenschaftliche Verlagsgesellschaft mbH Stuttgart, Germany, 2010.

[78] Deutsche Gesellschaft für Fettwissenschaft e.V., *DGF-Standard Methods C-VI 11a (98), Fatty acid methyl ester, Bortrifluorid methode,* Münster, Germany: Wissenschaftliche Verlagsgesellschaft mbH Stuttgart, Germany, 1998.

[79] G. Joshi, B. Y. Lamba, D. S. Rawat, S. Mallick und K. Murthy, „Evaluation of Additive Effects on Oxidation Stability of Jatropha Curcas Biodiesel Blends with Conventional Diesel Sold at Retail Outlets," *Industrial & Engineering Chemistry Research,* Bd. 52, Nr. 22, pp. 7586-7592, 2013.

[80] A. Munack, M. Petchatnikov, L. Schmidt and J. Krahl, "Spektroskopische Untersuchung zur Ergründung der Wechselwirkungen zwischen Biodiesel und Dieselkraftstoff bei Blends," J.H.v.Thünen-Institut-VDB Verband der Deutschen Biokraftstoffindustrie e.V., Braunschweig, Germany, 2009.

[81] P. M. Neu, *unpublisched data.*

[82] E. Mubiru, K. Shrestha, A. Papastergiadis and B. De Meulenaer, "Improved Gas Chromatography-Flame Ionization Detector Analytical Method for the Analysis of Epoxy Fatty Acids," *Journal of Chromatography A,* vol. 1318, pp. 217-225, 2013.

[83] J. Velasco, O. Berdeaux, G. Márquez-Ruiz and M. C. Dobarganes, "Sensitive and Accurate Quantitation of Monoepoxy fatty acids in Thermoxidized Oils by Gas-Liquid Chromatography," *Journal of Chromatography A,* vol. 982, pp. 145-152, 2002.

[84] S. Flitsch, P. M. Neu, S. Schober, N. Kienzl, J. Ullmann and M. Mittelbach, "Quantitation of Aging Products formed in Biodiesel during the Rancimat accelerated Oxidation Test," Manuscript submitted.

[85] G. J. Piazza, A. Nunez and T. A. Foglia, "Hydrolysis of Mono- and Diepoxyoctadecanoates by Aluminia," *Journal of the American Oil Chemists' Society,* vol. 80, no. 9, pp. 901-904, 2003.

[86] B.-J. K. Ahn, S. Kraft and X. S. Sun, "Chemical Pathways of epoxidized and hydroxylated Fatty acid methyl esters and triglycerides with phosphoric acid," *Journal of Materials Chemistry,* vol. 21, pp. 9498-9505, 2011.

[87] Y. Tanaka, N. Sawamura and M. Iwamoto, "Highly Effective Acetalization of Aldehydes and Ketones with Methanol on Siliceous Mesoporous Material," *Tetrahedron Letters,* no. 39, pp. 9457-9460, 1998.

[88] D. Swern, G. N. Billen and J. T. Scanlan, "Chemistry of Epoxy Compounds. V. Preparation of some Hydroxy-ethers from 9,10-Epoxystearic Acid and 9,10-Epoxyoctadecanol," *Journal of the American Chemical Society,* vol. 70, pp. 1226-1228, 1948.

[89] M. Guidotti, R. Psaro, N. Ravasio, M. Sgobba, F. Carniato, C. Bisio, G. Gatti and L. Marchese, "An Efficient Ring Opening Reaction of Methyl epoxystearate promoted by synthetic Acid Saponit Clay," *Green Chemistry,* vol. 11, pp. 1173-1178, 2009.

[90] H. Tang, A. Wang, S. O. Salley and K. Y. S. Ng, "The Effect of Natural and Synthetic Antioxidants on the Oxidative Stability of Biodiesel," *Journal of the American Oil Chemists' Society,* vol. 85, no. 4, pp. 373-382, 2008.

[91] Y. C. Liang, C. Y. May, C. S. Foon, M. A. Ngan, C. C. Hock and Y. Basiron, "The Effect of Natural and Synthetic Antioxidants on the Oxidative Stability of Palm Diesel," *Fuel,* vol. 85, pp. 867-870, 2006.